Comparative Study of Bovine Heart and Bacillus subtilis Cytochrome c Oxidase Vesicles and the Influence of Bulk pH on Cytochrome c Oxidase Components

by

Ivano Perin, Hons., B.Sc.,University of Guelph, Microbiology

A Thesis
submitted to the Department of Biological Sciences
in partial fulfillment of the requirements
for the degree of
Master of Science

October 1996
Brock University
St. Catharines, Ontario

©Ivano Perin, 1996

Abstract

Studies on the steady state behavior of soluble cytochrome *c* oxidase are extensive. These studies have examined the influence of ionic strength and pH and may provide answers to questions such as the link between proton translocation and charge separation. The present study examined the influence of external bulk pH on ΔpH formation, biphasic kinetics, and steady state reduction of cytochromes *c* and *a* of cytochrome *c* oxidase in proteoliposomes. Bulk pH has an appreciable effect on ΔpH formation and steady state reduction levels of cytochromes *c* and *a*. Bulk pH affected total V_{max} and K_m at the low affinity binding site of cytochrome *c*. This study also examined the influence of bovine serum albumin and free fatty acids on proton pumping activity in bovine heart proteoliposomes. Proton pumping activity decreased after treatment with BSA, and was subsequently reinstated after further treatment with FFA.

Much study in the superfamily of haem/copper oxidases has recently been devoted to the bacterial oxidases. The present study has examined some protein composition characteristics and bioenergetic features of *Bacillus subtilis* cytochrome caa_3 oxidase. Results provide evidence for the structural composition of the enzyme in relation to the covalently bound cytochrome *c* to the oxidase. Bioenergetically, caa_3 COV showed appreciable proton pumping activity. Steady state analysis of the caa_3 COV showed significantly different cytochrome *c* and *a* reduction characteristics compared to the bovine enzyme.

Acknowledgments

I would like to acknowledge the following people for their contribution and help in the writing of this thesis. Dr. Peter Nicholls for his support and encouragement to go in the direction that my experiments took me and for helping me understand where we've been and where we are going. Technical support was provided in abundance by Dr. Martyn Sharpe and Ms. Brenda Tattrie. Work on the free fatty acids and proton pumping was done in co-opperation with Dr. Martyn Sharpe. The three dimensional structure of cytochrome *c* oxidase was printed with the help of Ms. Mary Maj. I would also like to thank Dr. Bruce Hill of Queens University, Kingston, Ontario for providing samples of *Bacillus subtilis* caa_3 enzyme for this study. A personal appreciation is extended to Dr. Martyn Sharpe.

Table of Contents

List of Tables

List of Figures

Figure 5.5: Representative models of observed cytochrome *c* to *a* ratios in *B. subtilis* caa_3.

Figure 5.6: Representative populations of enzyme in *B. Subtilis* caa_3 COV.

Perspective

It was in 1925 that Keilin presented his discovery of what he termed 'cytochromes' involved in aerobic respiration (Keilin, 1925). He also observed that these 'cytochromes' were composed of three distinct species which were linked, but independent of each other in their redox reaction. This cytochrome system would later be referred to as the respiratory chain (Keilin, 1925). Since his death in 1963, many conceptual debates concerning the respiratory chain have surfaced. One of the most contested forums was Peter Mitchell's chemiosmotic hypothesis, which eventually became a firmly established principle. The central ideas to Mitchell's chemiosmotic coupling mechanism were first published in 1961 (Mitchell, 1961). Together, this paper and two privately published books (Mitchell, 1966; 1968), 'the little grey books' as they are known, form a comprehensive account of the underlying principles of the chemiosmotic mechanism. The introduction of these ideas was met with considerable resistance. During the 1950's and 60's, much research was put into finding a biochemical understanding of cell energetics and transport. The chemiosmotic hypothesis has four basic proposals: (1) the electron respiratory chain is vectorially arranged such that electron transfer is linked to proton translocation across the membrane, (2) ATP synthase is located in this membrane and uses the proton gradient to drive ATP synthesis, (3) the membrane is impermeable to protons, and (4) there are proton linked transporter systems for metabolite transport. Mitchell was able to show that Keilin's redox

active cytochrome system was capable of generating a proton motive force consisting of a difference pH, (ΔpH) and difference in charge ($\Delta\Psi$) to drive energetically unfavourable reactions such as ATP synthase and secondary active transport systems.

The respiratory oxidases, are those enzymes responsible for the reduction of molecular oxygen to water in the final respiratory event. As with the other members of the respiratory chain, they are also involved in the generation of a proton motive force. The respiratory oxidases play an important role in the physiology of virtually all aerobic organisms. Most of the respiratory oxidases of both eukaryotes and prokaryotes have recently been categorized as members of a single superfamily, the haem-copper oxidase superfamily (Brown *et al.*, 1993; Hosler *et al.*, 1993). As members of the same family, cytochrome oxidases share similar structural and functional characteristics.

As the cytochrome oxidases are membrane bound proteins, structural determinations in the past have been very difficult. X-ray crystal structures were limited to only a few membrane proteins, including the bacterial photosynthetic reaction centre. Crystallographic studies on cytochrome *c* oxidase showed minimal structural data (Yonetani, 1961; Yoshikawa *et al.*, 1988). With the recent structural determination of cytochrome *c* oxidase in mitochondria and *Paracoccus denitrificans*, a greater understanding to the structure/function relationship of the enzyme has become evident. Haem location and their relative intra-enzyme distances have aided in the determination of electron

movement within the enzyme. Physical structural analysis of the enzyme has allowed for the proposal of pores for proton movement to the binuclear centre and across the membrane. The new found structure of cytochrome *c* oxidase will undoubtedly provide the basis for the elucidation of the structure / function relationship in this family of enzymes.

Despite the importance of the structural data obtained through the X-ray crystal studies, understanding the relation of form to function concerning the respiratory oxidases, requires answers to several remaining questions: (1) the mechanism of oxygen reduction to form water, (2) the mechanism of proton translocation, and (3) the interrelationship between these two mechanisms. From these basic questions, a multitude of other questions arise concerning such things as physiological and environmental factors, or possible co-factors involved in the reactions. In studying this enzyme, or any other system, one must relate findings *in vitro* to possible situations as they are *in vivo*. No one study can answer all possible questions, but it can bring a better understanding to the overall relationship, however small. This study is not an exception. It is however an exercise in the scientific process, which as often as not brings about more questions than it may answer.

Chapter 1

Literature Review and Introduction

1.1 General Overview Cytochrome c oxidase

Cytochrome c oxidase (ferrocytochrome c : O_2 oxidoreductase; 1.9.3.1) is the terminal enzyme of the electron transport chain located in the eukaryotic inner mitochondrial membrane and the plasma membrane of some prokaryotes. Its catalytic reaction involves the four electron reduction of oxygen to water and the oxidation of ferrocytochrome c as follows:

$$4\ \text{cyt.}c^{2+} + O_2 + 4H^+ \longrightarrow 4\ \text{cyt.}\ c^{3+} + 2\ H_2O \qquad (1)$$

Additionally, cytochrome *c* oxidase is capable of translocating $4H^+$ outside across the membrane.

The components of cytochrome *c* oxidase are distinct. It contains two spectrally distinct haem iron centres (Keilin and Hartree, 1939) - *a* and a_3. These centres can be distinguished in that the former is a low spin centre which does not bind added ligands, while a_3 is high spin and can bind ligands such as O_2 and CO in its ferrous state, and HCN, NH_3, and H_2S in the ferric state. Two copper containing centres are also to be found, which are integral in electron movement through the enzyme. The Cu_A centre is the proposed entry point of electrons from cytochrome *c*, which then donates the electrons to haem *a*. This centre is composed of two copper atoms located in subunit II of the enzyme (Iwata *et al.*, 1995). A third copper atom forms part of the O_2 reduction site with haem a_3. Two other metal atoms include one zinc, and one magnesium atom

(Einarsdottir and Caughey, 1984, 1985). The roles of these metals have not been determined, but they may be involved in the formation of a structurally stable enzyme.

1.2 Superfamily of Haem/Copper Oxidases

Respiratory oxidases are ubiquitous among all aerobic organisms. All respiratory oxidases can be categorized into a single superfamily called the haem/copper oxidase superfamily. Members of this family all share similar structural and functional features. Figure 1.1 shows members of the haem copper oxidase superfamily. Within the haem-copper oxidase superfamily there exists diversity in the substrates used and the haem groups.

There are two distinct branches within the superfamily in terms of the substrate utilized and haem content. Class I oxidases are the cytochrome *c* oxidases which receive electrons from ferrocytochrome *c* and reduce molecular oxygen to produce water. Class II oxidases are, as far as is now known, unique to bacteria. They are the quinol oxidases, which receive electrons from ubiquinols and/or menaquinols and transfer them to molecular oxygen. The quinol oxidases do not react with cytochrome *c* nor do they have a Cu_A centre. Enzymes within Class I can be further divided into two subgroups based on their haem content. Class IA oxidases contain haem *a*, while those in Class IB contain haem *b* or haem *o*. Similarly, Class II oxidases have two subgroups. Enzymes of this class contain haem *a*, but no Cu_A $^{2+}$(Class IIA), or haem *b* and haem *o* (Class IIB).

Figure 1.1: A representation of subunits I and II of some well characterized members of the haem/copper superfamily of oxidases. This family is divided into two groups, A. cytochrome *c* oxidase, B. quinol oxidases. The cytochrome *c* oxidases include aa_3 from mitochondria and prokaryotes such as *Rhodobacter sphaeroides*; cytochrome caa_3 form *Bacillus subtilis*; cytochrome ba_3 from *Thermus thermophilus*; and cytochrome *cao* form *Bacillus* PS3. The quinol oxidases include cytochrome aa_3 from *B. subtilis;* cytochrome ba_3 from *Acetobacter aceti*; and cytochrome *bo* from *Escherichia coli*. The cytochrome *c* oxidases are characterized by the presence of a copper centre located in subunit II, which receives electrons from cytochrome *c*. The quinol oxidases lack the presence of a copper centre in subunit II, and receive electrons directly from the Q-pool (from Anraku, 1988).

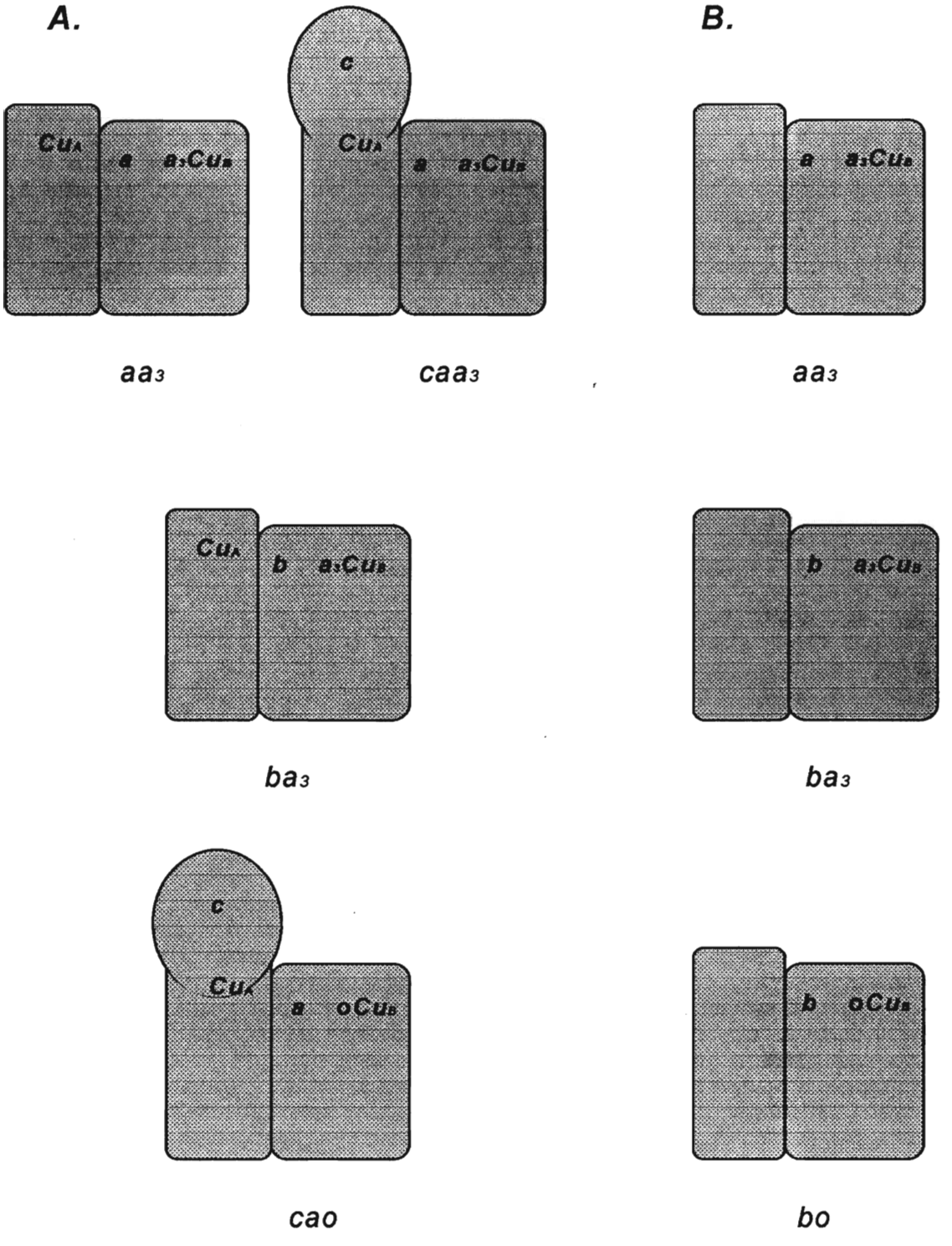
A.
B.
c
Cu_A
a
a_3Cu_B
Cu_A
a
a_3Cu_B
a
a_3Cu_B
aa_3
caa_3
aa_3
Cu_A
b
a_3Cu_B
b
a_3Cu_B
ba_3
ba_3
c
Cu_A
a
oCu_B
b
oCu_B
cao
bo

The cytochrome *bd* quinol oxidase from *E. coli* is unrelated to the haem/copper oxidase superfamily. The subunits of haem/copper oxidases have no sequence similarity to the subunits of cytochrome bd. It contains three redox centres (Meinhardt *et al.,* 1989). Cytochrome *bd* contains one haem *d* and two haem *b*. Haem *b*-558 is a six coordinate, low spin haem, and is the initial site reduced by quinol. Haem *b*-595 and haem *d* appear to be located near the cytoplasmic side of the membrane. Both these haems share a common binding pocket, but only haem *d* binds oxygen or CO (Hill *et al.,* 1993). Cytochrome *bd* oxidase is able to translocate protons with a H^+/e^-ratio of 1(Puustinen *et al.*, 1991; Calhoun *et al.*, 1993), but it does not involve a proton translocation channel. Protons are released to the outside at the time of oxidation of quinol near the top of the membrane. This suggests that cytochrome *bd* is a relatively simple proton translocating system that takes up and releases protons from opposite sides of the membrane. The haem/copper oxidases, in contrast, couple the translocation of protons across or through a channel to electron transfer within the enzyme.

Mammalian cytochrome *c* oxidase has been shown to contain 13 subunits, 10 of which are encoded in the nuclear genome, and 3 are mitochondrially encoded (Capaldi, 1990; Tsukihara *et al.*, 1996). Prokaryotic oxidases generally contain 3 or 4 subunits depending on the species. Sequencing of the genes encoding the subunits of several prokaryotic respiratory oxidases have revealed homologues of the mitochondrially encoded eukaryotic subunits I, II, and III. Subunit I is particularly highly conserved. The

sequence of subunit I from the *R. sphaeroides* aa_3-type and the *E. coli* cytochrome *bo* quinol oxidase are 50% and 40% identical to subunit I of bovine oxidase, respectively (Chepuri *et al.*, 1990). Studies on both the mammalian and *P. denitrificans* cytochrome *c* oxidases have revealed that subunit III is not essential for either cytochrome *c* oxidation or proton pumping (Gregory and Ferguson-Miller, 1988). Thus only subunits I and II are required for electron transfer-linked proton pumping.

1.3 Evolution of the Cytochrome oxidases

The evolution of the cytochrome oxidase has been suggested to the result of gene duplication followed by natural selection of oxidases from the genes of denitrification enzymes (Saraste and Castresana, 1994) (Figure 1.2). Terminal oxidases have been found in both eubacteria (Saraste *et al.*, 1991) and also in archaebacteria (Lubben *et al.*, 1992). These two domains of life share a common distant ancestor, and therefore an oxygen reducing respiratory oxidase must have existed prior to their divergence. Since this divergence occurred prior to an oxygenic atmosphere (Woese, 1987), then early oxidases may have been functioning at low oxygen concentrations (< 2-3%). Nitric oxide was present in the early atmosphere of the earth (Kasting, 1993). One can therefore assume that denitrification predates aerobic respiration and that denitrifying enzymes evolved prior to the first oxidases.

A novel cytochrome *c* oxidase has recently been characterized from *Bradyrhyzobium japonicum, Rhodobacter sphaeroides,* and *Paracoccus*

Figure 1.2: A proposed evolutionary history of cytochrome oxidase. The very first oxidase (FixN) developed from nitric oxide reductase (NOR). This adaptation required a change in the affinity of the iron/copper active site for NO and O_2. The mitochondrial cytochrome oxidase (COX) developed from the FixN complex, which lost the cytochrome *c* domain and acquired the Cu_A binding domain from the nitrous oxide reductase (N_2OR) lineage (from Castresana *et al.*, 1994).

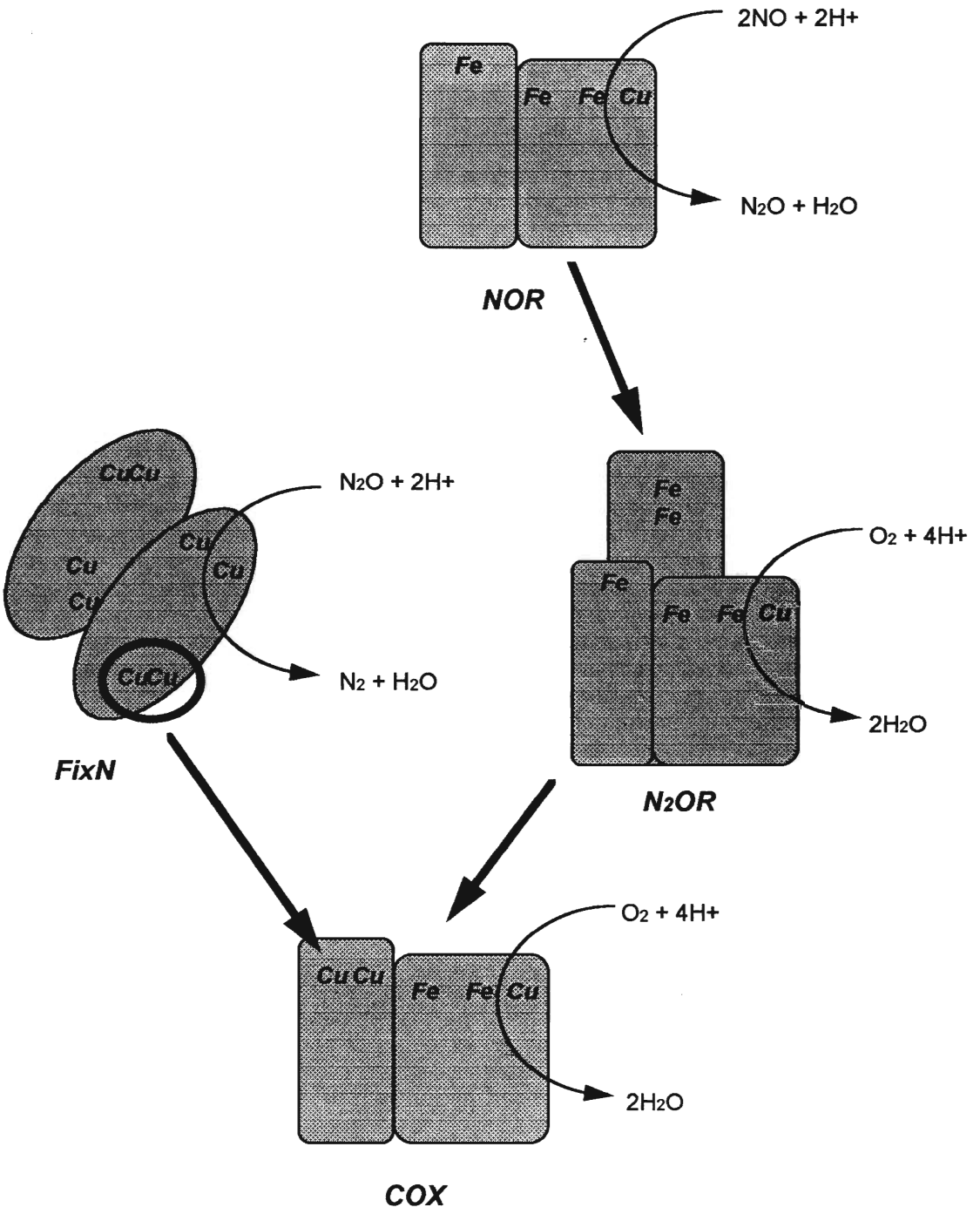
2NO + 2H+
Fe
Fe Fe Cu
N2O + H2O
NOR
CuCu
Cu
Cu
Cu
Cu
CuCu
N2O + 2H+
N2 + H2O
FixN
Fe
Fe
Fe
Fe Fe Cu
O2 + 4H+
2H2O
N2OR
Cu Cu
Fe Fe Cu
O2 + 4H+
2H2O
COX

denitrificans (Preisig *et al.*, 1993; Garcia-horsman *et al.*, 1994). This enzyme is encoded by the *fixNOQP* operon in *B. japonicum*. It is expressed in the nitrogen fixing bacteroids living in root nodules. Energy metabolism is supported by oxidative phosphorylation under conditions in which oxygen concentration is very low. Sequence analyses (Castresana *et al.*, 1994) has shown that the FixN complex is the most distant member of the cytochrome oxidase family, but it still shares the six histidine ligands that bind two haems and Cu_B in the catalytic subunit.

The cytochrome composition of the FixN complex is very similar to the nitric oxide reductase complex. Nitric oxide reductase is a membrane bound *bc* complex (Dermantia *et al.*, 1991), containing two subunits. The subunit NorB is a haem containing membrane protein, which is presumed to be the catalytic site for NO reduction to dinitrogen. It has 12 trans-membrane segments, similar to subunit I of the cytochrome oxidases. NorB is observed to contain six histidine residues that bind the haem groups and Cu_B. Phylogenetically, FixN is the closest branch to NorB. It is therefore proposed that a FixN-type oxidase developed from a nitric oxide reductase through a change in the catalytic reaction. A gene duplication may have resulted in the development of a O_2-reducing enzyme, by changing the distances between the copper and iron atoms.

A further development of the respiratory oxidases may have come from nitrous oxide reductase. N_2OR and the mitochondrial-type cytochrome *c*

oxidases are the only enzymes known to contain a binuclear copper centre. It therefore may be likely that the binuclear copper centre in the cytochrome *c* oxidases originated from nitrous oxide reductase.

1.4 Bacterial Oxidase Complexes

Although there exist both structural and functional similarities between the mitochondrial cytochrome *c* oxidase in eukaryotes and the oxidases in prokaryotes, the evolution of the branched bacterial oxidases permit optimal growth, depending on physiological and environmental conditions (Anraku, 1988). This can be seen in the variety of haem combinations found in the prokaryotic oxidases. Bacteria are often found in environments which are less than optimal for their growth and proliferation. Different oxidases may serve different functions depending on environmental conditions. Those bacteria whose energy needs are met by fermentation or photosynthesis, without oxidative phosphorylation, respiration may be needed simply as a method of maintaining a redox balance in the cytoplasm. Aerobic bacteria may require multiple oxidase systems depending on the level of oxygen in the environment. This is the case for *Escherichia coli,* where cytochrome *bd* predominates in environments of low oxygen tension, which has a higher affinity for molecular oxygen. Cytochrome *bo* has a low affinity for molecular oxygen, and therefore predominates in environments of high oxygen tension (Rice and Hempling, 1978). When *E. coli* is grown anaerobically, cytochrome *bd* is present and may

be used to scavenge for oxygen in order to protect oxygen sensitive enzymes required for anaerobic growth (Hill *et al.*, 1990).

Bacillus subtilis is a Gram-positive prokaryotic bacteria which contains an aa_3-600 quinol oxidase in addition to a cytochrome *c* oxidase (Lauraeus *et al.*, 1991). The *B. subtilis* cytochrome *c* oxidase also shows differences from other oxidases, in that it has a cytochrome *c* covalently bound to a carboxy-terminal extension of subunit II (Saraste *et al.*, 1991). It is thus a caa_3 type oxidase. In addition, *B. subtilis* can also synthesize cytochromes of *b, d,* and *o* types (von Wachenfeldt and Hederstedt, 1992). Cytochrome caa_3 oxidase is predicted from genetic data to be composed of four subunits, but only the two largest subunits have been found in the isolated product (Lauraeus *et al.*, 1991). Subunit I is a large subunit at 69 000 Da, and is larger than the corresponding subunits of either the mitochondrial or the *Paracoccus* enzyme. Subunit II has a molecular mass of 40 000 Da, and is homologous to the *Paracoccus* enzyme. Subunit III is the smallest subunit at 23 000 Da. A fourth subunit, has been identified to be approximately 12 600 Da. Spectrally, cytochrome caa_3 oxidase shows absorption peaks at 604 and 442 nm due to the cytochrome *a*, at 550, 520, and 417 nm from the cytochrome *c* domain. Different environmental conditions will see the production of different haems to be incorporated into the oxidase. In glucose supplemented media, or from haem *a* deleted mutants, *B. subtilis* will express a *d* type of cytochrome. This cytochrome has not been isolated, but is predicted that it functions as an

oxidase. Spectroscopic evidence has also suggested the presence of at least one type of cytochrome *o* oxidase, but structural and genetic data have yet to be obtained. A *b*-type cytochrome, that binds carbon monoxide, and exhibits an absorption maxima at 556 nm has been partially purified by de Vrij and Konings (1987). This *b*-type cytochrome also showed oxidase activity with yeast cytochrome *c*.

The existence of at least two types of respiratory oxidases in *B. subtilis,* as in other prokaryotic bacteria, poses the question of the functional role of these oxidases in relation to the organism and to each other. Mutations of both the oxidases have been studied. Mutants lacking the cytochrome caa_3 show similar growth properties and colony morphology as the wild-type strain. However, when mutants lacking the quinol aa_3-type cytochrome are grown on minimal media supplemented with succinate or citrate, small colonies and slower growth are observed compared to the wild-type strain (Santana *et al.*, 1992). A double deletion of both types of oxidases shows poor but viable growth. They also show an increase in the expression of cytochrome *d*, in the absence of any haem *a*. Of the two oxidases, it appears that the quinol aa_3-600 oxidase is functionally more important during vegetative growth.

1.5 Structure of Cytochrome c Oxidase Protein

Cytochrome *c* oxidase is a large, membrane bound protein. The mitochondrial enzyme is composed of up to 13 subunits (Tsukihara *et al.*, 1996) with a molecular weight of 200 kDa. The prokaryotic enzyme is generally

composed of between 2 and 4 subunits (Poole, 1988; Gai *et al.*, 1990). Up until recently, the major problem in determining the structure of cytochrome c oxidase, was its large size and the fact that it is a membrane protein. Previous attempts to crystallize cytochrome c oxidase resulted in minimal structural data (Yonetani, 1961; Yoshikawa *et al.*, 1988).

Recently, the 3-dimensional structure of cytochrome *c* oxidase was finally obtained for both the mitochondrial enzyme (Tsukihara *et al.*, 1996) and for the bacteria *Paracoccus denitrificans* (Iwata *et al.*, 1995). Surprisingly, two different methods were used in obtaining these structures. The mitochondrial enzyme was crystallized using the more traditional method involving non-ionic detergents (Yoshikawa *et al.*,1988). For cytochrome *c* oxidase, decyl maltoside was used in the purification of the enzyme. The *Paracoccus* enzyme was crystallized using the F_V fragment of a monoclonal antibody (Iwata *et al.*, 1995; Ostermeier *et al.*, 1995). Both enzymes were resolved at a resolution of 2.8 A by X-ray crystallography.

The crystal structure of bovine heart cytochrome *c* oxidase reveals 13 different subunits, while the cytochrome *c* oxidase of *P. denitrificans* is composed of four subunits. For both enzymes, subunits I, II, and III form the functional unit of the enzyme. The general structure of the functional unit of both species are very similar. The enzyme unit comprises a roughly cylindrical or trapezoid shaped membrane portion, with a domain extending above the membrane into the intermembrane space or periplasm. Figure 1.3 presents a

diagram of the three dimensional structure of subunits I, II, and III of the bovine heart cytochrome *c* oxidase. The central part of the enzyme consists of subunit I, which binds both haem groups and Cu_B. Subunit I is flanked by subunits II and III. A globular portion of subunit II protrudes into periplasmic space and contains Cu_A.

Subunit I consists of 12 membrane spanning segments with a helical secondary structure. The 12 segments appear to form three symmetrical semi-circular arcs. When viewed from the top of the enzyme, the semicircles have a pore like appearance. The segments of subunit I together form 'pores' of the enzyme involved in proton translocation for the reduction of molecular oxygen and proton pumping (Figure 1.4). Two of the pores hold haems *a* and a_3 respectively and are perpendicular to the membrane plane. A third pore is blocked mostly by aromatic residues. The helices of subunit I are not completely perpendicular to the membrane surface, but are at a 20° to 35° angle against the vertical line from the membrane plane.

Subunit II is composed of three segments: an N-terminal loop, two transmembrane helices, and a C-terminal globular domain, which contains the Cu_A centre. The N-terminal domain comprise of residues which interact with the C-terminal domain on the periplasmic side, directly above the pore containing the binuclear centre. The Cu_A site is in fact two copper atoms bridged by two cystein thiolates, at a distance of 2.6 A. This copper centre is the entrance point for electrons from cytochrome *c*. The binding site for cytochrome *c* is therefore in close proximity to copper centre. The corner formed by the globular domain of

Figure 1.3: Three dimensional structural representation of subunits I, II, and III of bovine heart cytochrome *c* oxidase. Structure was created in Quanta for Silicon Graphics. Subunit I (light blue) contains haems *a* and a_3 (red), a Mg atom (green), and a Cu_B atom (purple). The Zn atom (dark blue) is located near the bottom of subunit II. Subunit II (brown) contains the Cu_A site (yellow) which is composed of two copper atoms. Subunit III (grey) is located adjacent to subunit II. The exact function of subunit III is not known, but it does not contain any redox active sites (Tsukihara *et al.,* 1996).

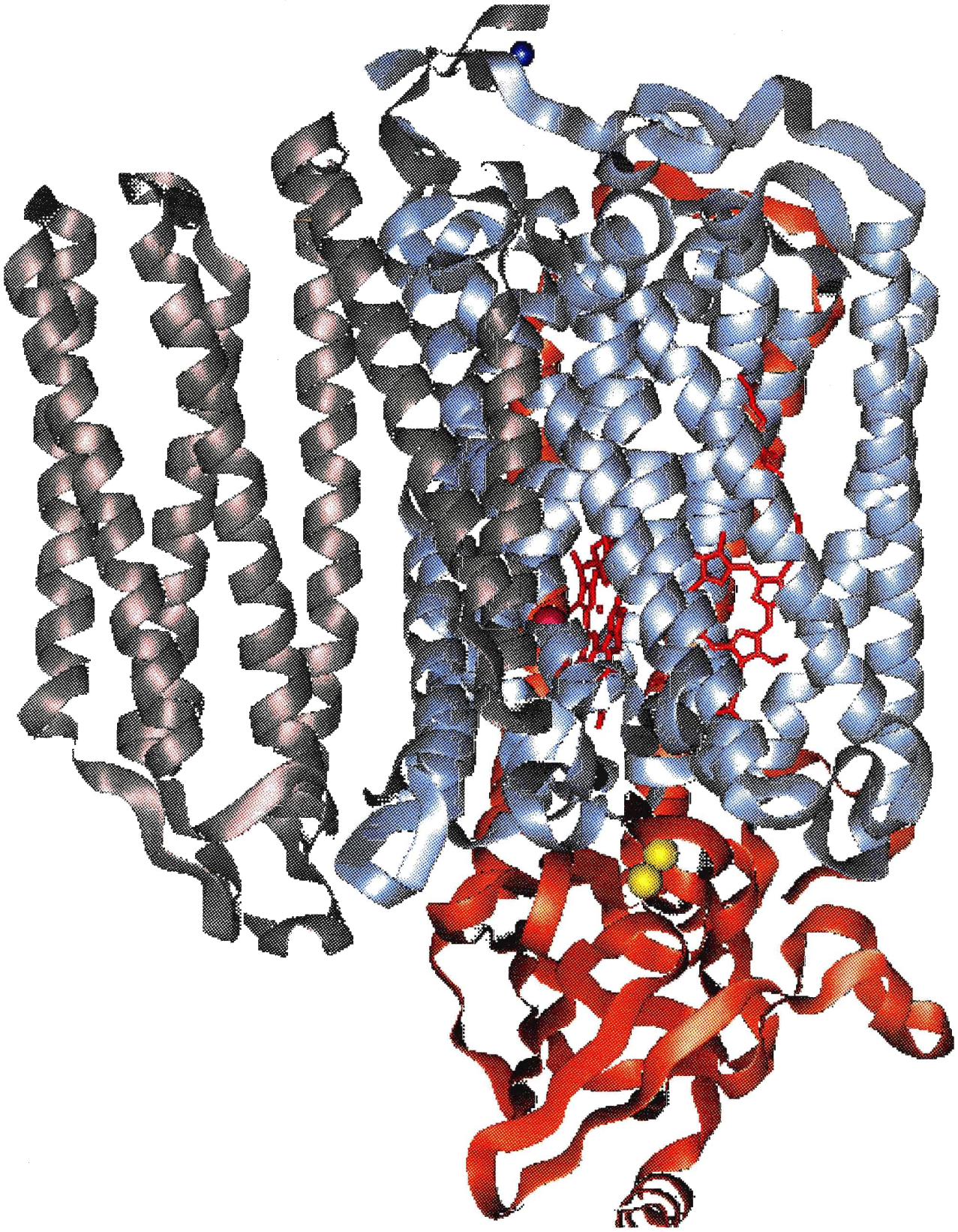

Figure 1.4: Representation of the pores associated with subunit I (top view). The 12 transmembrane helices of subunit I are arranged to form three pores. These pores have a channel like appearance. The pores are blocked, pore A (bottom) by mostly conserved aromatic residues, pore B (upper right) by haem a_3 and Cu_B, and pore C (upper left) by haem *a*. These pores are thought to be involved in proton translocation to the binuclear centre.

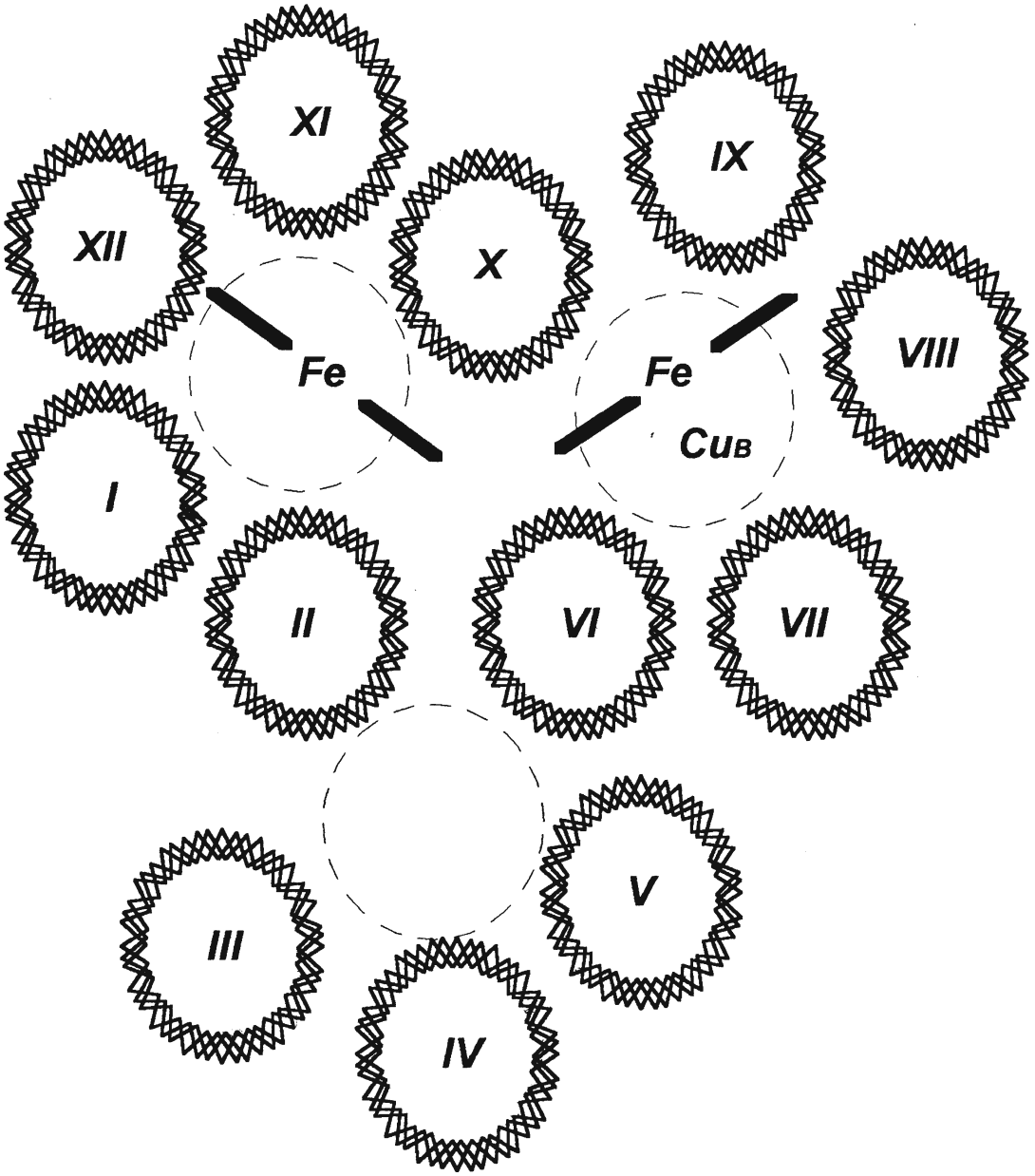
XI
IX
XII
X
VIII
Fe
Fe
CuB
I
II
VI
VII
III
V
IV

subunit II and the flat periplasmic surface of subunit I may be part of the cytochrome *c* binding site. Part of the loop connecting transmembrane helices III-IV of subunit III may also be involved in cytochrome *c* binding. This area contains 10 acidic residues, which could interact with lysine residues on cytochrome *c*.

Subunit III is composed of seven transmembrane helices that are arranged in a slightly irregular manner. The seven helices are divided into two groups, helices I and II forming one bundle, and remaining helices forming a second bundle. The two bundles are separated by a large V-shaped cleft, which contains lipid molecules bound at its bottom. The role of the lipid molecule is not known, but it may be involved in structural stability or as lipid pool. The function of subunit III is unknown, as it does not contribute to the binding of redox-active groups.

The possible involvement of subunit III in proton pumping activity has been studied extensively. Although subunit III is highly conserved throughout the haem/copper family of oxidases, and therefore seems evolutionarily a necessity, the most recent studies have shown it to be unnecessary. Removal of subunit III does not prevent the enzyme from reducing molecular oxygen to water or from proton pumping (Hendler *et al.*, 1991). It may however, be involved in the assembly of the cytochrome *c* oxidase (Haltia *et al.*, 1989). The V-shaped cleft may be a docking site for other membrane proteins, such as the membrane

anchored cytochrome c_{552}, which seems to be a physiological electron donor to Cu_A of the *Paracoccus* cytochrome *c* oxidase.

The discovery of subunit IV in the *Paracoccus* enzyme is recent, with only the N-terminal sequence published (Haltia, 1990). The subunit consists mainly of a single transmembrane helix, with the N terminus on the cytoplasmic side. This subunit is in contact with all three of the other subunits. Its function is unknown; but it may be involved in the stabilization of the *Paracoccus* cytochrome *c* oxidase.

The extra subunits of the eukaryotic enzyme are nuclear encoded and each contains a transmembrane helix. In the bovine enzyme, subunit IV looks like a dumbbell with a transmembrane helix in the middle of two extramembranous domains. The transmembrane helix of subunit IV is in contact with subunit I at a 50° angle, and is sandwiched in-between subunit I and the subunit VIIb helix. Subunit Va is an extra membranous subunit located on the matrix side below subunit I. It contains five α-helices which forms a right-handed super helix. Subunit Vb is located below subunits I and III, adjacent to subunit Va and toward the matrix domain of subunit IV. This subunit contains a zinc site with four cysteine residues as ligands and a zinc finger motif. The transmembrane helix of subunit VIa interacts with helix IV of subunit III opposite the site of attachment of subunits I and III. Ten residues of the N-terminal region of subunit VIa are in contact with subunit I of the second molecule of the dimeric unit. It is thought that this contact stabilizes the dimeric unit. Subunit VIb is an

extramembranous subunit associated with subunits II and III. Subunit VIc is a dumbbell shaped subunit with a transmembrane helix in contact with subunit II. It also contains an extended peptide segment on the matrix side and a α-helix on the cytosolic side parallel to the membrane. Subunit VIIa is a transmembrane helix with an extramembranous region on the matrix side on the surface of subunit III. The transmembrane helix is against subunit III with the C-terminal end located near the C-terminal end of subunit VIIc. The transmembrane helix of subunit VIIb has an extended structure on the cytosolic side, but no extra domain on the matrix side. In between subunits VIIa and VIII against the surface of subunit I is subunit VIIc. It contains an N-terminal domain with an irregular conformation. Subunit VIII is parallel to the transmembrane helix of subunit IV, with close diagonal contacts with helices I and XII of subunit I. This subunit also contains an extended N-terminal domain on the matrix side.

1.6 Redox Metal Centres

There are four metal centres which are involved in the reduction of molecular oxygen and proton pumping. Three copper atoms are present, two of which are observed to form a bi-metalic centre (Cu_A centre) involved in accepting electrons from cytochrome *c*. A third copper (Cu_B) forms part of the binuclear centre, involved directly in the reduction of molecular oxygen. Two iron haem metal centres are also present in the enzyme, haems *a* and a_3. Haem *a* is involved in electron transfer from Cu_A to the binuclear centre. Haem a_3 forms the second part of the

binuclear centre with Cu_B. The relative positions of these redox centres have recently been deduced from the X-ray structures of both the mitochondrial and *Paracoccus* cytochrome *c* oxidases.

The position of the Cu_A centre has been confirmed in subunit II (Holm *et al.*, 1987; Iwata *et al.*, 1995; Tsukihara *et al.*, 1995). For both the mitochondrial and *Paracoccus* enzyme, the bi-metalic Cu_A centre contains of 6 metal ligands: 2 cysteins, 2 histidines, a methionine, and the carbonyl oxygen of a glutamate residue. The two coppers in Cu_A are bridged by sulphur atoms from cysteine residues. The estimated separation of the two coppers are 2.6 A and 2.7 A for the prokaryotic and mitochondrial enzyme respectively.

Both haem *a* and haem a_3 contain the same porphyrin, haem *a*. Differences in the two haems are a result of their distal and proximal ligands. Haem *a* is low-spin with two histidine residues as axial Fe-ligands. In the mitochondrial enzyme these ligands are identified as His 61 and His 378 form subunit I, while in the *Paracoccus* enzyme, they are His 94 and His 413. Haem a functions to transfer electrons from the Cu_A centre to the binuclear centre. For haem a_3, there is only one coordinated histidine residue, His 376 in the mitochondrial and His 411, *Paracoccus* enzyme. This allows a free position for a sixth ligand examples of which include O_2, CN^-, N_3, S^{2-}, CO, and NO. Haem a_3 thus forms part of the binuclear centre, involved in the binding of molecular oxygen, and subsequent formation of water.

The formation of the binuclear centre results from the close proximity of the Fe haem and Cu_B. In the mitochondrial enzyme this distance is 4.5A, whereas, in the *Paracoccus* enzyme this distance is 5.2A. This distance in the *Paracoccus* enzyme may be affected by the presence of azide within the 3-dimensional structure. This may in fact give a slightly larger distance between haem a_3 and Cu_B. Histidine residues form the ligands for Cu_B in both enzymes. Using their *Paracoccus* structure, Iwata *et al.* (1995) have suggested several possible pathways for electron transfer between haems: a direct pathway between the haems, a pathway using Fe-ligands His 413 (haem *a*) and His 411 (haem a_3) through the connecting peptide backbone, and a pathway involving Phe 412 and Met 416 with their side chains in contact with both haems.

1.7 Reconstituted Systems

Cytochrome *c* oxidase and other respiratory systems can be studied in intact mitochondria or bacterial membranes, or they can incorporated into artificial membrane systems. Both methods are useful, but can pose certain problems. The major advantage in using natural membrane systems, is their obvious realism in being the natural environment of the studied enzyme. Lipid and protein are natural and influence the enzyme system without the bias of unnatural factors. Unfortunately, it sometimes proves very difficult to obtain and maintain intact natural systems in such a way that makes them easy to study. Both mitochondria and bacterial membranes can be obtained, but are subject to inherent problems. Major problems include, heterogeneous populations in terms

of their coupling effectiveness. Other problems include light scattering during spectral studies, influence of other systems to a particular enzyme of study, and limited lifetime of sample.

The use of reconstituted systems or proteoliposomes proves to have several advantages over the intact lipid system. Initial work using cytochrome *c* oxidase vesicles (COV) was done by Racker, Hinkle and their co-workers (Racker, 1972; Hinkle *et al.*, 1972). They showed that COV could oxidize reduced ascorbate/cytochrome *c*, and could be influenced by uncoupling agents. The advantage in using reconstituted systems such as COV is simplicity. COV contain only the bare minimum of components to allow study of gradients and transport. This eliminates the influence of other systems. Another advantage of COV includes the ability to use pH probes such as phenol red or pyranine, which can be trapped inside the vesicle and allow for ΔpH measurements.

There are several methods for producing COV, all of which have both advantages and disadvantages. Two common methods involve sonicated liposomes and cholate dialyzed liposomes.

Sonicated liposomes are COV formed from a sonicated mixture of lipid and cytochrome *c* oxidase. A problem with sonication is that it forms a heterogeneous population of different sized vesicles, which can range between 50 and 160 nm or more in diameter. This size heterogeneity makes properties of the COV such as internal pH and membrane potential difficult to determine reliably (Wrigglesworth *et al.*, 1990). Another problem is that the proportion of

'right side out' facing cytochrome *c* oxidase,(the mitochondrial orientation) is approximately 50% (Nicholls *et al.*, 1980). This produces two major problems when studying steady state cytochrome redox levels: (1) 50% of the enzyme stays oxidized until membrane permeable reductants are added, and (2) when using TMPD; the reduced species can cross the membrane, and then be oxidized by cytochrome *c* oxidase in the absence of cytochrome *c* producing $TMPD^+$ which is blue and membrane impermeant and therefore collects inside the vesicle.

Many problems associated with COV formed by sonication, are eliminated through proteoliposome production by cholate dialysis. Cholate dialysis produces a reasonably homogeneous population of small, unilamellar vesicles with an average size of approximately 30 nm (Wrigglesworth *et al.*, 1985). The proportion of cytochrome *c* oxidase externally facing is greatly increased over that produced by the sonication method and is normally greater than 70% (Nicholls, 1990; Steverding *et al.*, 1990). The major disadvantages in using the cholate dialysis method are the time required and large quantity of dialysate used. This can be expensive when attempting to entrap a pH probe inside the vesicles.

1.8 Chemiosmotic Hypothesis

The chemiosmotic hypothesis developed by Peter Mitchell, states that mitochondria, chloroplasts and bacteria couple the transfer of electrons in redox reactions to the production of ATP, via the formation of a proton electrochemical

gradient $\Delta\mu H^+$ (Mitchell, 1961; 1966; 1968). The proton electrochemical gradient is composed of two separate component gradients: a transmembrane proton gradient, ΔpH, and a transmembrane charge gradient or membrane potential, $\Delta\Psi$. During the turnover of cytochrome *c* oxidase, contributions to the proton electrochemical gradient occur via two separate processes. Electrons flow from cytochrome c which is bound to the external face of the membrane to a reduction site within the protein. Four protons are consumed from the matrix of the mitochondria or cytoplasm of bacteria in the reduction of oxygen to water. This lowers the matrix pH, and contributes to the ΔpH and $\Delta\Psi$. Cytochrome *c* oxidase is also able to transport four additional protons across the membrane to the outside (Wikstrom, 1977). The proton pumping also generates a ΔpH gradient (alkaline inside), and a membrane potential (negative inside). The combined ΔpH and $\Delta\Psi$ is used to drive the thermodynamically unfavourable production of ATP, via the F_1 F_o ATP synthase.

For cytochrome *c* oxidase, turnover is controlled in part by both substrate concentration and product inhibition. The substrates of cytochrome *c* oxidase are molecular oxygen, protons, and ferrocytochrome *c*. The resulting products of cytochrome *c* oxidase turnover are water, ΔpH, $\Delta\Psi$, and ferricytochrome *c*. The chemiosmotic control of cytochrome *c* oxidase turnover is therefore in the form of product inhibition i.e. by $\Delta\Psi$ and ΔpH (Figure 1.5). Control of turnover is not shared equally between ΔpH and $\Delta\Psi$. Although $\Delta\Psi$ is responsible for approximately 90% of $\Delta\mu H+$ in terms of mV, most of the chemiosmotic control of

cytochrome *c* oxidase activity is due to the remaining 10% mV resulting from the ΔpH contribution (Nicholls, 1990).

1.9 Routes of Intra-enzyme Electron Flux

Four redox active metal centres, are involved in the electron transfer from cytochrome *c* to oxygen. The free energy of this process is conserved in the form of the electrochemical gradient. Kinetic and spectroscopic studies have been used to characterize electron transfer reactions in different forms of the enzyme, although the precise route of intra-enzyme electron flow has not been established. From these studies however, a number of different models have been derived (Figure 1.5). In the first model, two electrons are transferred from the binuclear centre to oxygen forming a peroxy intermediate. This is followed by electron transfer from Cu_A and cytochrome *a* successively. Cu_A can donate electrons to the binuclear centre and cytochrome *a* is the site of electron entry from cytochrome *c*. However, in this model, the observed kinetic spectra do not correspond to the static spectra of cytochrome *a* and cytochrome a_3 (Wrigglesworth *et. al*, 1988). In a second model, there is a branched reaction that allows for a two electron transfer form either cytochrome a_3 and Cu_A or cytochrome a_3 and cytochrome *a*. This model involves a direct electron transfer form cytochrome *a* to the binuclear centre (Hill and Greenwood, 1984). The most recent model details a linear pathway of electron transfer from cytochrome *c* to the binuclear centre. Cu_A is the primary site of electron acceptance from cytochrome *c*. Cytochrome *a* acts to bridge the electron

Figure 1.5: Chemiosmotic control of electron transfer from cytochrome *c* to the cytochrome *a*-Cu_B binuclear centre. Both $\Delta\Psi$ and ΔpH are involved in the control of cytochrome oxidase. $\Delta\Psi$ has been implicated in controlling electron movement from cytochrome *c* to cytochrome *a*, where as ΔpH controls electron movement from cytochrome *a* to the binuclear centre. Although $\Delta\Psi$ is responsible for approximately 90% of $\Delta\mu H+$ in terms of mV, most of the chemiosmotic control of cytochrome *c* oxidase activity is due to the remaining 10% mV resulting from the ΔpH contribution. The solid lines represents the most conventional scheme of electron transfer through the enzyme. Electrons are first accepted by Cu_A, thought to be in closer proximity to cytochrome *c* than cytochrome *a*. Electrons are then passed to cytochrome *a*, and then onto the binuclear centre. The dashed lines represent other possible routes of electron transfer through the enzyme. Electrons from Cu_A can alternatively be transferred directly to the binuclear centre. Electrons from cytochrome *c* may bypass Cu_A and pass its electrons to cytochrome *a*.

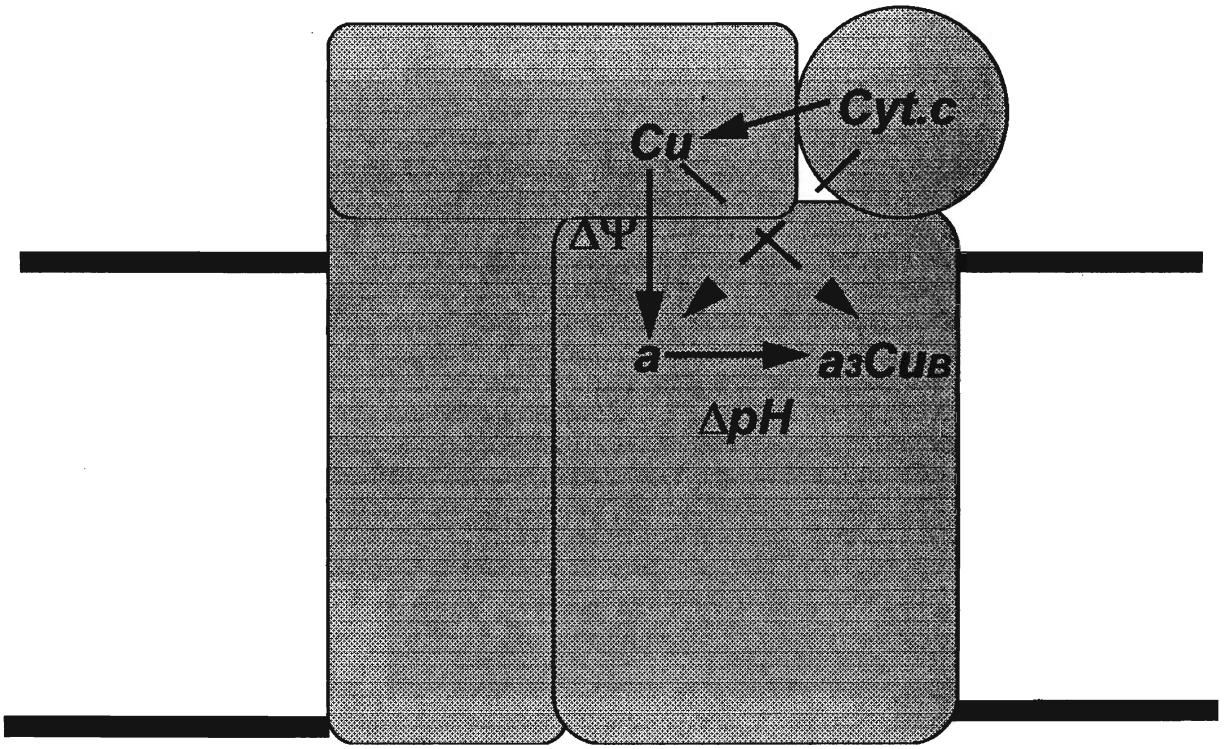
Cyt.c
Cu
ΔΨ
a
a3CuB
ΔpH

receiving site and the oxygen binding site. In this particular model there are at least two different rates for the oxidation of cytochrome *a*.

1.10 Proton Movement

For the proper function of cytochrome *c* oxidase, protons are required for two different purposes. Scalar protons are those protons used directly in the formation of water by the reduction of oxygen. Vectorial protons are protons which are translocated across the membrane resulting in the formation of an added proton electrochemical gradient. Recent work by Thomas *et al.* (1993) and Garcia-Horsman *et al.* (1995) suggests the possibility of two separate pathways for proton movement. In their 3-dimensional model of the *Paracoccus* enzyme, Iwata *et al.* (1995) have also proposed the existence of two separate proton channels.

Most terminal respiratory oxidases conserve energy of the oxygen reduction reaction by coupling it to the vectorial translocation of protons. The ability of cytochrome *c* oxidase to pump protons and the stoichiometry involved has been addressed for many years. It was first proposed by Wikstrom (Wikstrom, 1977) and Wikstrom and Krab (1979), that electron flow from cytochrome *c* to oxygen resulted not only in the formation of water, but also the release of additional protons. These original experiments were criticized by Mitchell (Moyle and Mitchell, 1978) and others (Papa *et al.*, 1980) as being due to other mechanisms. After much debate and discussion, the idea of pumped protons became generally accepted (Papa *et al.*, 1987). The stoichiometry of

proton pumping has been estimated by many groups. A H^+/e^- ratio = 1 has been reported (Casey *et al.*, 1979) while some groups have reported ratios of 1.5 (Beavis, 1987) and even as high as 2 (Alexander *et al.*, 1978; Azzone *et al.*, 1979).

Such differences in reported stoichiometries could be due to phenomena known as 'slip' and 'leak'. The occurrence of 'slip' is a process where at high proton electrochemical gradients, the oxidase is able to turnover, but no proton pumping occurs. The occurrence of 'slip' has been used to try to explain differences in stoichiometries by several groups. Murphy and Brand (1988a; 1988b), using intact mitochondria reported that H+/e- stoichiometry is dependent upon $\Delta\Psi$. With an increase in $\Delta\Psi$ there is a decrease in H+/e- stoichiometry. Papa and colleagues (Papa *et al.*, 1991; Capitanio *et al.*, 1991) using mitochondria and reconstituted systems concluded that proton pumping was subject to 'slip' at high turnover. Membranes may have a passive leak for protons, such that a large proportion of protons pumped across during enzyme turnover, may leak back across the membrane without being coupled to ATP synthesis or transport phenomena. Proton leak rates have also been measured at high $\Delta\Psi$ (Krishnamoorthy and Hinkle, 1984; Brown and Brand, 1986) by first inhibiting all proton transport process and then inducing an artificial $\Delta\Psi$. The rate of proton leak was much greater, with an exponential dependence on $\Delta\Psi$. Slips and leaks may be an unavoidable consequence of membrane structure and cause a significant wastage of free energy.

1.11 Proton Translocation Schemes

This discovery of proton pumping immediately raised questions concerning mechanism and control. Assuming that there is a common mechanism for proton pumping, it can be concluded that neither cytochrome *a* nor Cu_A are involved, since some members of the oxidase family do not have these groups, but are still able to pump protons (Calhoun *et al.*, 1994), unless different mechanisms for proton pumping in different complexes have evolved. All members of the haem/copper oxidases transfer protons to the outside through a channel system. For each molecule of oxygen reduced, eight protons are taken up from the mitochondrial matrix or bacterial cytoplasm, four of which are deposited into the mitochondrial inter-membrane space or the periplasm. Cytochrome *bo* oxidase from *E. coli* also undergoes the oxidation ubiquinol near the upper membrane surface, resulting in the further release of four protons to the outside. A further four protons are translocated through a channel system from inside to the outside. Cytochrome *bd* from *E. coli* moves protons solely through the oxidation of ubiquinol.

The method by which protons are moved across the membrane remains an enigma. Current suggestions for a mechanism of proton pumping include a 'histidine cycle' (Wikstrom *et al*, 1994; Morgan *et al.*, 1994), which couples the chemistry of oxygen reduction directly to proton pumping. From their 3-dimensional model of the *P. denitrificans* oxidase, Iwata and colleagues (1995) have proposed an alternate mechanism for proton pumping. The structure of the

oxidase suggests a pathway for pumped protons, with an entrance-gap located between subunit I loops II-III and III-IV. Residues on subunit I, Asp 124, Thr 203, and Asn 199 form a gate. This is followed by residues Asn 113, and Asn 131. Replacement of these residues by hydrophobic ones results in the loss of proton pumping (Garcia-Horsman *et al.*, 1995). The remaining cavity is lined primarily with hydrophilic residues, leading to Glu 278. On the periplasmic side of Glu 278, two possible pathways are suggested. From Glu 278, protons may be shuttled to one of the cytochrome a_3 propionate groups. A more likely pathway involves the Cu_B-ligand His 325. His 325 may be involved in cycling through the imidozolate, imidozole, and imidozolium states, and shuttle between two positions. A switching between these two alternate conformations may allow the conduction of protons to the formyl group of cytochrome a_3, the carbonyl oxygen of Leu 393, and Asp 399. Ultimately, protons from His 325 are released into an exit pathway towards the periplasm.

1.12 Effect of $\Delta\Psi$ on Cytochrome c oxidase activity

The influence of $\Delta\Psi$ on cytochrome *c* oxidase turnover can be observed by the addition of the ionophore valinomycin to reconstituted systems such as respiring COV. Valinomycin can be used to abolish the membrane potential (Sharpe *et al.,* 1995) so that chemiosmotic control is only due to ΔpH (Figure 1.6). At high valinomycin concentrations resulting turnovers increase with a slight decrease in ΔpH (Shaughnessy and Nicholls, 1985; Capitanio *et al.*,

1991). At low concentrations of valinomycin, the turnover is lower, and accompanied by a slight increase in ΔpH (Nicholls, 1990).

Prior to the steady state, during the first few turnovers ΔpH is very low and $\Delta\Psi$ is large (Nicholls *et al.*, 1990). This low ΔpH is due to the buffering capacity of the vesicles. A large number of protons will be required to move from inside the vesicle to the outside in order to generate a substantial ΔpH. The capacitance of the COV allows a large $\Delta\Psi$ to be produced from a few charges crossing the membrane (Wrigglesworth *et al.*, 1990). Therefore, during the first few turnovers of the enzyme, $\Delta\Psi$ is the major component of $\Delta\mu_H^+$

Mechanistically, where does $\Delta\Psi$ influence the turnover of the enzyme? According to Mitchell and Hinkle (1970), $\Delta\Psi$ solely affects electron transfer between cytochrome *c* and cytochrome *a*, with no influence from ΔpH. A direct effect of $\Delta\Psi$ on the midpoint potential of Cu_A is extremely small (Rich *et al.*, 1988). The redox potential of Cu_A in fact, appears to be linked to the redox state of cytochrome *c* (Rich *et al.*, 1988). As the redox state of cytochrome *c* changes, so does that of Cu_A. The influence of $\Delta\Psi$ on the redox potential of cytochrome *a* has been studied extensively. Upon the addition of valinomycin to COV, cytochrome *a* becomes more reduced (Mitchell and Hinkle, 1970; Nicholls, 1990). Therefore, the removal of $\Delta\Psi$ can either increase the rate of electron flux from cytochrome *c* to cytochrome *a*, or decrease the rate of electron flux to the binuclear centre, or both.

Figure 1.6: Ionophore interaction with cytochrome *c* oxidase vesicles. Valinomycin is an electrophoretic ionophore, which provides for the movement of charge across the membrane. It acts to eliminate the membrane potential $\Delta\Psi$ by allowing K^+ ions to move across the membrane, at which point chemiosmotic control is governed solely by ΔpH. Nigericin is a electroneutral ionophore, which allows the movement of charged ions both in and out of COV. There is no change in net charge across the membrane through the movement of ions. The movement of H^+ ions into the COV eliminates ΔpH, but $\Delta\Psi$ is maintained by the movement of K^+ outwards.

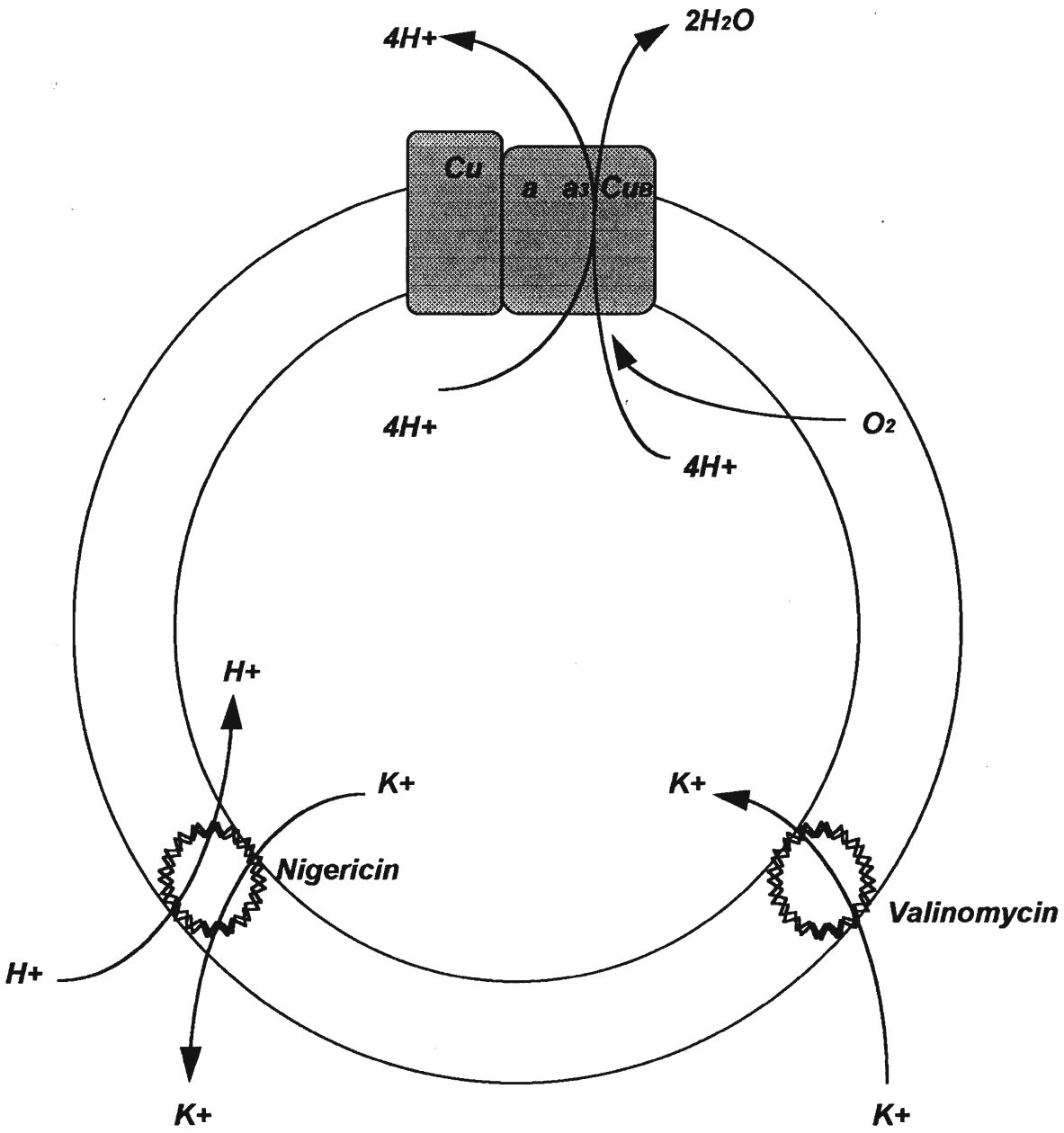
4H+
2H2O
Cu
a
a3
CuB
4H+
O2
4H+
H+
K+
K+
Nigericin
Valinomycin
H+
K+
K+

The effect of $\Delta\Psi$ on the steady state redox potential of cytochrome *a* at different levels of cytochrome *c* reduction has been examined in the presence of nigericin (Nicholls, 1990). It was found that with an increase in $\Delta\Psi$, and abolition of ΔpH, cytochrome *a* become more oxidized. A decrease in $\Delta\Psi$ also produced a decrease in the redox potential of cytochrome *a*. Capitanio *et al.* (1990) found that the redox reduction level of cytochrome *a* increased upon the addition of valinomycin, but with no increase in turnover of the enzyme. Upon the addition of nigericin, there was a decrease in the reduction level of cytochrome *a*, along with an increase in the turnover of the enzyme. With both ionophores present, there was a further increase in turnover, and a decrease in steady state reduction level. The steady state redox level of cytochrome *a* was approximately 53% if valinomycin was added first, and 38% if nigericin was added before valinomycin.

1.13 Effect of ΔpH on Cytochrome c oxidase Activity

The major gradient across the membrane of mitochondria or of COV is $\Delta\Psi$ but, ΔpH may be the predominant controlling element of cytochrome *c* oxidase activity. One problem involved in the study of ΔpH effects is that they may be due to ΔpH or to changes of pH inside the COV. This question can be examined by observing the effects of bulk pH on the respiratory control in COV. COV have been reported to show the highest respiratory control ratios at bulk pH values ranging between 6.4 and 7.4, with an optimum at pH 7.0 (Maison-Peteri and Malmstrom, 1989). But, the pH optimum for enzyme turnover in the solubilized

form is much lower, close to pH 5.0, which is near the limit of enzyme acid stability (Cooper, 1990).

The activity of the enzyme in COV with an imposed pH gradient was examined using stopped flow. At a fixed pH of 7.4 outside the COV, the turnover of COV with an internal pH ranging form pH 5.4 to 8.4 was examined (Maison-Peteri and Malmstrom, 1989). The highest turnover occurred with an acidic pH inside the COV, but at high ferrocytochrome *c* concentrations. When the internal pH was kept constant at 7.4, and the bulk pH ranged between 5.4 and 8.4, the relationship between turnover and pH was reversed, that is turnover was greatest at acidic pH (Maison-Peteri and Malmstrom, 1989). For the solubilized enzyme, a low bulk pH affects cytochrome *c* binding and leads to an increase in both V_{max} and K_m (Cooper, 1990).

1.14 Study Proposals

Cytochrome *c* oxidase oxidizes cytochrome *c* and reduces molecular oxygen to water. This process generates both an electrical and pH gradient ($\Delta\Psi$ and ΔpH) which inhibit enzyme turnover. This respiratory control process is seen in both mitochondria and reconstituted proteoliposomes. The first step in turnover is electron transfer from cytochrome *c* to the enzyme. Ferrocytochrome *c* oxidation involves two distinct kinetic phases, each with a characteristic TN_{max} and K_m. The occurrence of two phases suggests two catalytically competent cytochrome *c* binding sites (Ferguson-Miller *et al.*, 1976). The discovery of proton and charge translocation (Wikstrom, 1977; Hinkle *et al.,* 1972) by the

enzyme raised questions concerning details of mechanism and control. Are the steps involved the same or different for both phenomena? Do they involve a common pathway? Does proton translocation occur with constant or variable stoichiometry? A constant H^+/e^- stoichiometry suggests a close relationship between proton and charge translocation. A more distant coupling would imply a variable stoichiometry. This variability could be evolutionary in nature, or be a result of 'slippage' as postulated by Petronilli *et al.* (1991). How is respiratory flux influenced by $\Delta\Psi$ and ΔpH? The gradients created by enzyme turnover are a function of enzyme flux (Nicholls *et al.,* 1987). The gradients created are characteristically linear ('ohmic') or non-linear ('nonohmic'). In general, the enzyme responds more 'ohmically' to ΔpH and 'nonohmically' to $\Delta\Psi$ (Nicholls, 1990). The controlling gradient can be varied through the addition of ionophores (small amounts of valinomycin to abolish $\Delta\Psi$, or small amounts of nigericin to abolish ΔpH). These profiles also show an 'ohmic' or 'nonohmic' character. The major gradient across the membrane of mitochondria and COV is $\Delta\Psi$, but, ΔpH is reported to be the predominant controlling element of cytochrome *c* oxidase activity.

Studies of ferrocytochrome *c* kinetics indicate different ionic strength and pH dependencies for the two kinetic phases (Pan *et al.,* 1991). For the solubilized enzyme, a low bulk pH affects cytochrome *c* binding and leads to an increase in both V_{max} and K_m (Cooper, 1990). Studies on the influence of bulk pH on pre-steady state COV (Maison-Peteri and Malmstrom, 1989) have indicated

that at constant external bulk pH, turnover is greatest at acidic internal pH. When the internal pH was kept constant, turnover was greatest at an acidic bulk pH. This study will attempt to examine the influence of external bulk pH on bovine heart COV.

Prokaryotes are found in a large variety of environmental niches. It is common for bacteria to have more than one terminal oxidase. In the Gram-positive bacteria *Bacillus subtilis* two terminal oxidases are known, the quinol aa_3 -600 oxidase and the cytochrome caa_3 oxidase. The caa_3 enzyme of *B. subtilis* is probably a secondary oxidase to the quinol aa_3 -600 enzyme. What role does caa_3 play as a secondary oxidase? Structurally, caa_3 is unique because it has a cytochrome *c* covalently bound to subunit II. What is the function of covalently attached cytochrome *c*? The plasma membrane of Gram-positive bacteria is inside of a cell wall composed of peptidoglycan, formed by polysaccharide chains cross-linked covalently to each other by short peptide chains. It is generally assumed that the peptidoglycan layer of the Gram-positive cell wall is not a major permeability barrier, so that if a *c*-type cytochrome were translocated across the plasma membrane, it would be lost into the environment unless a mechanism for membrane anchoring is present. One method to prevent this loss is by attachment of cytochrome *c* to the cytochrome oxidase molecule. The presence of a covalently bound cytochrome *c* molecule is also associated in thermal resistance in thermophilic bacteria (Buse *et al.,* 1989; deVriij *et al.,* 1989). The cytochrome *c* species in *B. subtilis* are all membrane

bound. The removal of the cytochrome *c* from the membrane would prevent electrons from reaching the caa_3 enzyme. However, electrons from the bc_1 complex may be passed directly to the cytochrome *c* portion of the caa_3 enzyme, bypassing membrane bound cytochrome *c* molecules. Bioenergetically, cytochrome caa_3 may behave as a secondary oxidase to the quinol 600-aa_3 enzyme. Turnover of the caa_3 enzyme are much less than those of the mitochondrial type or other bacterial aa_3 enzymes (Oshida and Fee, 1984; Hill *et al.,* 1993). The presence of multiple oxidases is energetically favourable to the organism.

Bioenergetically cytochrome caa_3 performs an essential function as a secondary terminal electron acceptor. The caa_3 oxidase is unlike the eukaryotic enzyme or other bacterial *aa3* oxidases. In this study I shall attempt to (1) examine the structure of the *caa3* enzyme as it relates to the cytochrome *c* to cytochrome *a* ratio; (2) to use this enzyme with its covalentlly attached cytochrome *c* to study cytochrome oxidase bioenergetics without the problems associated with the use of exogenous cytochrome *c* in reconstituted systems. Respiratory control, proton pumping activity, and the steady state reduction of cytochromes *c* and *a* during steady state respiration of the caa_3 enzyme in proteoliposomes will be examined.

Chapter 2

Materials and Methods

2.1 Materials

The following are the materials used in this study.

Bovine heart cytochrome *c* oxidase

Bacillus subtilis caa_3 cytochrome oxidase

di-oleoyl-sn-glycero-3-phosphatidyl-choline (DOPC)

di-oleoyl-sn-glycero-3-phosphatidyl-ethanolamine (DOPE)

HEPES (4-(2-hydroxyethyl)-1-piperazine-ethane-sulphonic acid)

Sodium cholate

Horse heart cytochrome *c* Type IV (Sigma Co.)

Sodium ascorbate

N,N,N',N'-tetramethyl-*p*-phenylenediamine (TMPD)

Bovine serum albumin #7511 (<0.05% fatty acids)

Free fatty acids: tridecanoic acid, pentadecanoic acid
heptadecanoic acid

Pyranine (8-hydroxy-1,3,6 -pyrene trisulphonate trisodium salt)

Valinomycin, Sigma Co. #0627 (ethanolic solution)

Nigericin, Sigma Co. #7143 (ethanolic solution)

methanol (5%, 100%)

acetic acid (7.5%, 9%)

Coomassie Blue R-250 staining solution

0.5 M Tris-HCL buffer

3,3'-diaminobenzoic acid (DAB)

2.2 Methods

Enzyme and Proteoliposome Preparation

Bovine heart cytochrome *c* oxidase was purified according to Kuboyama *et al.* (1972), with Tween-80 substituting for Emasol in the final stage. The enzyme was stored at -80 °C in 100 mM sodium phosphate buffer containing 0.25% Tween-80. Protein concentration was determined by the biurette method of Gornall *et al.* (1949), and cytochrome *c* oxidase concentration using an extinction coefficient of 27 mM^{-1} cm^{-1} for reduced minus oxidized enzyme at 605-630 nm. *Bacillus subtilis* cytochrome caa_3 oxidase was purified according to Henning *et al.* (1995) and was donated by Dr. Bruce Hill. Proteoliposomes were prepared as described by Wrigglesworth *et al.* (1990) using either asolectin or DOPE/DOPC. Lipids were dissolved in chloroform, and the solvent removed by rotary evaporation under nitrogen. The remaining film of lipid was dispersed by mixing in the appropriate buffer (and in the case of pH gradient experiments, 5 mM pyranine), with the addition of 2% sodium cholate. The sample was vortexed and sonicated on ice under a nitrogen stream for 8 minutes in the pulsed mode at 30% duty cycle (Heat Systems, Ultrasonics W-375 sonicator). Cytochrome *c* oxidase was added to a final concentration of 6 µM aa_3 and sonicated a second time for 30 seconds. For COV without pyranine, the mixture was then centrifuged for 10 minutes at 13 000 rpm for 10 minutes. The lipid solution was dialyzed against 2X100 vol. of buffer, and a further 200 vol. of buffer for 3 days at 4°C. For pyranine containing

COV, excess dye was removed by filtration on a G-25 Sephadex column equilibrated with buffer *B. subtilis* caa_3 COV were prepared as described above.

The proportion of outwardly facing cytochrome *c* oxidase was determined according to Wrigglesworth *et al.* (1987), and was typically >65% for bovine heart COV, and ≥ 55% for the caa_3 COV.

COV turnover and respiratory control were measured polarographically using a Clark type oxygen electrode (Yellow Springs Instruments). The electrode was placed in a thermostatically controlled, magnetically stirred, glass jacketed reaction vessel, with a working volume of 4 mL or 3.6 mL. For standard respiratory control ratio measurements, the medium used was 100 mM HEPES, 64 mM K^+, pH 7.0 equilibrated at 30°C. To this were added 180 μM TMPD, 10 mM ascorbate, and 10 μM cytochrome *c*. For cytochrome *c* kinetic studies turnover of the COV (100 nM aa_3) was measured in 100 mM HEPES, 64 mM K^+, with 10 mM sodium ascorbate at pH values between 6.0 and 7.8, in the controlled, partially controlled, and fully uncontrolled states. Turnover of the enzyme was initiated through the addition of horse heart cytochrome *c*. For partially uncontrolled samples, mixtures were as above except for the addition of 10 nM valinomycin ($\Delta\Psi$ eliminated), 1.4 μM nigericin (ΔpH eliminated) or both ionophores in the uncontrolled state. In the case of caa_3 COV, no cytochrome *c* was added unless otherwise stated. The respiratory control ratios of caa_3 COV were examined in three different respiratory media of either low or moderately high ionic strength. Respiratory control ratios were measured at a low ionic strength, (5 mM HEPES, 3mM K^+, pH 7.0) in the presence of high ascorbate concentrations (40 mM), or at low ascorbate

concentration (5 mM) with 200 μM TMPD and 40 μM cytochrome *c* at both low and high (100 mM HEPES, 64 mM K^+) ionic strength. Turnover was initiated by the addition of 10 nM COV. The ionophores valinomycin and nigericin were added in ethanolic solutions.

Proton Pumping

Proton pumping was assayed using a Radiometer Copenhagen GK2321C pH electrode attached to a Radiometer Copenhagen PHM64 Research pH meter. Changes in pH were recorded on a Radiometer Copenhagen REC61 Servograph connected to the pH meter via a REA100 interface. The pH electrode was placed in a sealed 4.4 mL reaction chamber, with a syringe access port. The vessel was thermostatically controlled and magnetically stirred. The reaction mixture contained 64 mM K^+, pH 7.0, DOPE/DOPC COV with 0.2 μM outwardly facing aa_3 or 0.5 μM caa_3, 400 nM valinomycin, and/or 10 nM FCCP, at 30°C. Proton pulses were initiated by the addition of 30 nmol ferrocytochrome *c*. The pH of the ferrocytochrome *c* was adjusted to pH 7.0 just prior to injection into the vessel. After equilibrium was reached the pH was readjusted to pH 7.0. A total of four ferrocytochrome *c* pulses were recorded. In the case of the bovine heart COV, following the last ferrocytochrome *c* pulse, 10 mM ascorbate and 150 μM TMPD were added . After anaerobiosis, the pH was readjusted to pH 7.0. The COV were then pulsed four times with 50 μL of 64 mM K_2SO_4. Nigericin was then added and the COV were pulsed twice more. Electrode response was calibrated with aliquots of standard 0.01N H_2SO_4 and 0.02N KOH solutions.

Bovine serum albumin (150 μM) was added to COV and incubated overnight at 4^0C. They were then passed through a Sepharose 6B column equilibrated 64 mM K_2SO_4, pH 7.0 at 25°C, to separate COV from BSA. H^+/e^- ratios were measured as described above. Free fatty acids were added to BSA-treated COV by incubating the latter with 10 mM ascorbate, 10 μM cytochrome *c*, and appropriate quantities of free fatty acids for 1 h at 4^0C. They were then passed through a Sepharose 6B column equilibrated 64 mM K_2SO_4, pH 7.0 at 25°C. H^+/e^- ratios were measured as described above.

SDS-Polyacrylamide gel electrophoresis

Polyacrylamide gel electrophoresis analysis of the caa_3 enzyme was done as described in Kadenbach *et al.* (1982). Electrophoresis was performed at 80 mV for 17 minutes and 200 mV for 83 minutes. Gels were stained overnight with a 45.5% methanol, 9.5% glacial acetic acid, and 0.006% Coomassie Blue R-250 staining solution. Destaining was done with a 5% methanol, 7% acetic acid destaining solution. Haem stain analysis of the caa_3 enzyme was done as described by DiSpirito (1990). The gel was first fixed in 7% acetic acid for 15 minutes, followed by incubation in 0.5 M Tris-HCL, pH 7.0 for 15 minutes. Incubation in 0.5 M Tris-HCL was repeated 4 to 5 times, until the solution pH reached 7.0. Staining of the bands was achieved by incubation in 0.5 M Tris-HCL, 1.4 mM 3,3' -diaminobenzidine, pH 7.0 for 30 minutes at room temperature. The DAB-Tris-HCL buffer was decanted and the gel incubated in a solution of 50 mM citrate, 2,8 mM DAB, pH 4.0. The reaction is started by adding 40

mL of 30% H_2O_2 per mL of the citrate-DAB solution. The gel was then incubated overnight in the dark at 4°C. Labeled proteins appeared as a reddish brown band.

ΔpH Formation and Bulk pH

Pyranine containing bovine heart COV were prepared as described above in 100 mM HEPES, 64 mM K^+, pH 7.0. COV were passed down a G-25 Sephadex column to remove extraneous pyranine. Fluorescence changes were monitored with a Perkin Elmer LS50 Spectrometer, with excitation at 470 nm, and emission at 514 nm, with 3 mL COV samples (90 nM aa_3) at varying pH ranging between 6.2 and 7.8 at 30°C. Turnover was initiated with cytochrome *c* (5 μM) and sodium ascorbate (10 mM). Upon reaching steady state, valinomycin was added (10 nM) to eliminate the membrane potential $\Delta\Psi$. At the second steady state, nigericin (1.4 μM) was added to produce uncontrolled turnover. The sample was removed and its pH was measured. Upon the return of the sample to the cuvette holder, it was titrated with 2N KOH or 1N H_2SO_4. The pH of the sample was measured after each successive addition of base or acid.

Steady State Reduction

Bovine heart or *B. subtilis* caa_3 COV were prepared as described above in 100 mM HEPES, 64 mM K^+, pH 7.0. Cytochrome *c* and *a* redox levels were monitored at varying ascorbate concentrations in the controlled state, partially uncontrolled or the fully uncontrolled states spectrophotometrically with a Beckman DU-7400 diode array spectrometer at 30°C. In the controlled state the bovine heart COV samples contained 600 nM aa_3 and 6.25 μM horse heart cytochrome *c* in 100 mM HEPES, 64 mM K^+ at varying pH values ranging between 6.2 and 7.8. For partially uncontrolled samples,

cuvette mixtures were as above except for the addition of 10 nM valinomycin ($\Delta\Psi$ eliminated), 1.4 μM nigericin (ΔpH eliminated) or both ionophores in the uncontrolled state. At each pH and energized state, enzyme turnover was initiated through the addition of increasing concentration of ascorbate. Steady state reduction was monitored over an increasing flux titration. Full reduction was achieved through the addition of solid dithionite crystals. For *B. subtilis* caa_3 COV, each 800 μL sample contained 0.35 μM caa_3 in 100 mM HEPES, 64 mM K^+, pH 7.0. Enzyme turnover was initiated by the addition of ascorbate. Valinomycin (15 nM) was added to eliminate $\Delta\Psi$ upon reaching a steady state. Similarly upon reaching the $\Delta\Psi$ free steady state, nigericin (1.4 μM) was added for an uncontrolled state. Full reduction was achieved through the addition of solid dithionite crystals.

Chapter 3

Bovine Heart Cytochrome c Oxidase in Proteoliposomes: Proton Pumping and Bulk pH Effects

3.1 Proton Translocation

Proton pumping activity in proteoliposomes can be monitored spectrophotometrically through the use of pH probes, or polarographically, using a pH electrode. Experiments here involved the latter method, in which the pH of the external medium was monitored in a sealed chamber. The pH of sample mixtures was maintained at pH ≈ 7.0 prior to the addition of ferrocytochrome *c*. The pH of the ferrocytochrome *c* was also kept at pH ≈7.0. Turnover was initiated through the addition of ferrocytochrome *c*. Typical traces are represented in Figure 3.1. After the initial proton pulse, the pH of the mixture was restored to pH 7.0 through the addition acid or base. In this way successive proton traces were observed. The addition of ferrocytochrome *c* induced an immediate decrease in the pH of the medium, indicating the release of protons. The protons are directly translocated across the membrane due to the pumping activity of the oxidase. After enzyme turnover has ceased, there is a gradual alkalinization of the medium, as protons move back across the membrane due to the difference in proton gradient. The number of protons moving back across the membrane is equal to the sum of the number of protons translocated and those consumed in the reduction of oxygen. The buffering capacity of the system was taken into account by measuring acid signal due to buffering outside the COV, and dividing it by the total acid signal. The H^+/e^- stoichiometry was obtained by comparing the number of protons initially translocated to the total number of protons consumed in oxygen reduction and multiplying by this buffering capacity ratio. The four electrons donated by ferrocytochrome *c* induce the consumption of 4 protons in oxygen reduction. The H^+/e^- stoichiometry observed here was between 0.55 to 0.8 indicating that each of the four electrons donated by ferrocytochrome *c* is associated with the translocation of 0.55 to 0.80 of a proton. Successive proton pulses are characterized by a decrease in the H^+/e^- stoichiometry. Oxygen induced proton pulses were also

Figure 3.1: Horse heart cytochrome *c* proton pulses of bovine heart COV. Proton pulses were measured using pH electrode. The pH electrode was placed in a sealed 4.4 mL reaction chamber, 64 mM K_2SO_4, DOPC/DOPE COV 0.2 μM aa_3, 400 nM valinomycin, 10 nM FCCP, pH 7.0 at 30 °C. Reduced horse heart cytochrome *c* (30 nM) (▲) was added through a syringe port to intiate a proton pulse. After euilibrium was reached, the pH was readjusted through the additon of H_2SO_4 (Δ).

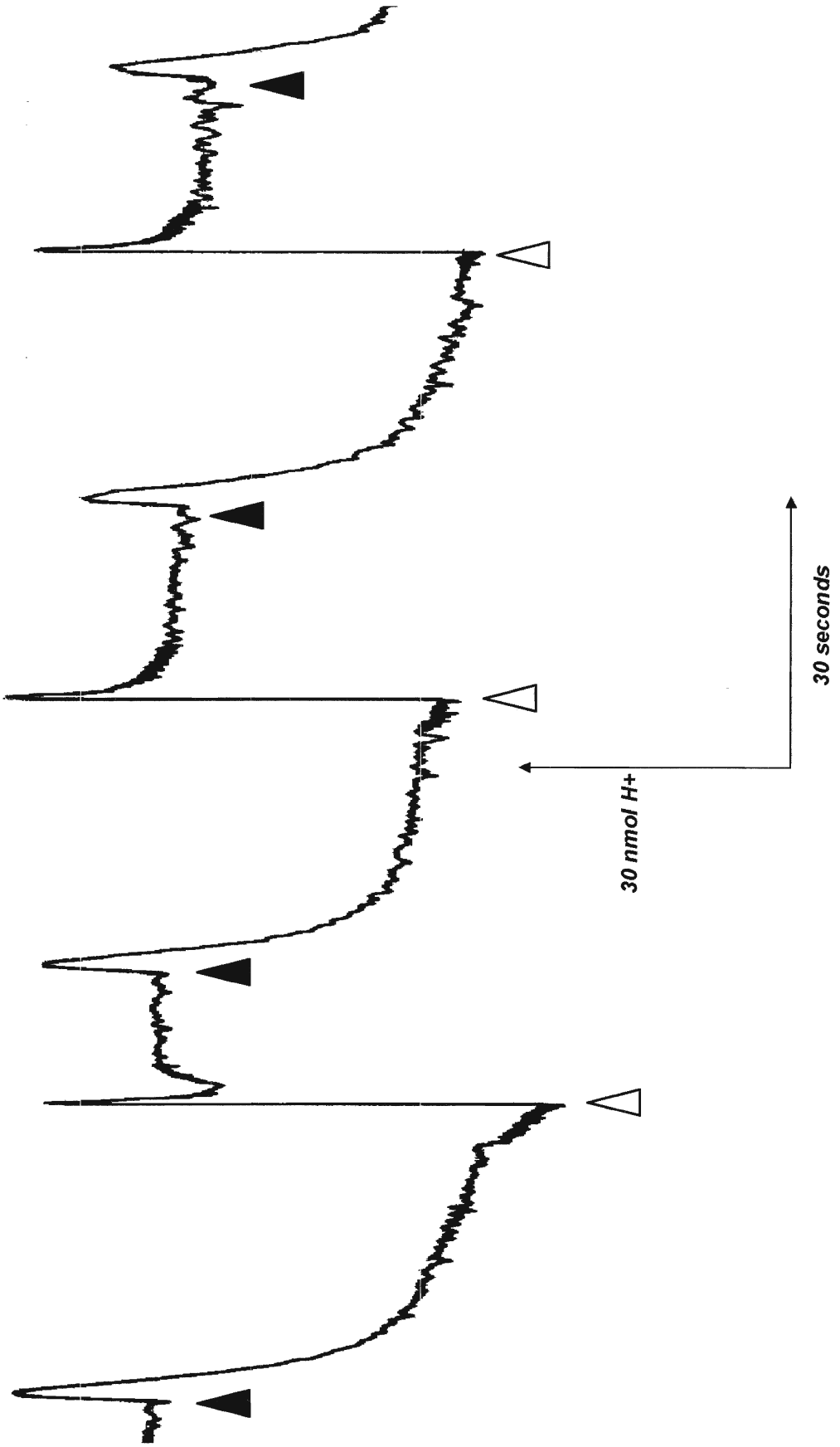
30 nmol H+
30 seconds

Figure 3.2: Oxygen induced proton pulses of bovine heart COV. Conditions and methods are as in Figure 3.1. After the final cytochrome *c* pulse, 10 mM ascorbate and 150 μM TMPD was added. After anaerobiosis, the pH was readjusted to pH 7.0 and the COV were pulsed four times with 50 μL K_2SO_4 (▲).

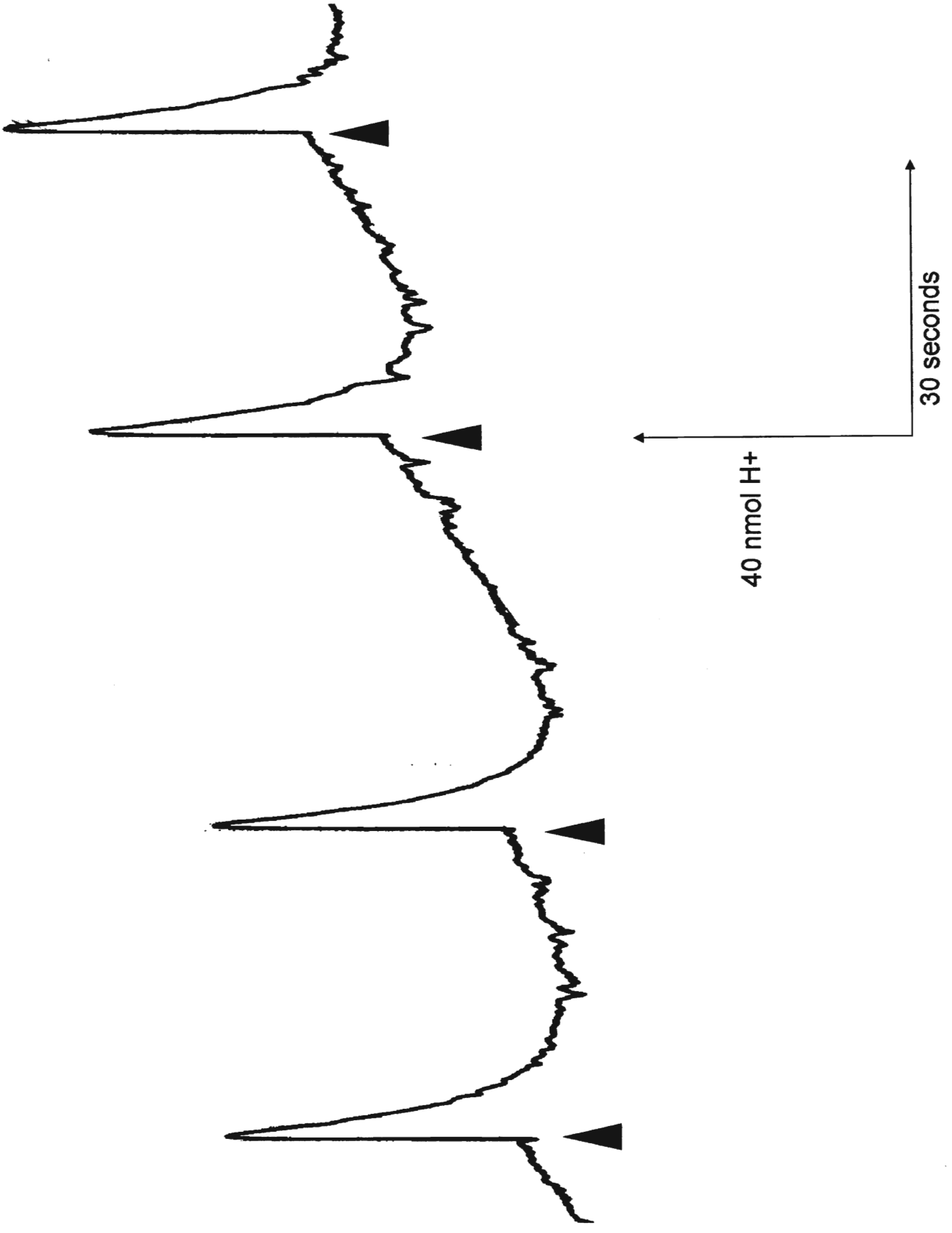
40 nmol H+
30 seconds

performed on the same COV mixture (Figure 3.2). After the final cytochrome *c* pulse, 10 mM ascorbate and 150 μM TMPD was added. After anaerobiosis, the pH of the sample was adjusted to pH 7.0, and four oxygen pulses were performed by the addition of 50 μL airrated aliquots of 64 mM K_2SO_4. The addition of oxygen induced the turnover of the enzyme and the subsequent translocation of protons across the membrane. The proton signal observed is composed of two sources of protons, those translocated during enzyme turnover, and those released upon the oxidation of ascorbate. The proton ratio between these two components is approximately 1:1. The alkalinization of the medium is due to the re-equilibration of protons inside the COV. The number of protons moving back across the membrane is equal to the number protons translocated plus those consumed in water formation. A H^+/e^- stoichiometry is obtained by comparing the oxygen signal, to that which occurs upon alkalinization. Fifty percent of the signal represents those protons released upon the oxidation of ascorbate. The remainder of signal are those protons translocated by the enzyme. This value, as in the ferrocytochrome *c* pulses, may be compared to the alkalinization signal which represents those protons consumed in water formation, which is constant. The H^+/e^- stoichiometry for the oxygen pulses range between 0.73 and 1.0. As in the ferrocytochrome *c* pulses, the H^+/e^- stoichiometry decreases with pulse number.

Biomembranes are known to contain free fatty acids (Gutknecht, 1988). Biochemically, FFA have been shown to act as electrophoretic protonophores, and catalyze cation exchange (Gutknecht, 1988; Wrigglesworth *et al.*, 1990). FFA efects on liposomes (Sharpe *et al.*, 1991, 1994) have shown them to be weak acid uncouplers. The work presented here, is part of a larger study which examined the influence of BSA and FFA on proteoliposomes (Sharpe *et al.*, 1996). Proton pumping activity was examined under the influence of BSA and FFA. BSA treatment of COV involved the incubation with 150 μM BSA for 16 h at 4°C. The COV mixture was then passed down a Sepharose 6B column to remove the BSA. The COV samples were then pulsed 4

times with cytochrome *c* and a further 4 times with 50 μL of airated 64 mM K_2SO_4. Typical ferrocytochrome *c* traces are observed if Figure 3.3, while Figure 3.4 shows typical oxygen induced proton pulses. Restoration of proton pumping activity was attempted through the addition of a mixture of FFA to BSA treated COV. The FFA mixture consisted of 100 μM pentadecanoic acid, 50 μM tridecanoic acid, and 50 μM heptadecanoic acid. Typical FFA treated cytochrome *c* and oxygen pulses are presented in Figure 3.5 and 3.6. Calculated H^+/e^- stoichiometries are presented in Table 3.1. It is observed that there is a decrease in the H^+/e^- stoichiometry upon incubation of COV with BSA. The H^+/e^- stoichiometry is then partially restored upon treatment of the BSA COV with the FFA mixture.

Figure 3.3: Horse heart cytochrome *c* proton pulses of bovine serum albumin treated bovine heart COV. Conditions are as in Figure 3.1. Reduced horse heart cytochrome *c* (30 nM) (▲) was added through a syringe port to intiate a proton pulse. After euilibrium was reached, the pH was readjusted through the additon of H_2SO_4 (Δ).

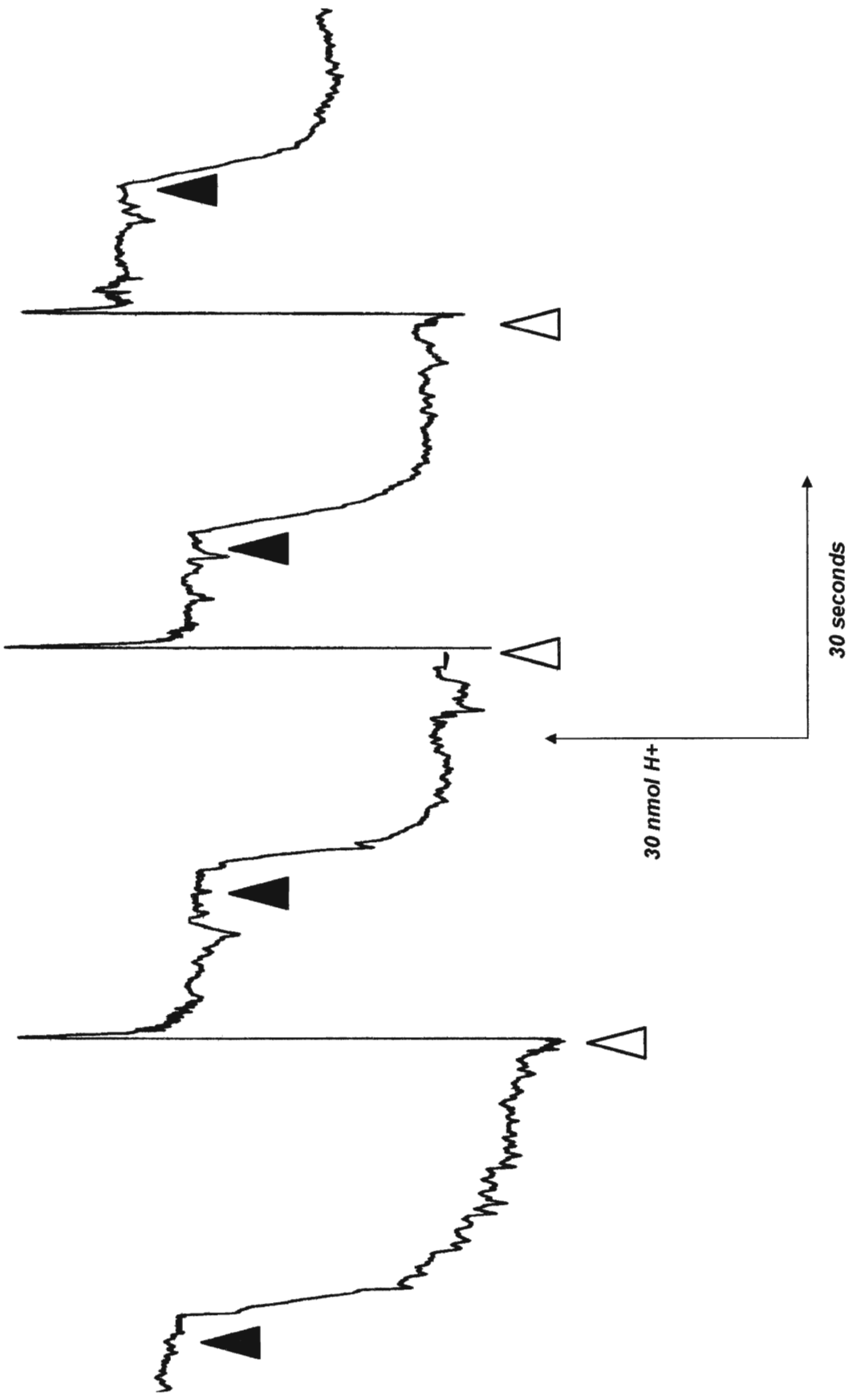
30 nmol H+
30 seconds

Figure 3.4: Oxygen induced proton pulses of bovine serum albumin treated bovine heart COV. Conditions are as in Figure 3.1. After the final cytochrome *c* pulse, 10 mM ascorbate and 150 μM TMPD was added. After anaerobiosis, the pH was readjusted to pH 7.0 and the COV were pulsed four times with 50 μL K_2SO_4 (▲).

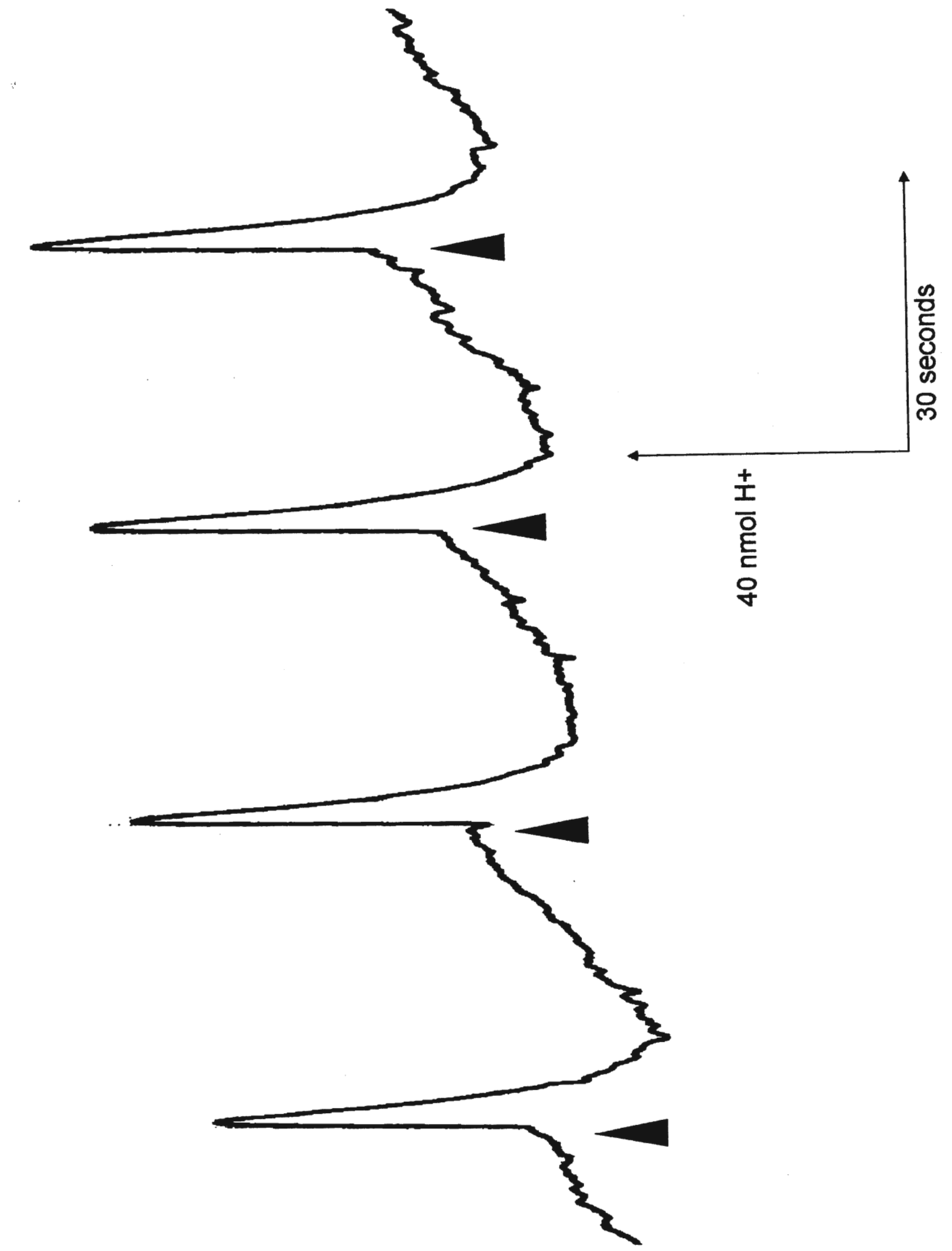
40 nmol H+
30 seconds

Figure 3.5: Horse heart cytochrome *c* proton pulses of free fatty acid treated BSA incubated bovine heart COV. Conditions are as in Figure 3.1. Reduced horse heart cytochrome *c* (30 nM) (▲) was added through a syringe port to initiate a proton pulse. After equilibrium was reached, the pH was readjusted through the addition of H_2SO_4 (Δ).

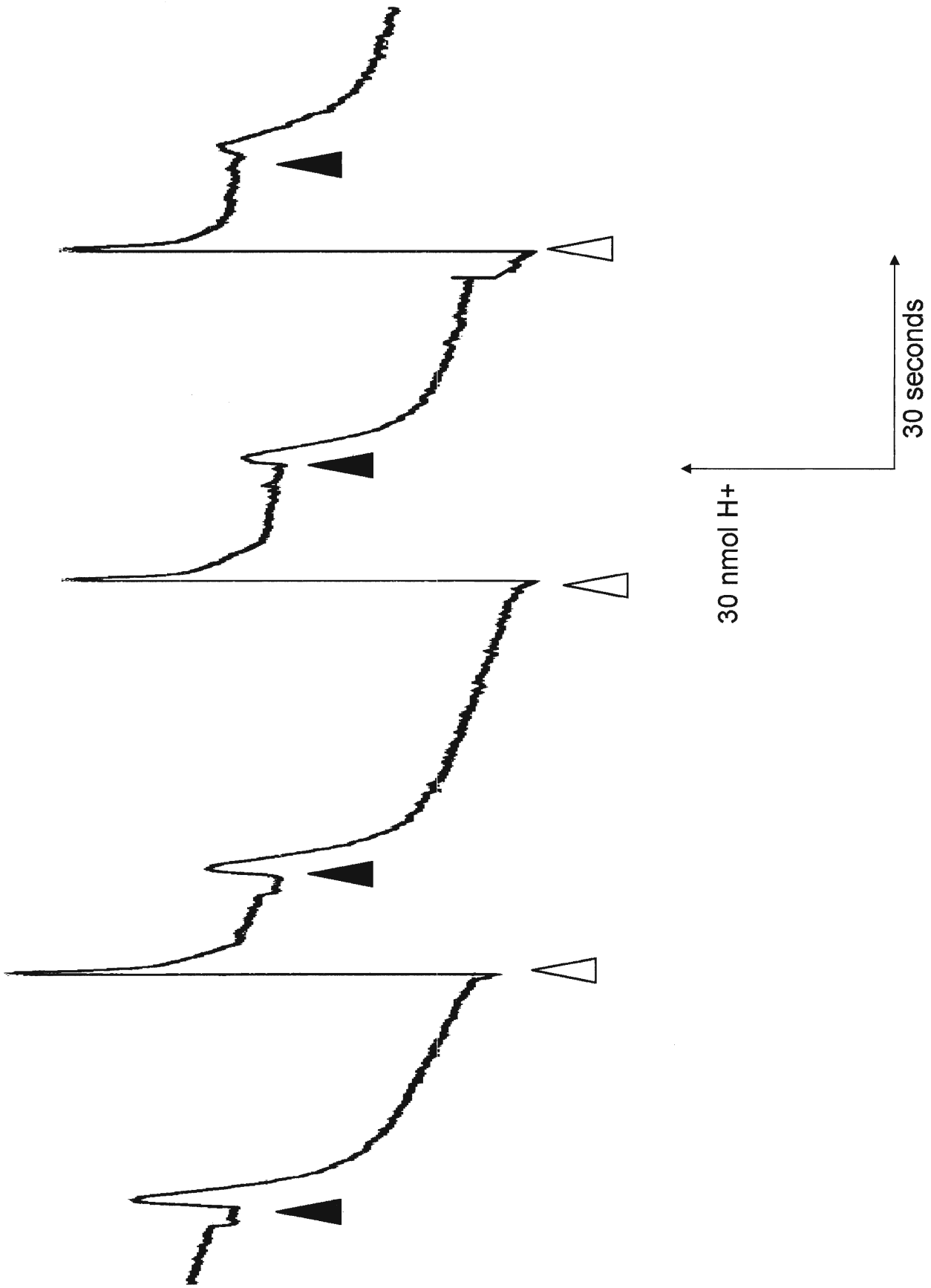
30 nmol H+
30 seconds

Figure 3.6: Oxygen induced proton pulses of free fatty acid treated BSA incubated bovine heart COV. Conditions are as in Figure 3.1. After the final cytochrome *c* pulse, 10 mM ascorbate and 150 μM TMPD was added. After anaerobiosis, the pH was readjusted to pH 7.0 and the COV were pulsed four times with 50 μL K_2SO_4 (▲).

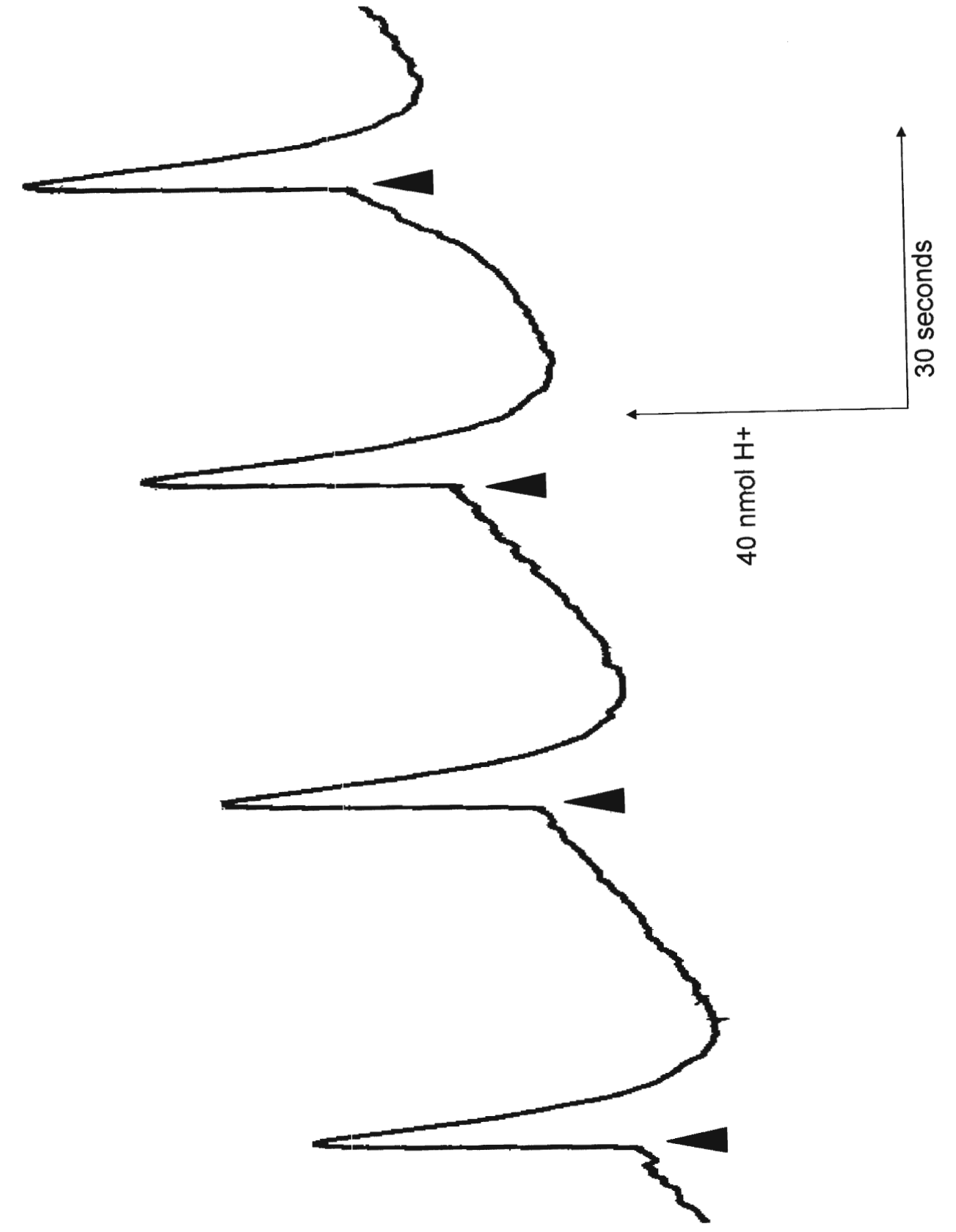
40 nmol H+
30 seconds

Table 3.1: Calculated H^+/e^- stoichiometry for bovine heart COV. For ferrocytochrome *c* pulses, pulse values were determined by dividing the initial proton pulse signal (translocated protons) by the alkalinization signal resulting solely from protons consumed in water formation (chemical protons). Oxygen pulses were determined in a similar manner, except that 50 % of the initial proton pulse signal is due to oxidation of ascorbate, a process which releases protons. Buffering effects were determined by the ratio of the buffering capability outside the COV to the total buffering capability of the system. H^+/e^- stoichiometries were determined by multiplying the observed pulse by the buffering ratio.

	H^+/e^- (ferrocytochrome c)				H^+/e^- (oxygen)			
Pulse #	***1***	***2***	***3***	***4***	***1***	***2***	***3***	***4***
Control								
pulse	1.1	0.95	0.80	0.75	1.37	1.11	1.06	1.0
H^+/e^- *	0.80	0.70	0.58	0.55	1.0	0.81	0.77	0.73
BSA								
pulse	0	0	0	0	0.66	0.64	0.56	0.56
H^+/e^- †	0	0	0	0	0.45	0.44	0.39	0.39
FFA								
pulse	1.0	0.85	0.67	0.49	1.04	0.93	0.85	0.63
H^+/e^- ✣	0.65	0.56	0.44	0.32	0.68	0.61	0.55	0.41

* H^+/e^- =(buffering(out)/buffering(total) = 0.73) * pulse
† H^+/e^- =(buffering(out)/buffering(total) = 0.69) * pulse
✣ H^+/e^- =(buffering(out)/buffering(total) = 0.65) * pulse

3.2 Effect of Bulk pH on ΔpH Formation

Control of turnover is not shared equally between ΔpH and ΔΨ. Although ΔΨ is responsible for approximately 90% of $\Delta\mu H+$ in terms of mV, most of the chemiosmotic control of cytochrome *c* oxidase activity is due to the remaining 10% mV resulting from the ΔpH contribution. Are ΔpH effects on cytochrome *c* oxidase the result of ΔpH or to changes of pH inside the COV? This problem can be studied by examining the effects of bulk pH on enzyme activity in COV. This section discusses results obtained in examining the effect of bulk pH on ΔpH formation in bovine heart COV.

Experimental procedures involved the use of a trapped pH probe inside the proteoliposome. Bovine heart COV were prepared as described in Chapter 2, in the presence of the pH probe pyranine. When in its protonated form, pyranine shows less fluorescent intensity than in its non-protonated form. During enzyme turnover, protons are being consumed in the formation of water, and being translocated across the membrane from inside the vesicle. Fluorescent intensity of pyranine increases due to the alkalinization inside the COV. This increase in fluorescent intensity indicates the formation of ΔpH. Figure 3.7 is a representative fluorescent trace. Fluorescent measurements were monitored using a Perkin Elmer LS50 Spectrometer, excitation 470 nm, emission 514 nm, with 3 mL COV samples (90 nM *aa3*). Turnover was initiated by the addition of horse heart cytochrome *c* (5 μM) and sodium ascorbate (10 mM). Upon the addition of sodium ascorbate, there is an increase in fluorescent intensity, as protons are being consumed. The addition of the electrophoretic ionophore valinomycin (10 nM) results in a decrease in enzyme control by ΔΨ by allowing for the movement of K^+ ions across the membrane. This change in the electrochemical gradient is compensated for by the movement of protons across the membrane. At this point, enzyme turnover is controlled solely by ΔpH. This is shown by an increase in the

fluorescent intensity upon the addition of valinomycin. The addition of nigericin collapses the ΔpH, and enzyme turnover is uncontrolled. Protons are now free to move back across the membrane. This is indicated by a decrease in fluorescent intensity. Fluorescent intensity is calibrated to ΔpH by observing change in pH of the solution upon the addition of acid or base to the change in fluorescent intensity. In this way, a change in fluorescent intensity can be directly compared to ΔpH formation. This procedure was used for pH ranges between 6.2 and 7.8. Figure 3.8 shows the steady state ΔpH measurements of bovine heart COV at varying external pH. ΔpH formation is greatest at an acidic pH, ranging between 0.40 and 0.50. At an alkaline bulk pH, ΔpH formation decreases between 40% to 50% upon reaching pH 7.8. This represents only a small change in ΔpH. Nicholls *et al.* (1990) showed that a ΔpH of 0.1 unit can diminish enzyme turnover by ≈ 10%. The difference in ΔpH formation between the alkaline and acidic pH, suggests only a possible 15% to 25% change in enzyme turnover over two magnitudes of proton concentration. This indicates that there is very little change in ΔpH formation with change in the bulk pH.

Figure 3.7: Representative fluorescent measurement trace of pyranine trapped bovine heart COV. Fluorescent measurements were monitored using a Perkin Elmer LS50 Spectrometer, excitation 470 nm, emission 514 nm, of 3 mL COV samples (90 nM *aa3*). Turnover was initiated by the addition of horse heart cytochrome *c* (5 μM) and sodium ascorbate (10 mM). Fluorescent intensity is calibrated to ΔpH by observing change in pH of the solution upon the addition of acid or base to the change in fluorescent intensity.

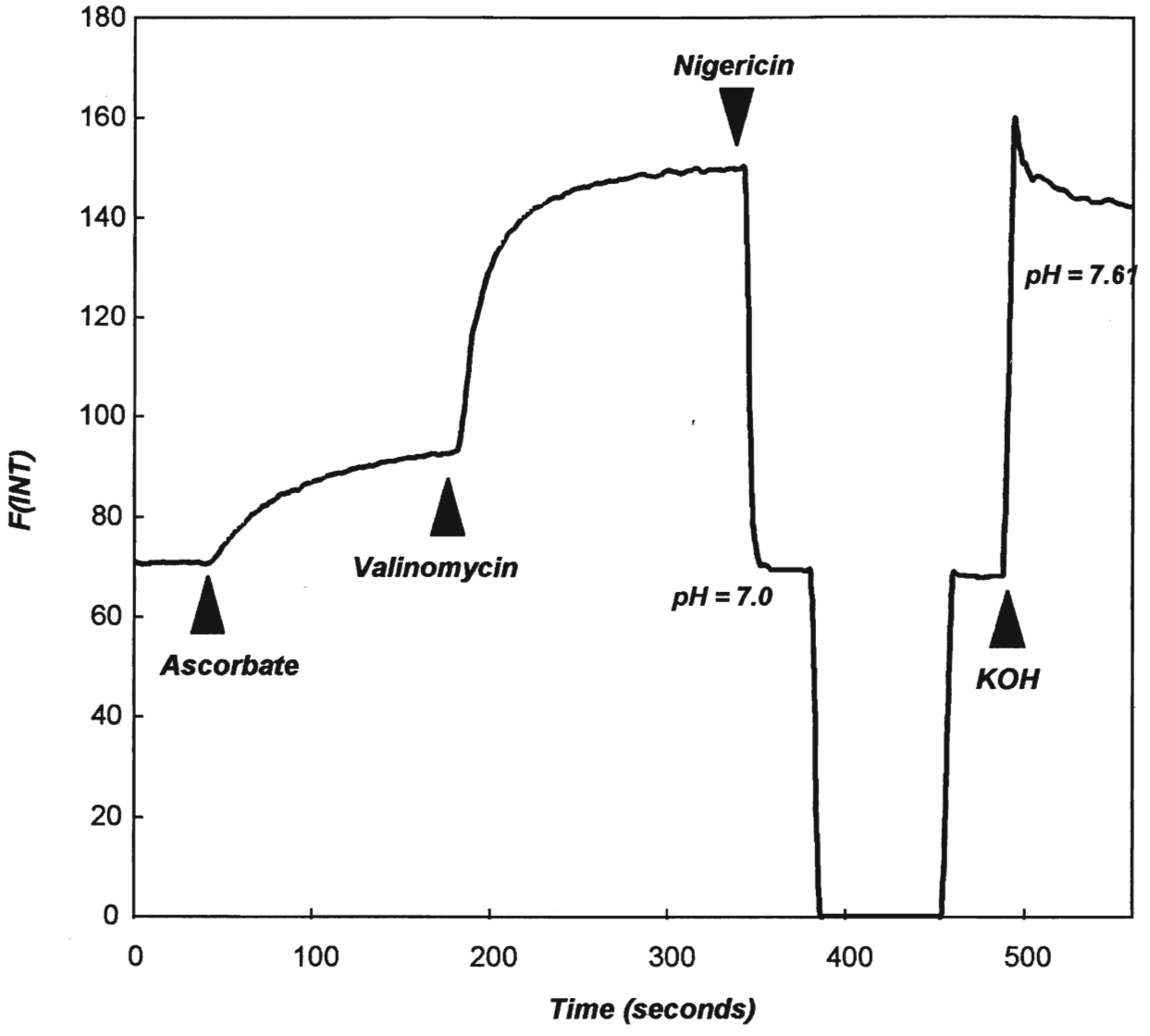
180
160
140
120
100
80
60
40
20
0
F(INT)
0
100
200
300
400
500
Time (seconds)
Nigericin
Valinomycin
Ascorbate
pH = 7.0
KOH
pH = 7.61

Figure 3.8: Measured steady state ΔpH formation in bovine heart COV versus bulk pH. ΔpH formation is greatest at an acidic pH, ranging between 0.40 and 0.50. At an alkaline pH, ΔpH formation decreases between 40% to 50% upon reaching pH 7.8. Data points are the average of three experiments.

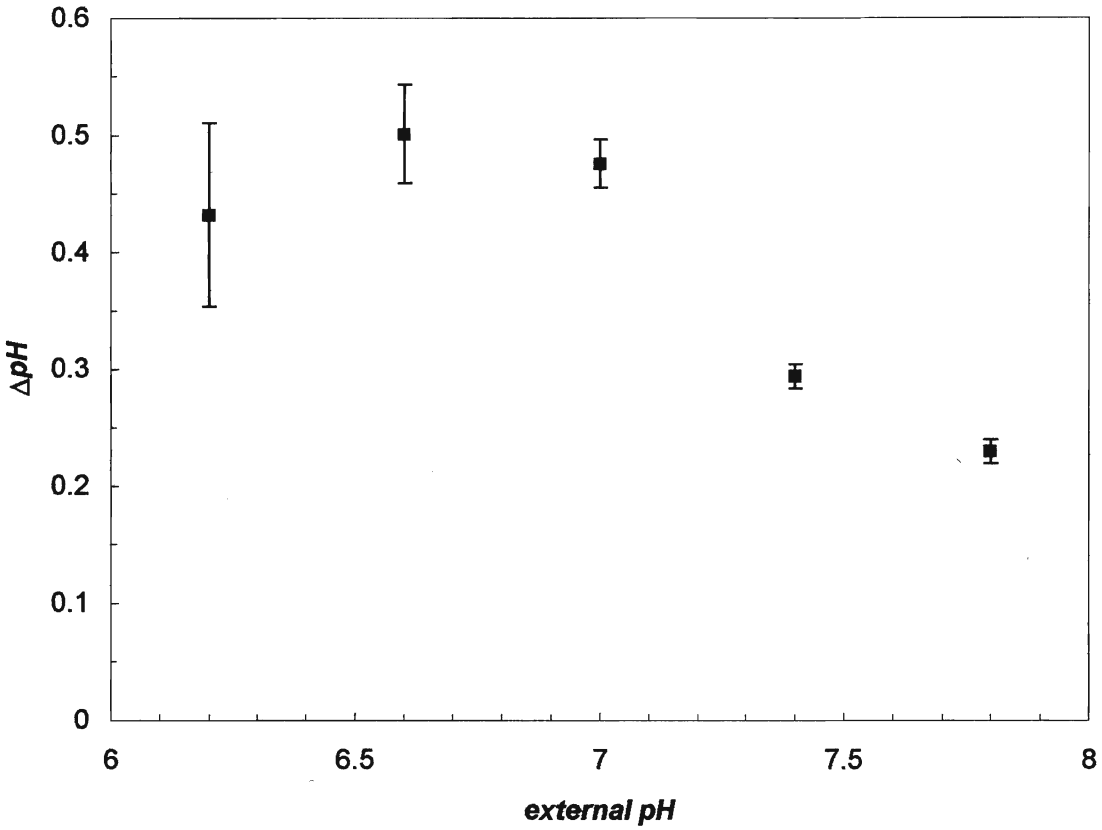
0.6
0.5
0.4
0.3
0.2
0.1
0
ΔpH
6
6.5
7
7.5
8
external pH

3.3 Effect of Bulk pH on the Kinetics of Vesicular Cytochrome c oxidase

Monoclonal antibody studies have indicated that subunit II provides the major contribution to the cytochrome *c* binding site (Taha and Ferguson-Miller, 1992). The cytochrome *c* - cytochrome *c* oxidase complex occurs through electrostatic attraction between carboxylic acid residues on the oxidase and lysine residues on the surface of cytochrome *c* (Bisson and Montecucco, 1982). The 3-dimensional structure of cytochrome *c* oxidase of *P. denitrificans* indicates that the globular domain formed by subunit II and the flat periplasmic surface of subunit I form the most probable cytochrome *c* binding region. This region also contains a portion of subunit III containing up to 10 acidic amino acid residues. Acidic amino acid residue Asp-158 is strictly conserved, and thought to be involved in direct binding of cytochrome *c* to the enzyme. Other acidic residues involved in cytochrome *c* binding include Asp-112, Glu-114, and Glu-98. This region of cytochrome *c* binding is in close proximity to the Cu_A site, the possible entry point of electrons from cytochrome *c*.

The influence of bulk pH on the biphasic kinetics of cytochrome *c* oxidase activity in COV was examined under controlled, partially controlled, and fully uncontrolled states. Turnover was monitored polarographically using a standard oxygen electrode apparatus over a range of cytochrome *c* concentrations at varying bulk pH. A typical polarographic trace is presented in Figure 3.9. V_{max} and K_m values for cytochrome *c* oxidase were determined through equation (2) using the spread sheet Delta Graph Professional version 2.

$$V = \frac{Vmax * [S]}{K_m + [S]} + \frac{Vmax^* [S]}{K_m + [S]} \qquad (2)$$

Figure 3.9: Polarographic trace of cytochrome *c* titration of bovine heart COV in the controlled state at pH 7.0. COV were in 100 mM HEPES, 64 mM K^+, pH 7.0 at 30°C. COV (100 nM aa_3) were added to medium containing 10 mM ascorbate. Turnover was initiated by the addition of cytochrome *c*. Cytochrome *c* concentrations ranged between 10 nM and 40 μM.

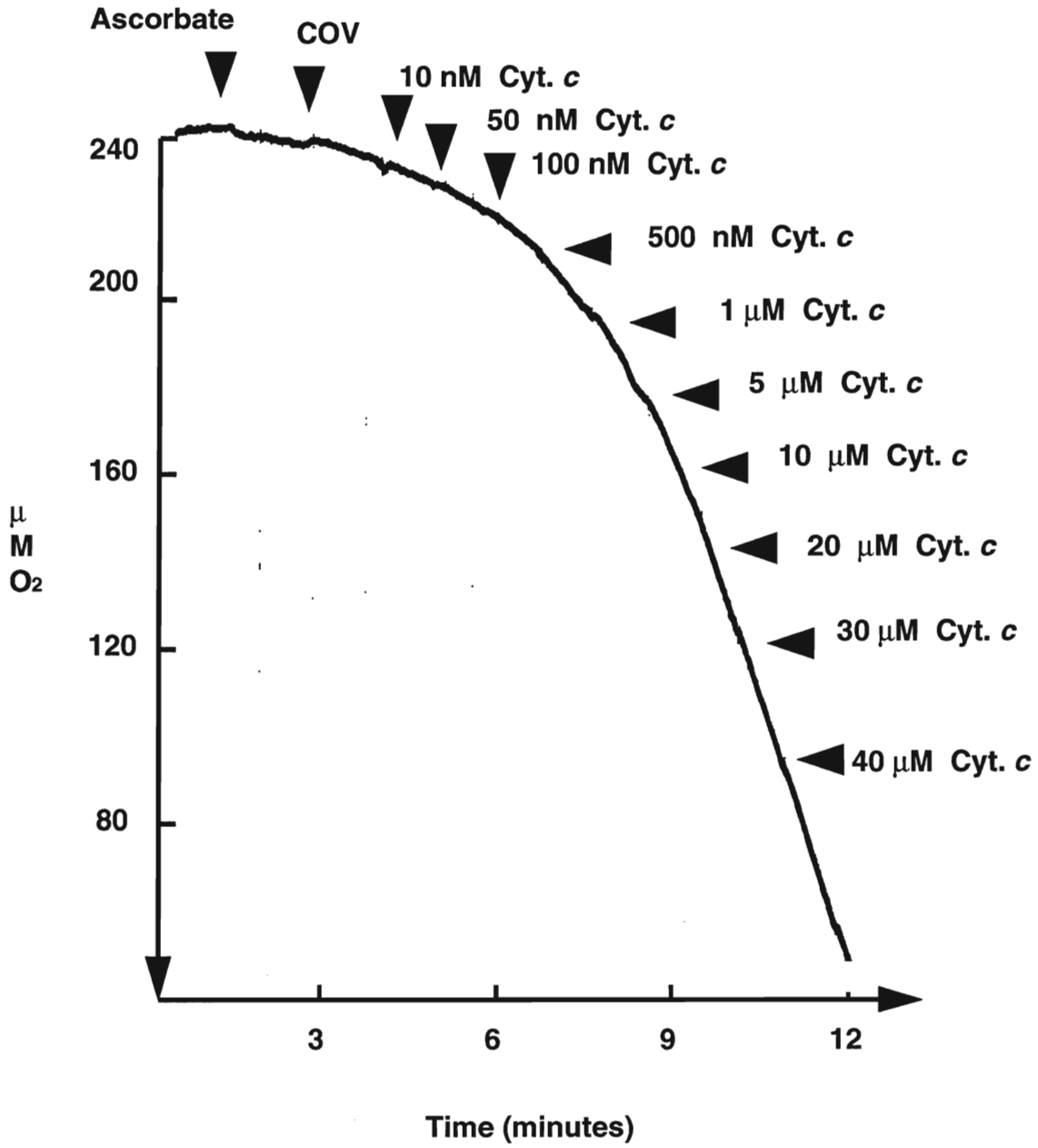
Ascorbate
COV
10 nM Cyt. c
50 nM Cyt. c
100 nM Cyt. c
500 nM Cyt. c
1 μM Cyt. c
5 μM Cyt. c
10 μM Cyt. c
20 μM Cyt. c
30 μM Cyt. c
40 μM Cyt. c
240
200
160
120
80
μ
M
O2
3
6
9
12
Time (minutes)

Values for V_{max} and K_m were separated into its four component parameter: V_{max} (high affinity), V_{max} (low affinity), K_m (high affinity), K_m (low affinity). Table 3.2 summarizes the calculated values.

Figure 3.10A compares the V_{max} values at the high affinity binding site as a function of bulk pH. Neither under controlled conditions (both $\Delta\Psi$ and ΔpH) nor in the presence of ionophores does turnover of the enzyme shows any significant change with change in bulk pH. A more marked effect of bulk pH on enzyme turnover occurs when V_{max} is measured at the low affinity binding site (Figure 3.10B). For the controlled and partially controlled states, there is a slight increase in enzyme turnover with a decrease in bulk pH. The greatest change in enzyme turnover occurred in the fully uncontrolled state, where turnover increased dramatically as the pH decreased. From the data in Figure 3.10B, the respiratory control ratio (RCR) of the COV can be obtained. Figure 3.11 shows such RCR for the COV at varying bulk pH. RCR values increase with bulk pH, reaching a maximum of approximately 2.5 at pH 7.0. RCR values then declined with increasing alkalinity.

The biphasic behaviour reflects K_m values of ≤ 0.1 μM (high affinity) and ≥ 1 μM (low affinity). Figure 3.12A shows the determined K_m values for the high affinity binding site. For the controlled, partially controlled, and fully uncontrolled states, there is no significant change in K_m over the bulk pH range. The K_m (low affinity) values are however dependent both on pH and on the energized state of the COV (Figure 3.12B). There is an increase in the measured K_m as control is released. Significant increases in K_m are seen as pH declines.

Table 3.2: Calculated V_{max} and K_m values of cytochrome *c* oxidase at the high affinity and low affinity binding sites at varying external bulk pH. Values were calculated using a modified Michaelis-Menten equation (see text) and the spreadsheet Delta Graph Pro. Turnover values expressed in e^-/sec/aa_3 and K_m in μM.

Bulk pH	Control				+val				+nig				val+nig			
	V_{max} (hi)	V_{max} (lo)	K_m (hi)	K_m (lo)	V_{max} (hi)	V_{max} (lo)	K_m (hi)	K_m (lo)	V_{max} (hi)	V_{max} (lo)	K_m (hi)	K_m (lo)	V_{max} (hi)	V_{max} (lo)	K_m (hi)	K_m (lo)
6.0	23	206	0.012	5.19	52	118	0.047	4.33	12	215	0.018	3.54	30	460	0.007	2.80
6.4	43	153	0.048	4.35	55	83	0.027	2.10	25	163	0.012	2.69	33	401	0.004	2.40
6.8	59	89	0.170	3.69	42	74	0.031	2.50	27	147	0.008	2.53	26	379	0.006	2.20
7.0	91	48	0.120	2.70	51	63	0.020	3.70	20	149	0.120	2.17	36	331	0.017	2.00
7.4	31	67	0.063	2.30	30	41	0.005	1.01	10	109	0.028	1.32	38	213	0.009	1.30
7.8	35	34	0.012	1.74	31	33	0.080	1.27	30	46	0.010	1.10	42	109	0.009	0.95

Figure 3.10: Cytochrome *c* oxidase turnover at the high and low affinity cytochrome *c* binding sites at varying bulk pH (see text for conditions). A. High affinity binding site. B. Low affinity binding site. (◆) control conditions; (■), +val (no $\Delta\Psi$); (Δ) +nigericin (no ΔpH); (O) uncontrolled (no $\Delta\Psi$ or ΔpH). Data points are obtained from a single experiment.

A.

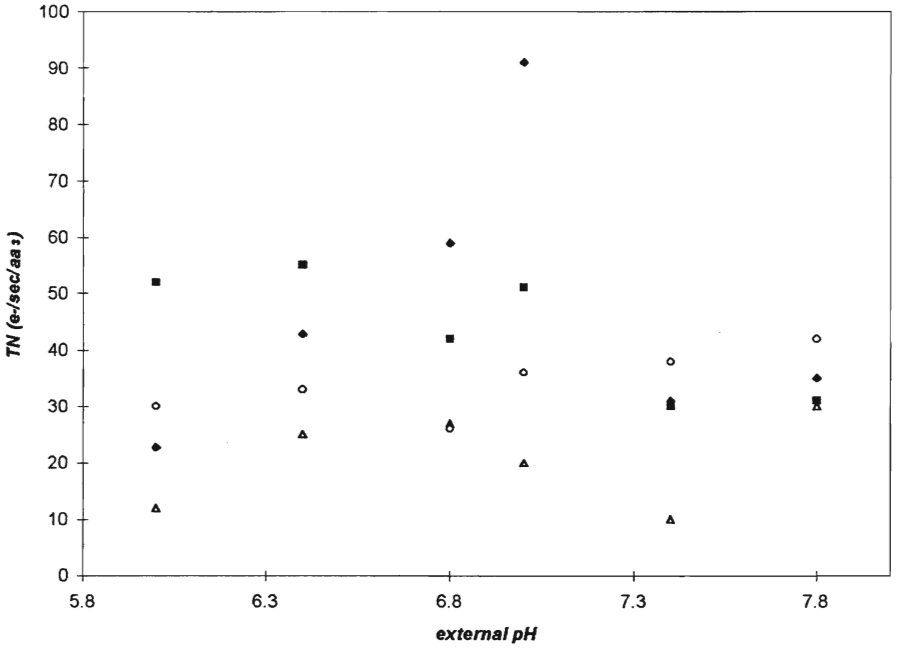
100
90
80
70
60
50
40
30
20
10
0
TN (e-/sec/aa2)
5.8
6.3
6.8
7.3
7.8
external pH

B.

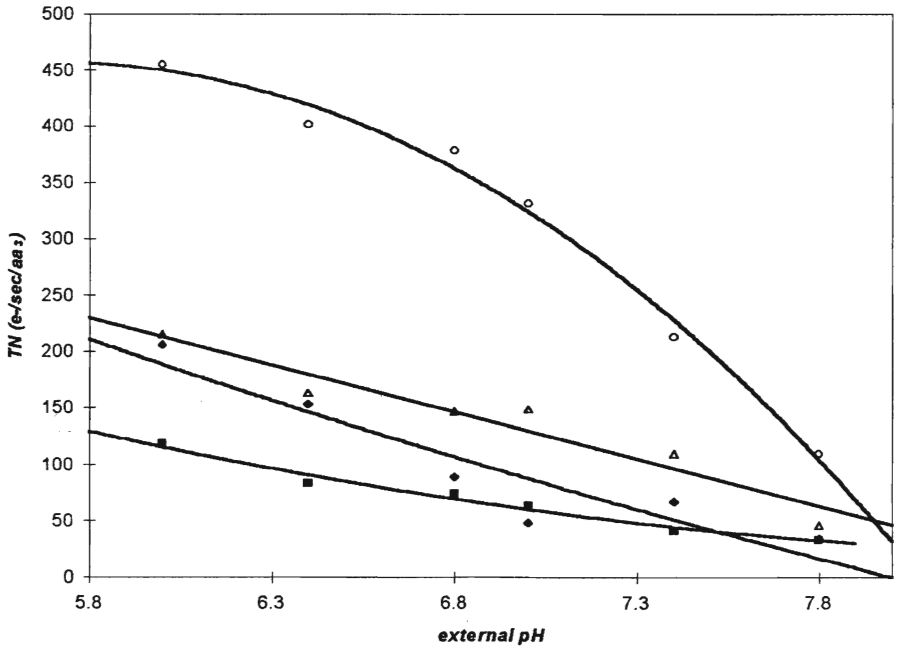
500
450
400
350
300
250
200
150
100
50
0
TN (e-/sec/aa2)
5.8
6.3
6.8
7.3
7.8
external pH

Figure 3.11: Respiratory control ratios of bovine heart COV at varying bulk pH. RCR values were determined from Table 3.2 above. Cytochrome *c* oxidase turnover in the uncontrolled state was divided by the turnover in the controlled state

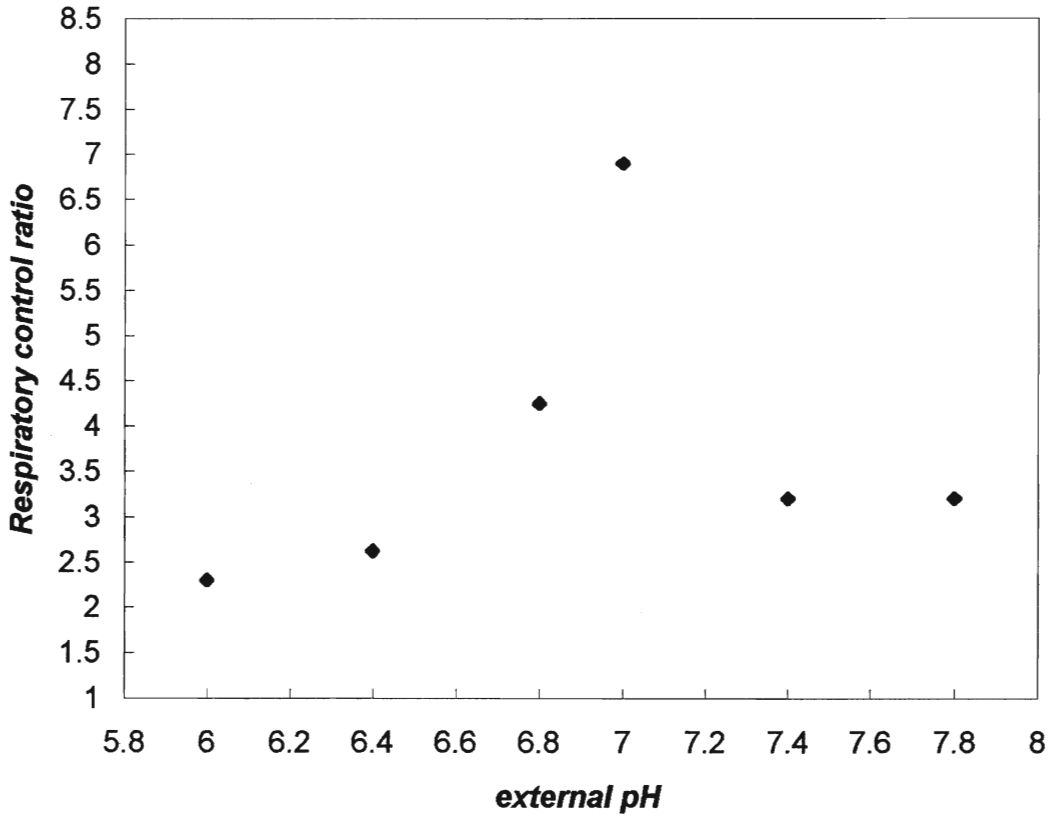
Respiratory control ratio
8.5
8
7.5
7
6.5
6
5.5
5
4.5
4
3.5
3
2.5
2
1.5
1
5.8
6
6.2
6.4
6.6
6.8
7
7.2
7.4
7.6
7.8
8
external pH

Figure 3.12: K_m at the high and low affinity cytochrome *c* binding sites at varying bulk pH (see text for conditions). A. High affinity binding site. B. Low affinity binding site. (◆) control conditions; (■), +val (no $\Delta\Psi$); (Δ) +nigericin (no ΔpH); (O) uncontrolled (no $\Delta\Psi$ or ΔpH). Data points are obtained from a single experiment.

A.

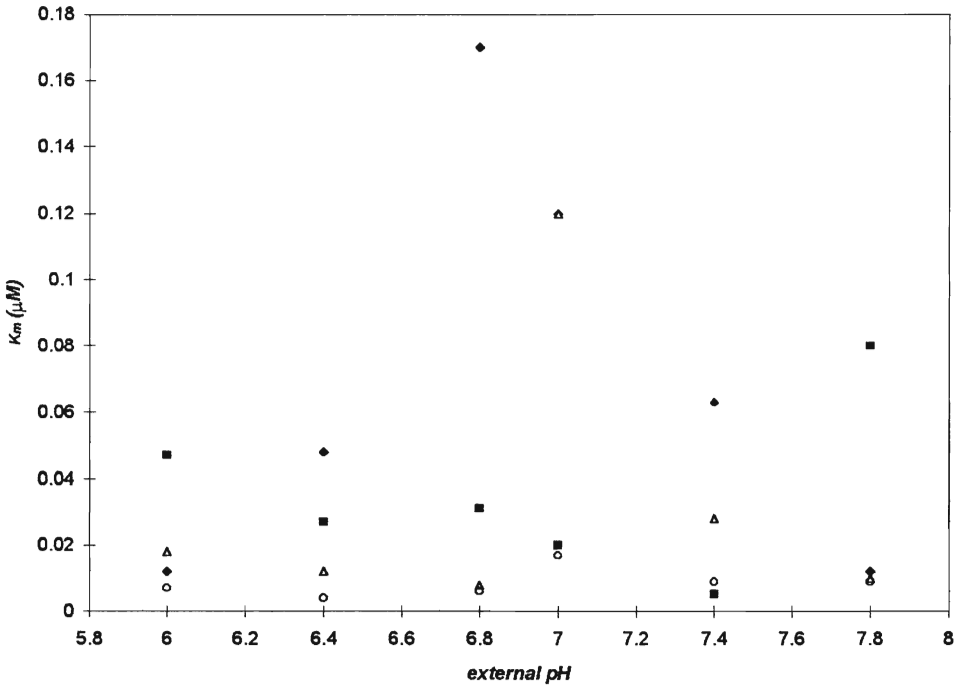
0.18
0.16
0.14
0.12
0.1
0.08
0.06
0.04
0.02
0
Km (μM)
5.8
6
6.2
6.4
6.6
6.8
7
7.2
7.4
7.6
7.8
8
external pH

B.

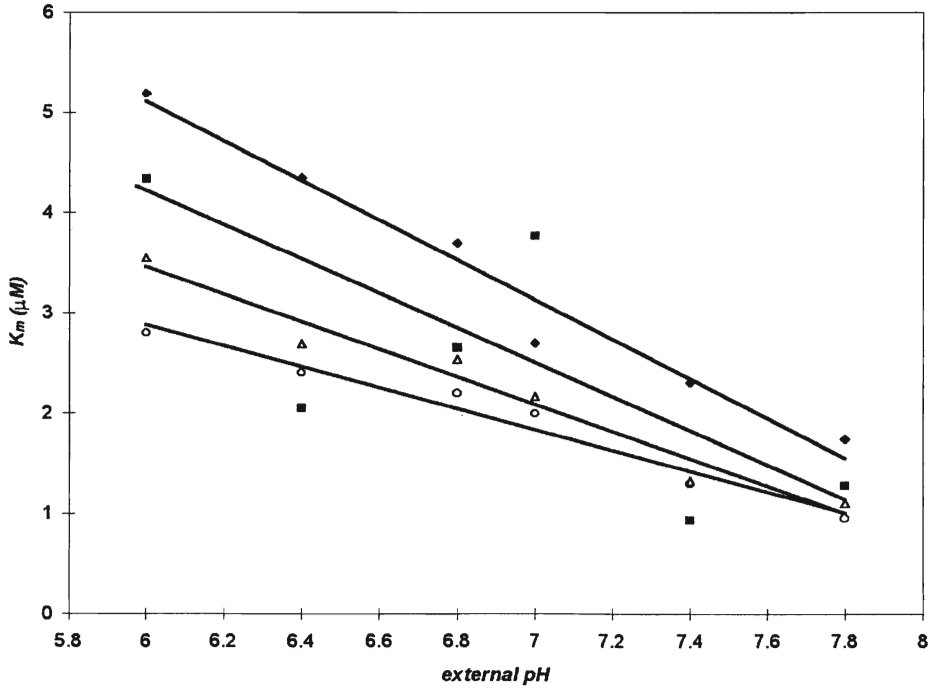
6
5
4
3
2
1
0
Km (μM)
5.8
6
6.2
6.4
6.6
6.8
7
7.2
7.4
7.6
7.8
8
external pH

3.4 Steady State Kinetics of Bovine Heart COV at Varying Bulk pH

The recent determination of the 3-dimensional structure of cytochrome *c* oxidase for both bovine heart (Tsuikihara *et al.*, 1995, 1996) and *P. dinitrificans* (Iwata *et al.*, 1995) cytochrome *c* oxidase has provided for better structural understanding of the enzyme. Mechanistically however, many questions remain concerning the movement and control of electrons through the enzyme. Steady state studies of the enzyme designed to investigate the steps involved in turnover can help answer these questions. Two types of method exist for measuring steady state parameters: (a) spectrophotometric methods, in which the oxidation-reduction of cytochrome *c* and cytochrome *c* oxidase components are measured; and (b) polarographic methods in which, oxygen consumption by the enzyme is measured. Much of the work concerning the steady state kinetics of cytochrome *c* oxidase has involved the free enzyme, and the effects of substrate concentration, pH, and ionic strength. The present study examined the influence of bulk pH on the steady state kinetics of cytochrome *c* oxidase in proteoliposomes. The redox state of cytochrome *c* and cytochrome *a* was monitored spectrophotometrically with a diode array spectrophotometer. Cuvette samples contained COV (600 nM aa_3), horse heart cytochrome *c* (5 μM) and/or valinomycin (10 nM) or nigericin (0.7 μM). Turnover was initiated and monitored over a range of sodium ascorbate concentrations.

Figure 3.13 presents the % reduction of cytochromes *c* at 550-540 nm and cytochromes *a* at 605-630 nm versus ascorbate concentration at pH 7.0. These results indicate that the reduction level of cytochrome *c* is linearly dependent on ascorbate concentration. Unlike cytochrome *c*, cytochrome *a* reduction reaches a maximum value independent of ascorbate concentration or enzyme flux. A plot of the cytochrome *a* reduction as a function of cytochrome *c* reduction at bulk pH 7.0 is presented in Figure 3.14. A lower maximum cytochrome *a* reduction is observed in the presence of nigericin and in the fully uncontrolled state. A higher cytochrome *a*

Figure 3.13: Steady state reduction of cytochromes *c* and *a* from bovine heart COV. Reduction was measured on Beckman DU-7400 Diode Array Spectrometer in 100 mM HEPES, 64 mM K^+, pH 7.0 at 30°C. A. Steady state reduction of cytochrome *c* with increasing ascorbate concentration (550-540 nm). B. Reduction of cytochrome *a* with increasing ascorbate concentration. Cytochrome *a* reduction was measured from 605-630 nm wavelength pair. Complete reduction (100%) was measured after the addition of dithionite.(◆) control conditions; (■), +val (no $\Delta\Psi$); (Δ) +nigericin (no ΔpH); (O) valinomycin + nigericin (no $\Delta\Psi$ or ΔpH). Data points were obtained from the average of 4 spectra of a single experiment. Experimental error is estimated to occur within the data point region

A.

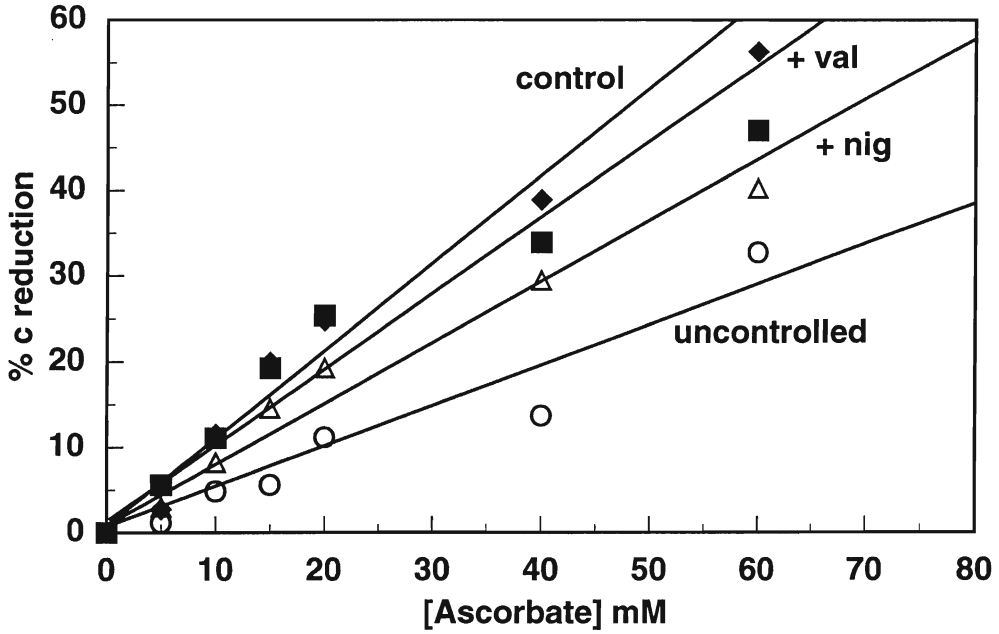
60
50
40
30
20
10
0
% c reduction
control
+ val
+ nig
uncontrolled
0
10
20
30
40
50
60
70
80
[Ascorbate] mM

B.

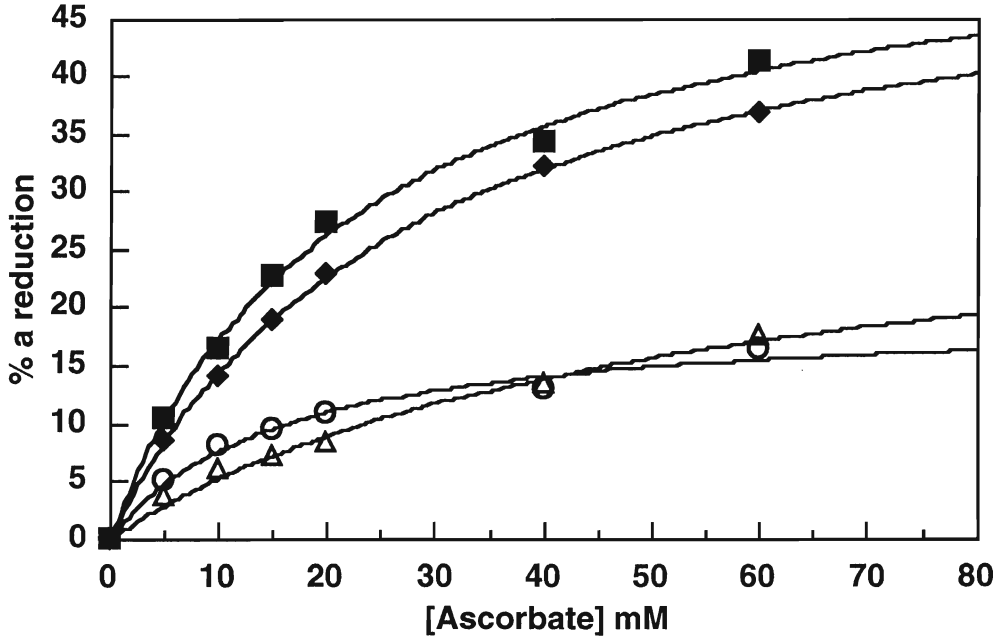
45
40
35
30
25
20
15
10
5
0
% a reduction
0
10
20
30
40
50
60
70
80
[Ascorbate] mM

Figure 3.14: Comparison of steady state reduction of cytochrome *a* as a function of cytochrome *c* reduction. Conditions are as in Figure 3.13.(◆) control conditions; (■), +val (no $\Delta\Psi$); (Δ) +nigericin (no ΔpH); (O) valinomycin + nigericin (no $\Delta\Psi$ or ΔpH).

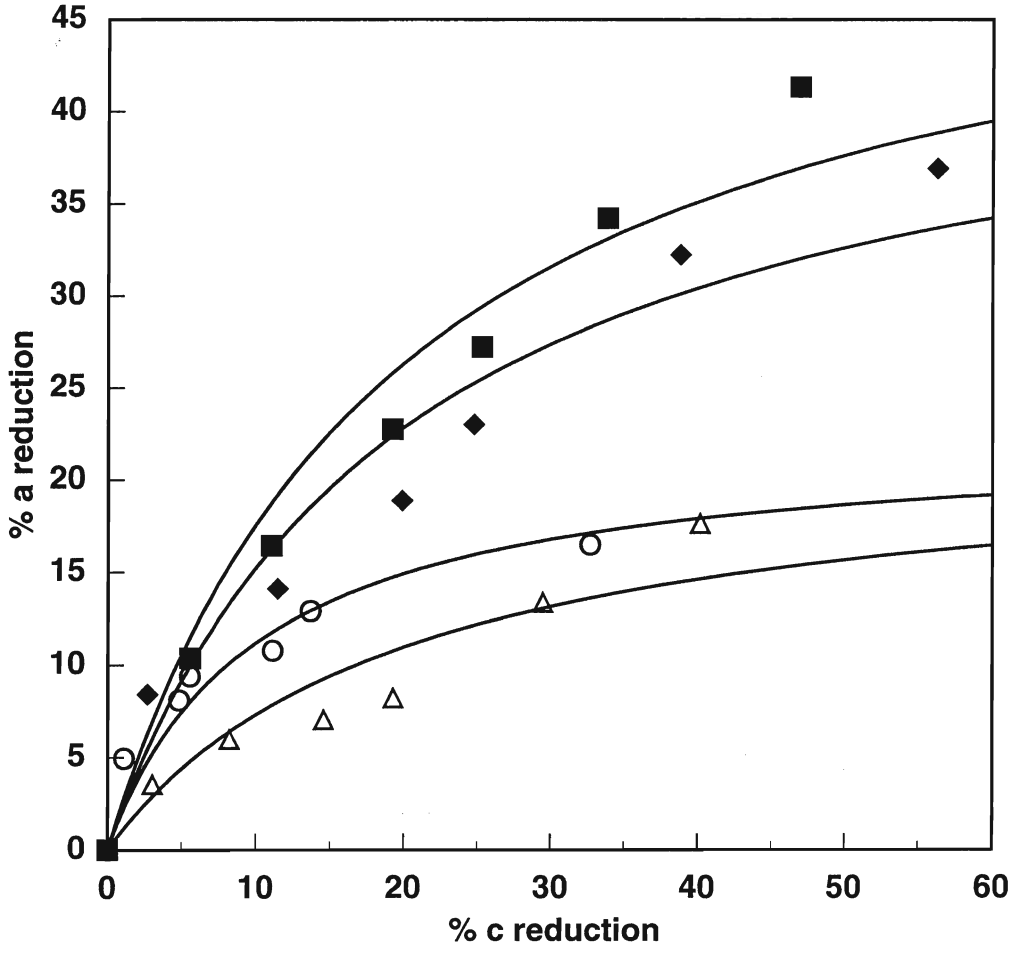
45
40
35
30
25
20
15
10
5
0
% a reduction
0
10
20
30
40
50
60
% c reduction

reduction is observed when ΔpH control is exerted (+valinomycin or fully controlled). Similar trends are observed for cytochrome *c* and *a* reduction in the acidic and alkaline pH range.

Further analysis has indicated a regular relationship between cytochrome *a* reduction and bulk pH. The equilibrium constant K_{eq} is a measure of the apparent redox potential of cytochrome *a*. K_{eq} can be measured for the different conditions. Figure 3.15 plots the ratio of oxidized/reduced cytochrome *a* versus that of cytochrome *c* at pH 7.0. The slope is proportional of the apparent K_{eq} (equation 3).

$$\text{Slope} = \frac{[a^{3+}]\,[c^{2+}]}{[a^{2+}]\,[c^{3+}]} = \frac{1}{K_{eq}} \qquad (3)$$

The intercept on the y-axis, is the maximum $[a^{3+}]/[a^{2+}]$ value. Table 3.3 presents the calculated K_{eq} values and $[a^{2+}]_{max}$ values at the varying bulk pH. The K_{eq} value increases with pH in all energetic states which indicates a decrease in the redox potential of cytochrome *a* with increasing pH (Figure 3.16A). The apparent increase of E_o' with decreasing pH is independent of the energetic state. The log K_{eq} at the varying bulk pH are plotted in Figure 3.16B. The K_{eq} values are high in the $\Delta\Psi$ controlled state and the fully controlled state over the pH range. The $[a^{2+}]_{max}$ as a function of pH is plotted in Figure 3.17. The value of $[a^{2+}]_{max}$ increases with pH under all energized states. The degree of reduction of cytochrome *a* appears to be dependent on the energized state. An increase in $[a^{2+}]_{max}$ occurs in the presence of valinomycin, as compared to the control state. In the presence of nigericin, or both valinomycin and nigericin (uncontrolled), there is only a slight increase in $[a^{2+}]_{max}$ with increasing pH. Cytochrome *a* reduction is smaller in the presence of nigericin as compared to the control state. Cytochrome *a* reduction shows a dependence on pH. This suggests that that the uptake of protons may be associated with cytochrome *a* reduction (equation 4).

Figure 3.15: Oxidized/Reduced ratio of cytochrome *a* versus oxidized/reduced ratio of cytochrome *c*. Linear slope is representative of K_{eq}. The y -intercept is representative of $[a^{3+}] / [a^{2+}]_{max}$.

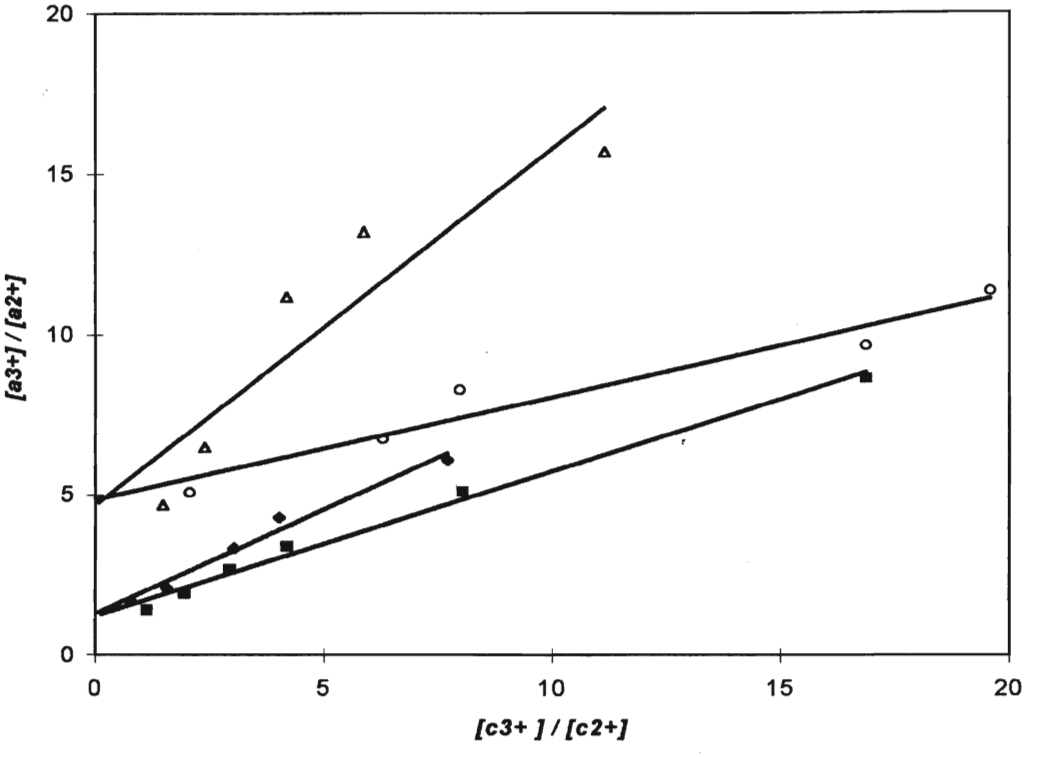
20
15
10
5
0
0
5
10
15
20
[a3+] / [a2+]
[c3+] / [c2+]

Table 3.3: Calculated K_{eq} and $\%[a^{2+}]_{max}$ of the various energized states at varying bulk pH. K_{eq} values were obtained from the slopes as in Figure 3.15. $\%[a^{2+}]_{max}$ values were obtained from $[a^{3+}] / [a^{2+}]_{max}$ intercept ratios as in Figure 3.15.

External Bulk pH	K_{eq}				$\%[a^{2+}]_{max}$			
	con	+val	+nig	val+nig	con	+val	+nig	val+nig
6.2	0.131	0.163	0.136	0.088	23.5	20.7	18.6	17.4
6.6	0.426	0.215	0.388	0.193	25	32.6	22.6	15.8
7.0	0.647	0.450	1.113	0.321	45.6	50.4	16.6	22.3
7.4	0.803	0.669	2.530	0.974	44.5	52.1	32.1	32.6
7.8	4.306	1.907	2.100	3.100	-	66.5	43.1	37.1

Figure 3.16: The influence of bulk pH on K_{eq}. A. K_{eq} values versus bulk pH at the varying energized states. All values are from Table 3.3. B. Log K_{eq} versus bulk pH.

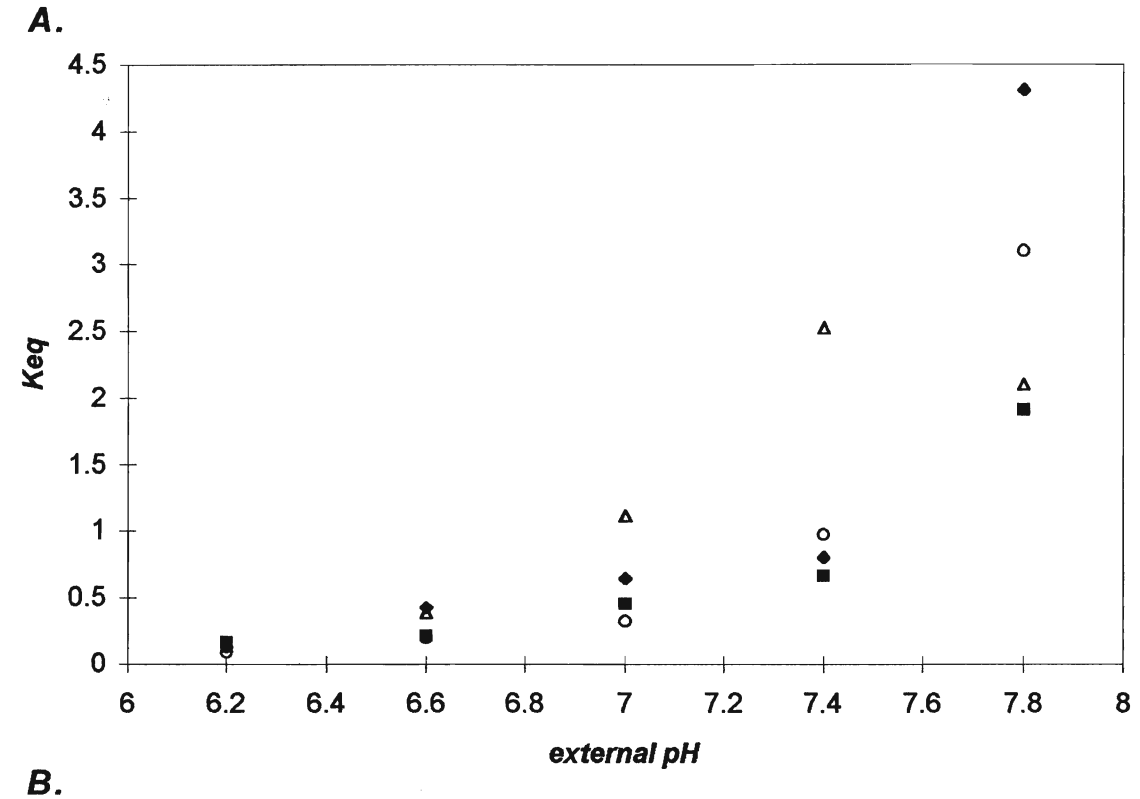
A.
Keq
4.5
4
3.5
3
2.5
2
1.5
1
0.5
0
6
6.2
6.4
6.6
6.8
7
7.2
7.4
7.6
7.8
8
external pH

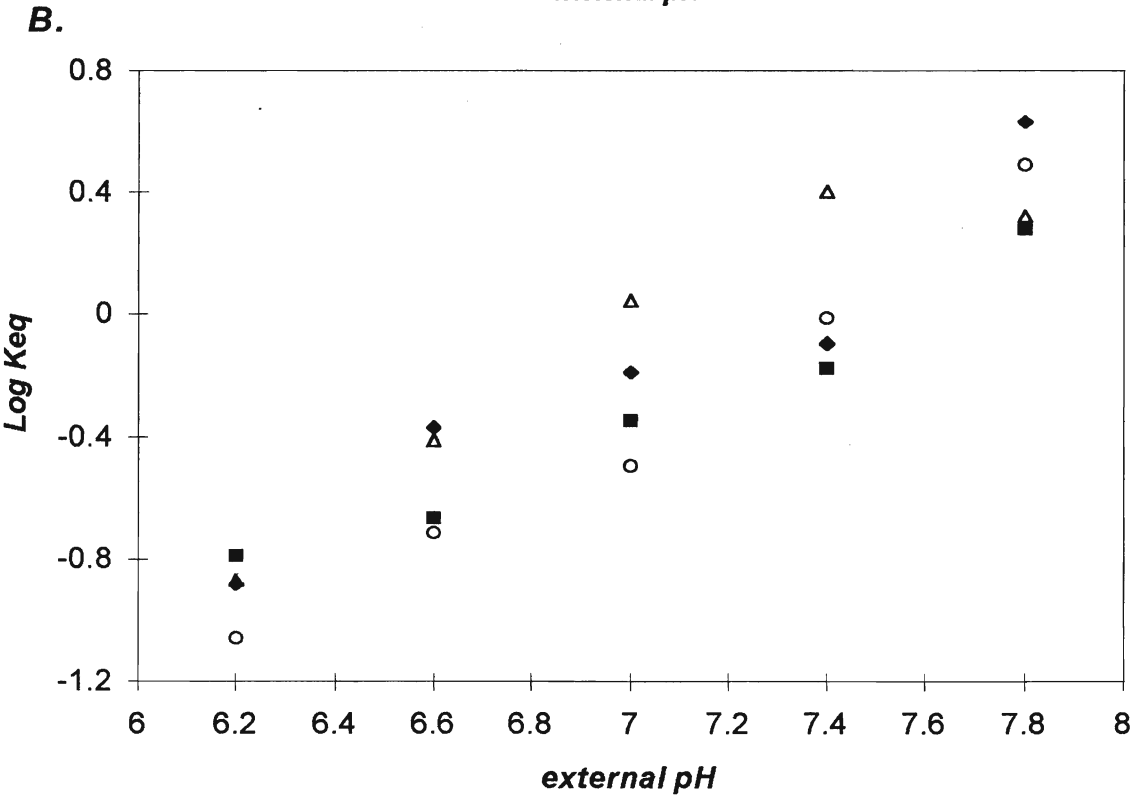
B.
Log Keq
0.8
0.4
0
-0.4
-0.8
-1.2
6
6.2
6.4
6.6
6.8
7
7.2
7.4
7.6
7.8
8
external pH

Figure 3.17: The influence of bulk pH on $\%[a^{2+}]_{max}$ at various energized states. Values were obtained from Figure 3.15.

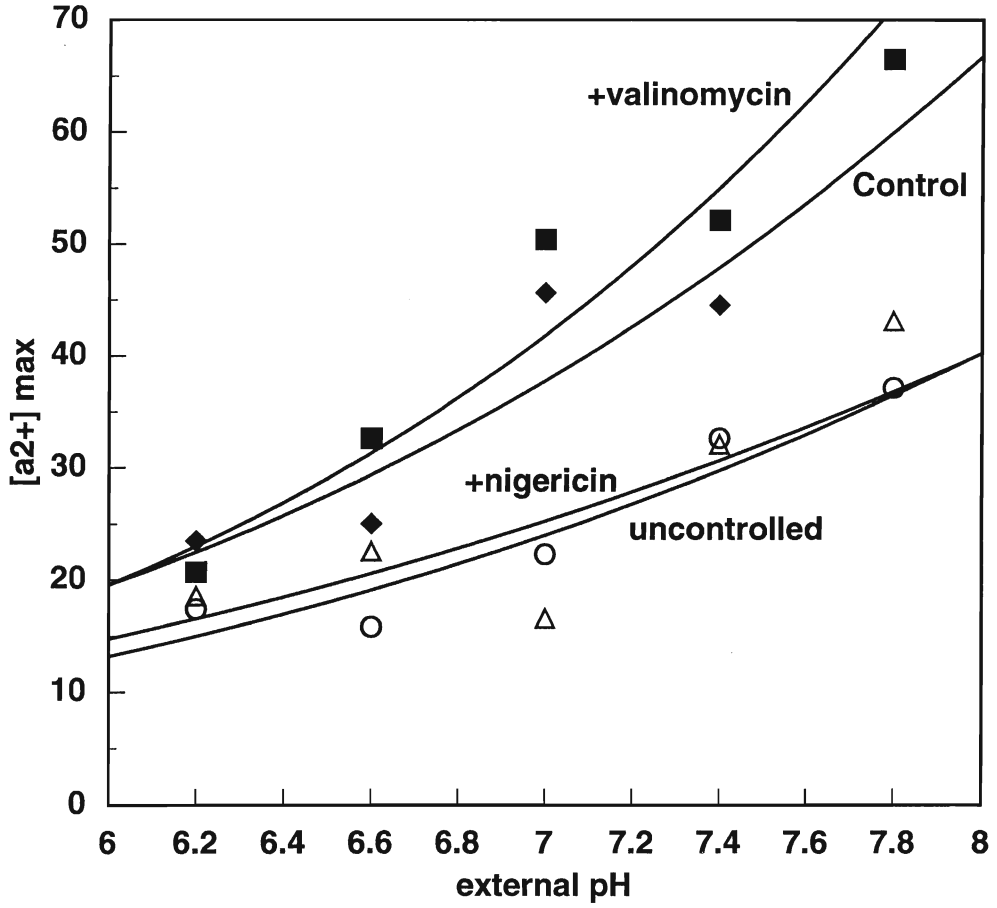
70
60
50
40
30
20
10
0
[a2+] max
6
6.2
6.4
6.6
6.8
7
7.2
7.4
7.6
7.8
8
external pH
+valinomycin
Control
+nigericin
uncontrolled

In this case, the reoxidation of cytochrome *a*, possibly by reduced cytochrome *c*, would result in the release of a proton (equation 5).

$$H^+ + \text{Cyt. } c^{2+} + \text{Cyt. } a^{3+} \longleftrightarrow \text{Cyt. } c^{3+} + \text{Cyt. } a^{2+}\,H^+ \quad (4)$$

$$\text{Cyt. } a^{2+} + H^+ + \text{Cyt. } c^{3+} \longrightarrow \text{Cyt. } a^{3+} + \text{Cyt. } c^{2+} + H^+ \quad (5)$$

This may implicate cytochrome *a* involvement in proton translocation. This cytochrome *a* reduction dependence on pH is modulated by both ΔpH and $\Delta\Psi$.

Chapter 4

Protein Composition and Bioenergetics of Bacillus subtilis Cytochrome caa3 oxidase

4.1 Structural Analysis of B. subtilis Cytochrome caa3

4.1.1 Reduced Spectra and Ratio of Cytochromes c to a in caa_3

The original cytochrome *c* oxidase purified by de Vriij and co-workers (1983) was reported to oxidize cytochrome *c*. However, biochemical and genetic studies showed that the spectra reported by de Vriij and co-workers (1983) were in fact that of a quinol *aa3* oxidase. The spectral properties of the quinol aa_3 and cytochrome caa_3 oxidases are very similar to that of the mitochondrial enzyme. UV-visible spectra of highly purified samples of quinol oxidizing cytochrome aa_3 and cytochrome caa_3 from *B. subtilis* show only slight differences in absorbence peaks (Henning *et al.*, 1995). Cytochrome caa_3 has peaks in the visible region when reduced at 550 and 603 nm and in the Soret region at 416 and 443 nm. The extra peaks at 550 and 416 nm are due to the cytochrome *c* component. The quinol oxidase shows peaks when reduced at 600 nm and 442 nm, due to the haems of cytochrome aa_3.

Genetic studies of the cytochrome caa_3 have indicated the presence of a single cytochrome *c* like sequence, which is covalently associate with subunit II of the enzyme (Saraste *et al.*, 1991). This suggests a haem *c* to haem *a* ratio of 1. This ratio can be compared by examining the reduced-oxidized spectra of the enzyme (550-540 nm/604-630 nm). Figure 4.1 shows the difference spectra of *B. subtilis* cytochrome caa_3 (free enzyme). The enzyme was reduced in the presence of (I) ascorbate+TMPD; (ii) ascorbate+dithionite; and (iii) ascorbate/TMPD/dithionite+KCN. All three methods show a characteristic alpha peak at 604 nm, a cytochrome *c* peak at 550 nm, and Soret peaks at 416 and 442 nm. Cytochrome a_3 is capable of binding HCN in the ferric state at the binuclear centre. Spectrally this is indicated by the decreased Soret peaks at 605 nm and 443 nm indicating a partially reduced state of the enzyme (Figure 4.1).

The haem *c* to haem *a* ratio within the free enzyme was estimated. This ratio can be determined by comparing the 550-540 nm vs the 604-630 nm absorbance values. Table 4.1 shows the resulting haem *c* to haem *a* ratios of the various reduction

methods observed in Figure 4.1. In each condition, the value indicates a ratio greater than 2. This suggested the possibility that a second cytochrome *c* species might be associated with the enzyme.

4.1.2 Coomassie and Haem Stained Chromatograms of caa_3

Bacillus subtilis cytochrome caa_3 oxidase is composed of 3 subunits. Subunit I is the largest subunit, 69 000 Da, larger than the corresponding subunits of either the mitochondrial or *Paracoccus* enzyme (Saraste *et al.*, 1991). Subunit II has a molecular mass of 40 000 Da, and is partially homologous to subunit II of the *Paracoccus* enzyme. In addition about 100 C-terminal amino acid residues appear to form a cytochrome *c* domain. Subunit III is the smallest subunit (23 000 Da) smaller than the corresponding mitochondrial and *Paracoccus* subunits. A fourth 110 amino acid residue peptide (12 600 Da) may also be associated with the enzyme. However, it is not conserved within *Bacillus* cytochrome oxidase species (Sone *et al.*, 1990).

In order to examine subunit and haem composition SDS-PAGE analysis of the free enzyme was performed. Figure 4.3 shows a Coomassie stained SDS-PAGE chromatogram of the *B. subtilis* caa_3. Lane 1 contains horse heart cytochrome *c,* and shows a band with a molecular weight of 12 000 - 14 000 Da, as expected. The *B. subtilis* caa_3 enzyme (Lane 2) shows three bands. The upper most band shows a molecular weight of >80 000 Da. This is most likely due to a undissociable complex of subunits I and II. The second band has a molecular weight of approximately 64 000 Da, and most subunit I. The third band ($\approx$ 40 000 Da) is probably subunit II. A band is noticeably absent in the region expected for subunit III (23 000 Da) and no bands appear with molecular weights < 20 0000 indicating the absence of separate cytochrome *c*. Figure 4.4 is a SDS-PAGE chromatogram of *B. subtilis* caa_3 enzyme stained with the haem stain diaminobenzoic acid. Lanes 1 and 5 contain *B. subtilis* caa_3 enzyme. A single band in the 40 000 Da region appears indicating a haem group. The running time of this gel was then extended an further one hour to ensure the

Figure 4.1: Difference spectra of reduced *Bacillus subtilis* caa_3 free enzyme. Reduction of the enzyme was monitored using a Beckman 7400 Diode Array Spectrophotometer in 100 mM HEPES, 64 mM K^+, pH 7.0 at 30°C. Three different methods were used to reduce the enzyme. The solid line represents spectra of caa_3 which was initially reduced by ascorbate (6 mM); full reduction of was achieved by the addition of TMPD (375 μM). A second method (long dashes) reduction was initiated by the addition of ascorbate, and full reduction achieved by the addition of solid dithionite crystals. For the third method (short dashes) an ascorbate/TMPD mixture was added to reduce the KCN (500 μM)inhibited enzyme.

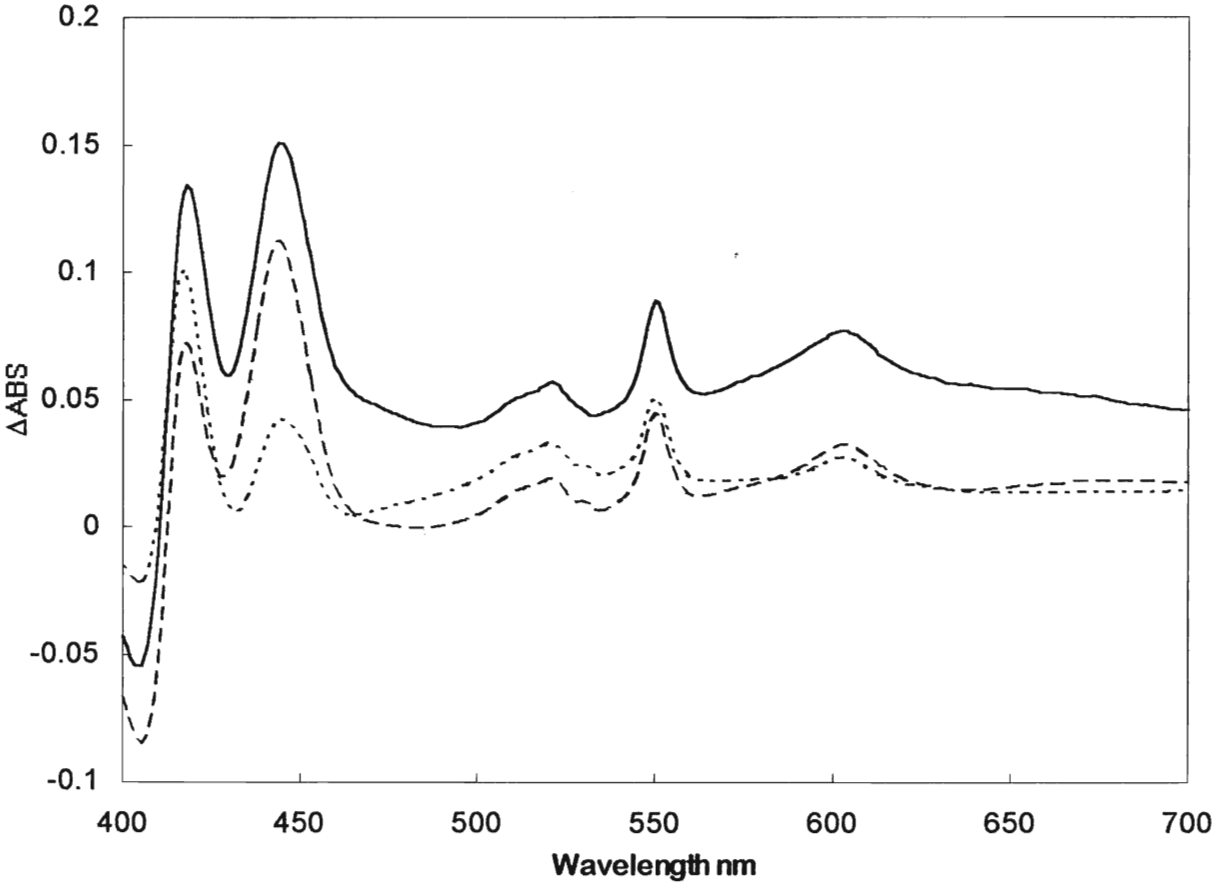
0.2
0.15
0.1
0.05
0
-0.05
-0.1
ΔABS
400
450
500
550
600
650
700
Wavelength nm

Table 4.1: Calculated haem *c* to aa_3 ratios in *B. subtilis* cytochrome caa_3. Ratios were obtained through difference spectra of reduced enzyme (c.f. Figure 4.1) at 550-540 nm (cytochrome *c*) and 604-630 nm (cytochrome *a*).

Conditions	*ΔA 550-540 nm*	*[Cyt. c]✣ μM*	*ΔA 604-630 nm*	*[aa_3] μM*	*[c]:[aa_3] ratio*
Ascorbate TMPD	0.0352	1.67	0.0176	0.65 †	2.60
Ascorbate Dithionite	0.0294	1.39	0.0175	0.65 †	2.15
Ascorbate TMPD+KCN	0.0235	1.09	0.0118	0.53 #	2.10

✣ $\Delta\varepsilon = 21.1\ mM^{-1}cm^{-1}$
† $\Delta\varepsilon = 27\ mM^{-1}cm^{-1}$
# $\Delta\varepsilon = 22.4\ mM^{-1}cm^{-1}$

Figure 4.2: Coomassie blue protein polyacrylamide gel electrophoresis analysis of the caa_3 enzyme was done as described in Kadenbach *et al.* (1982). Electrophoresis ran at 80 mV for 17 minutes and 200 mV for 83 minutes. Gels were stained overnight with a 45.5% methanol, 9.5% glacial acetic acid, and 0.006% Coomassie Blue R-250 staining solution. Destaining was done with a 5% methanol, 7% acetic acid destaining solution. Lane 1 contains horse heart cytochrome *c* from Sigma; Lane 2 contains *B. subtilis* caa_3 enzyme; Lane 3 contains molecular markers.

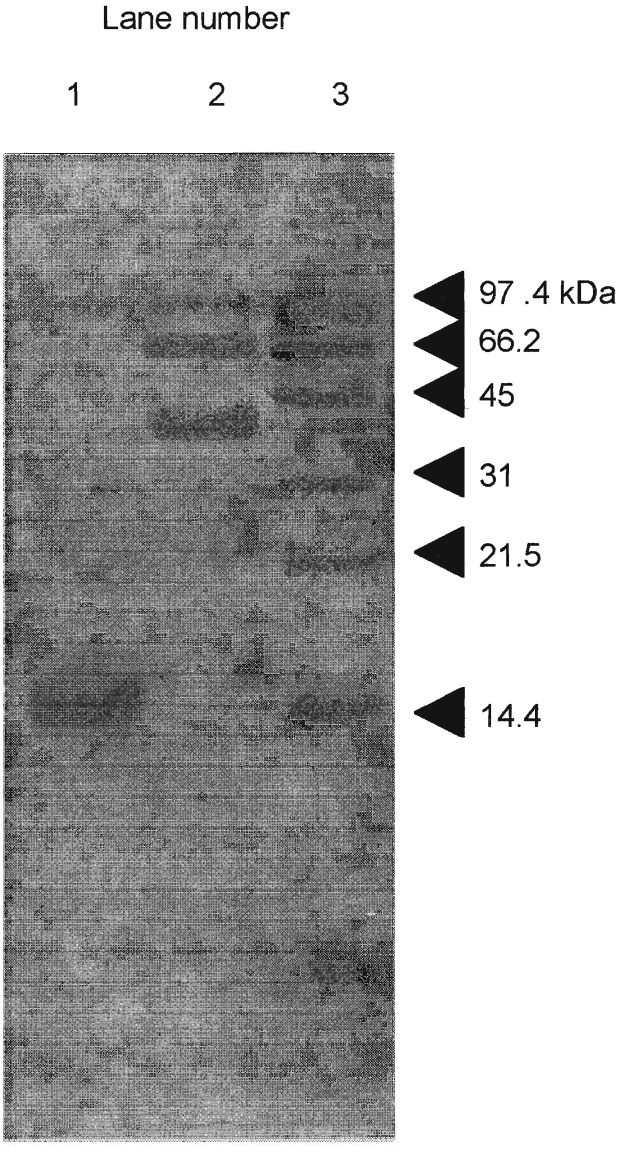
Lane number
1
2
3
97 .4 kDa
66.2
45
31
21.5
14.4

Figure 4.3: Polyacrylamide gel electrophoresis haem stain chromatogram of *B. subtilis* caa_3. Haem stain analysis of the *caa3* enzyme was done as described by DiSpirito (1990). The gel was first fixed in 7% acetic acid for 15 minutes, followed by incubation in 0.5 M Tris-HCL, pH 7.0 for 15 minutes. Incubation in 0.5 M Tris-HCL was repeated 4 to 5 times, until pH solution reached 7.0. Staining of the bands was achieved by incubation in 0.5 M Tris-HCL, 1.4 mM 3,3' -diaminobenzidine, pH 7.0 for 30 minutes at room temperature. The DAB-Tris-HCL buffer was decanted and the gel incubated in a solution of 50 mM citrate, 2,8 mM DAB, pH 4.0. The reaction is started by adding 40 mL of 30% H_2O_2 per mL of the citrate-DAB solution. The gel was then incubated overnight in the dark at 4 ^{o}C. Labeled proteins appeared as a reddish brown band. Lanes 1 and 5 contain *B. subtilis* caa_3 enzyme; Lanes 2 and 6 contain horse heart cytochrome *c* from Sigma; Lanes 3 and 4 contain bovine heart aa_3 enzyme.

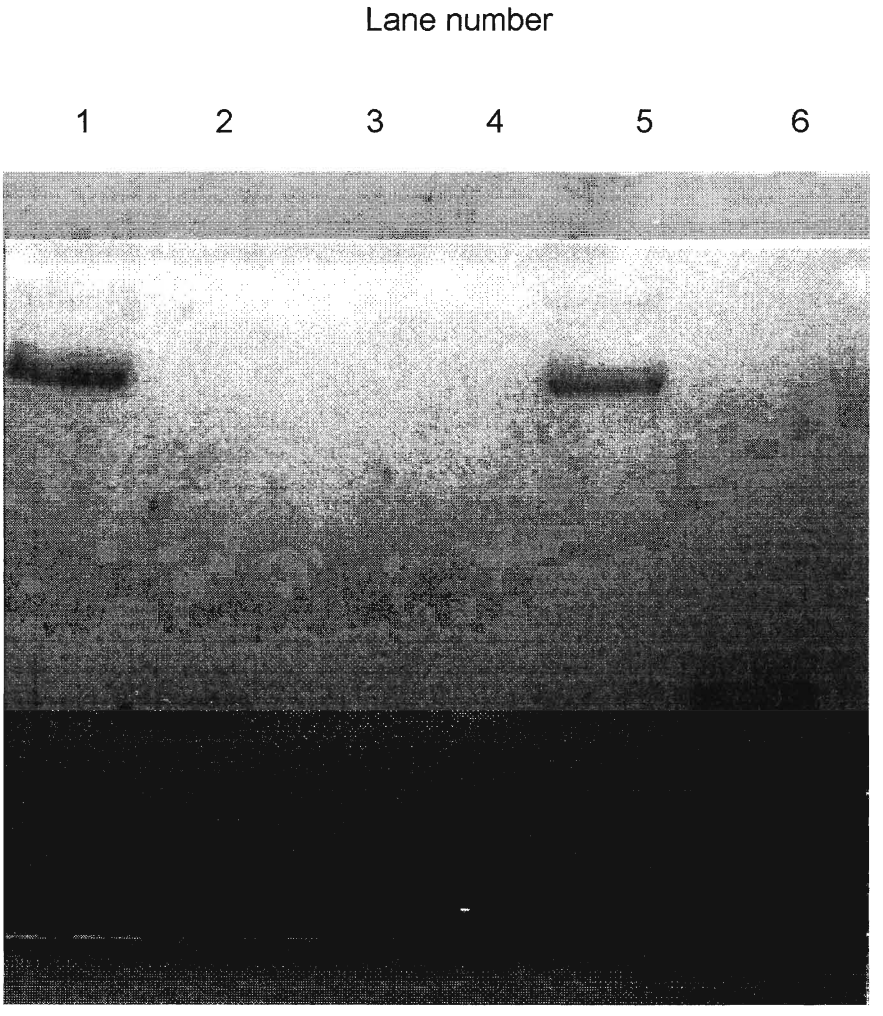
Lane number
1
2
3
4
5
6

separation of all subunits. Lanes 2 and 6 contain horse heart cytochrome *c* from Sigma. The *B. subtilis* caa_3 preparation does not show any haem containing band in the comparable region of molecular size. The suggests that no separate cytochrome *c* species are present within the enzyme sample.

4.2 Bioenergetic Analysis of Bacillus subtilis Cytochrome caa_3 COV

4.2.1 Respiratory Control In Bacillus subtilis Cytochrome caa_3 COV

The respiratory control ratio (RCR) of COV is measured by dividing the turnover of the enzyme in the fully uncontrolled state (both ΔpH and $\Delta\Psi = 0$) with that in the fully controlled state (both ΔpH and $\Delta\Psi$ present). RCR are normally in the range of 6 to 8 in beef heart COV; a RCR of 1 indicates no respiratory control.

Purified *Bacillus subtilis* caa_3 was incorporated into proteoliposomes by the method of detergent dialysis and a DOPC/DOPE mixture as lipid matrix. The proportion of externally facing caa_3 (as it exists in the bacterial plasma membrane) was determined as in Wrigglesworth *et al.* (1987). Figure 4.5 shows the reduced minus oxidized spectra of cyanide inhibited *B. subtilis* caa_3 COV. Initial reduction involved the addition of sodium ascorbate (20 mM), while full reduction was obtained by the addition of TMPD. Table 4.1 lists the proportion of externally facing caa_3 as determined by the given wavelength pairs. Figure 4.6 shows respiration of these caa_3 COV in an O_2 electrode with ascorbate+TMPD. Unlike COV containing mammalian oxidase, added cytochrome *c* is not required. Addition of valinomycin, an electrophoretic potassium ionophore, slows the respiration. Subsequent addition of nigericin, an electroneutral K^+/H^+ ionophore fully releases the respiration rate. The results suggest that the caa_3 is more sensitive to the full pH gradient (created by valinomycin) than to the mixture of ΔpH and $\Delta\Psi$ in the original controlled state.

Figure 4.5: Reduced minus oxidized spectra of cyanide inhibited *B. subtilis* caa_3 COV. Spectra were obtained through a Beckman DU-7400 Spectrophotometer for a 1.92 μM (total) caa_3 sample in 100 mM HEPES, 64 mM K^+, pH 7.0 at 30°C. KCN (500 μM) was added to the sample 15 minutes prior the addition of ascorbate (20 mM). The black line represents spectrum of ascorbate reduction 15 minutes after addition. Complete reduction was obtained with the addition of TMPD (1.1 mM) (grey line).

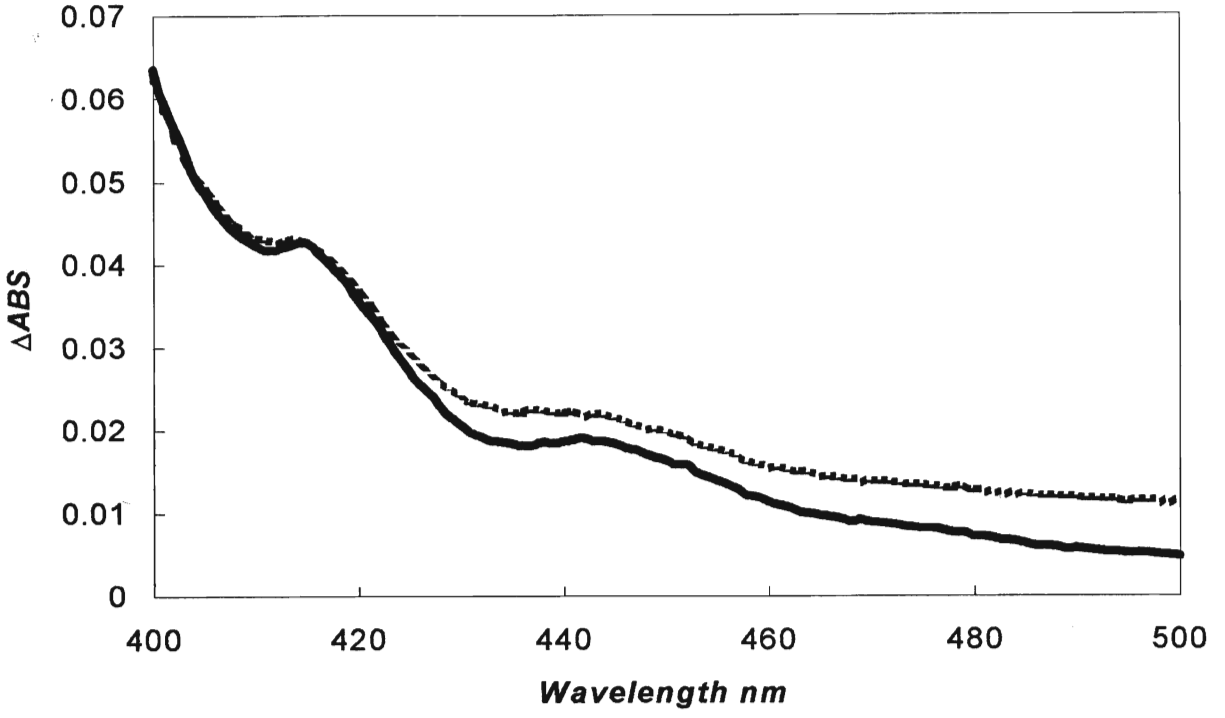
0.07
0.06
0.05
0.04
0.03
0.02
0.01
0
ΔABS
400
420
440
460
480
500
Wavelength nm

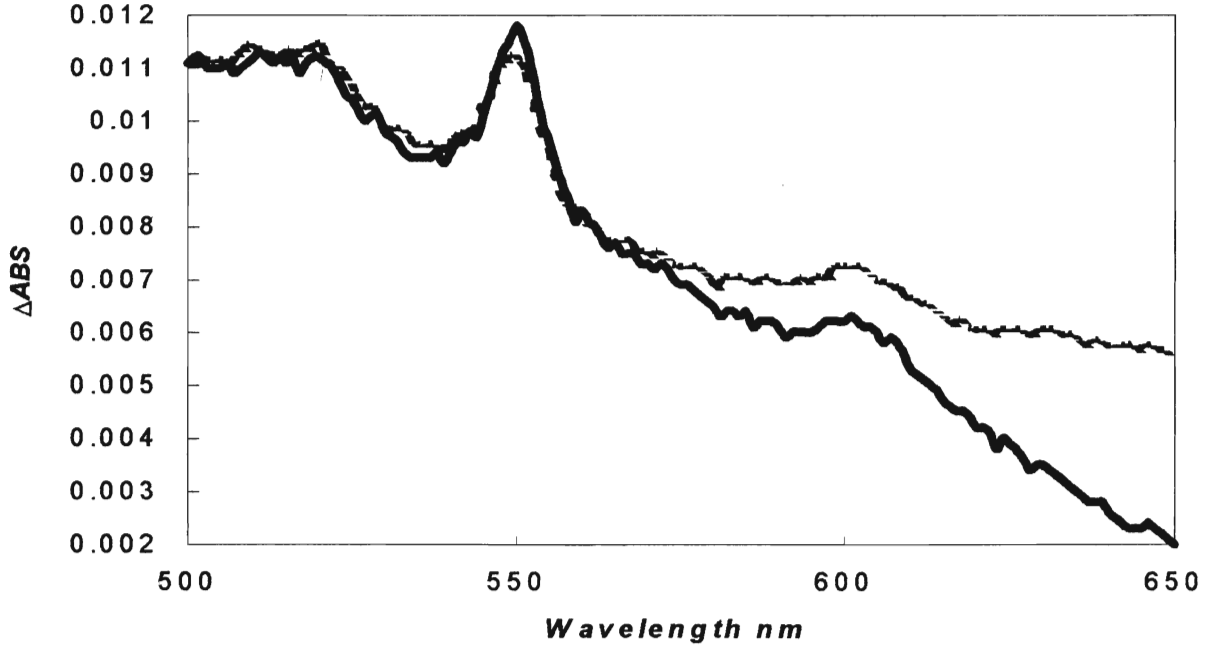
0.012
0.011
0.01
0.009
0.008
0.007
0.006
0.005
0.004
0.003
0.002
ΔABS
500
550
600
650
Wavelength nm

Table 4.2: Proportion of externally facing caa_3 in DOPC/DOPE proteoliposomes. The difference absorbence values of the wavelength pairs were obtained from the reduced minus oxidized spectra in Figure 4.5. The values below are obtained by dividing the absorbance under steady reduction by ascorbate to the steady state absorbence when fully reduced by TMPD.

Conditions	*ΔA Ascorbate*	*ΔA Ascorbate/TMPD*	*% outward facing caa_3 **
ΔA 550-540 nm Cyt. c	0.0017	0.0019	89
ΔA 604-630 nm Cyt. a	0.0012	0.0020	60
ΔA 444-470 nm Cyt. aa_3	0.0079	0.0094	84

* ΔA (ascorbate)/ΔA (Ascorbate/TMPD)*100

Figure 4.6: Polarographic determination of respiratory control ratio in *B. subtils* caa_3 COV. The electrode was placed in a thermostatically controlled, magnetically stirred, glass jacketed reaction vessel, with a working volume of 4 mL or 3.6 mL with the medium of 100 mM HEPES, 64 mM K^+, pH 7.0 equilibrated at 30°C. Turnover was initiated through the addition of COV (10 nM), to give the controlled respiratory rate. Ionophores valinomycin and nigericin were then added, to give the uncontrolled respiratory rate. RCR were determined by comparing the uncontrolled rate to the controlled rate.

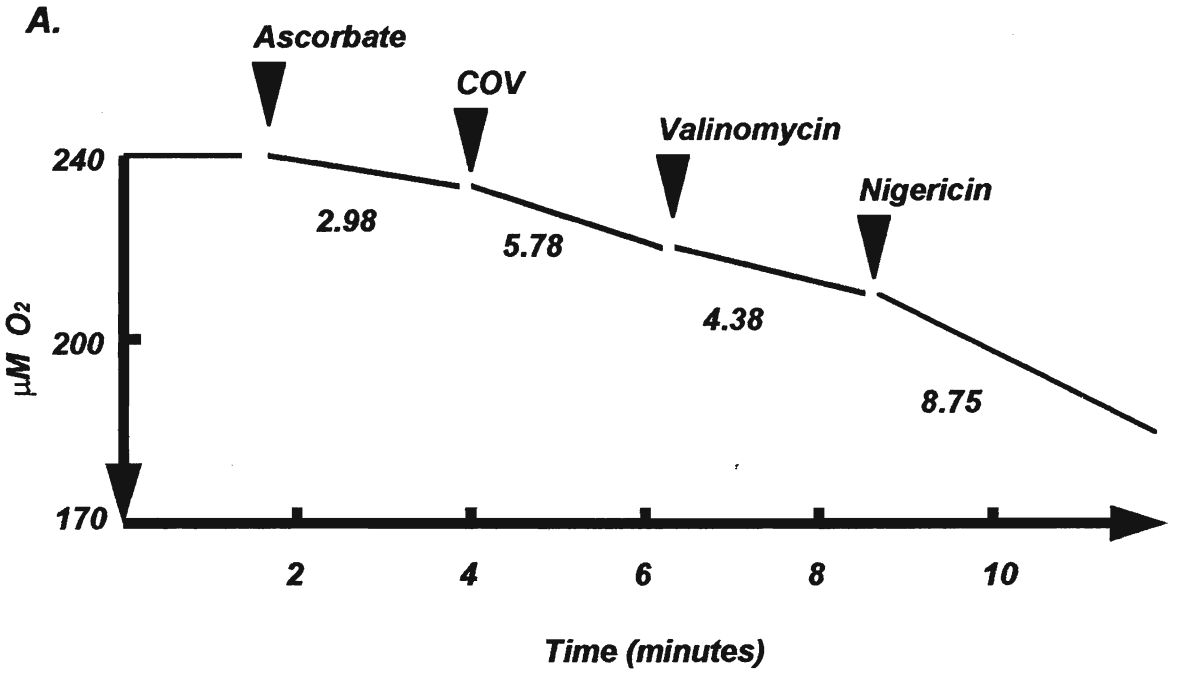
A.
Ascorbate
COV
Valinomycin
Nigericin
240
200
170
μM O2
2.98
5.78
4.38
8.75
2
4
6
8
10
Time (minutes)

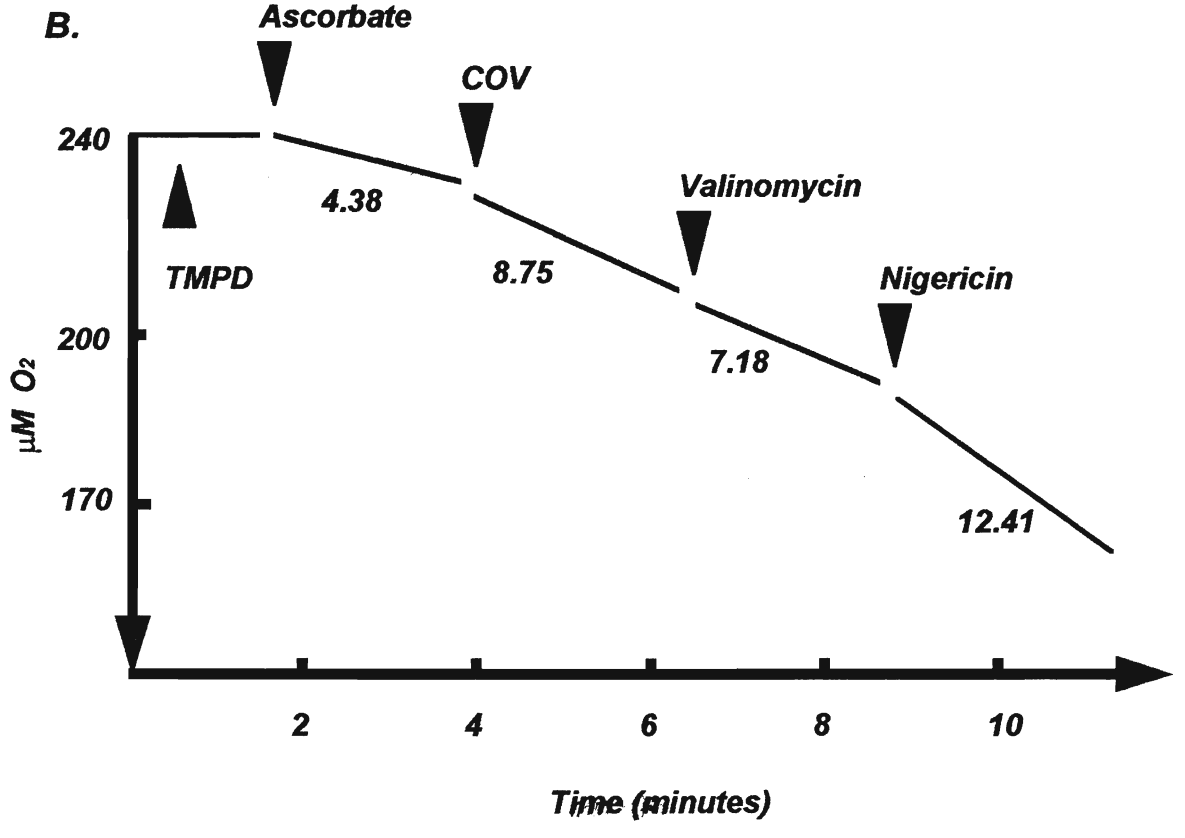
B.
Ascorbate
COV
Valinomycin
Nigericin
TMPD
240
200
170
μM O2
4.38
8.75
7.18
12.41
2
4
6
8
10
Time (minutes)

Respiratory control ratios are summarized in Table 4.3. Three different substrate systems were used . The highest control (RCR = 2.2) was obtained in a substrate system containing 5 mM HEPES, with ascorbate alone as the substrate. This reagent reduces bound cytochrome *c* rapidly at low ionic strength. At a much higher ionic strength, TMPD is needed as a redox mediator (cf. Figure 4.5). A slightly lower RCR of 1.8 was found using this system. When exogenous horse heart cytochrome *c* used, the respiration rate was substantially higher, but the COV no longer responded to respiratory control.

4.2.2 Proton Pumping Activity in Bacillus subtilis Cytochrome caa_3 COV

Two respective paths have been implicated in the movement of protons to the binuclear centre and translocation across the membrane in both the mitochondrial and *Paracoccus* enzyme (Tsukihara *et al.*, 1996; Iwata *et al.*, 1995). The translocation of protons by cytochrome *c* oxidase has previously been established (Wikstrom, 1977). In eukaryotic mitochondrial systems, proton translocation in cytochrome *c* oxidase functions to produce a proton electrochemical gradient. In prokaryotes, respiration is complicated by the presence of more than one different cytochrome oxidase. Both environmental conditions and energy requirements of the cell may influence the number and type of oxidase a particular species of bacteria may express at any given time. During times of low energy requirements, proton pumping activity may be less active, and may result in a less predominant proton pumping oxidase.

The *B. subtilis* caa_3 COV were tested for their ability to pump protons. An aerobic suspension in 100 mM HEPES, 64 mM K^+ at pH 7.0 and 30°C plus 10 nM

Table 4.3: Respiratory control ratios of *B. subtilis* caa_3 COV in different respiratory media. The respiratory control ratio of caa_3 COV were examined in three different respiratory media of either low or moderately high ionic strength. Respiratory control ratios were measured at a low ionic strength, (5 mM HEPES, 3mM K^+, pH 7.0) in the presence of high ascorbate concentrations (40 mM), or at low ascorbate concentration (5 mM) with 200 mM TMPD and 40 mM cytochrome *c* at both low and high (100 mM HEPES, 64 mM K^+) ionic strength.

Conditions	*TN (e^-/sec/aa_3)*			*RCR * +val*	*RCR ** val+nig*
	control	*+val*	*val+nig*		
Ascorbate; low	49	35	103	1.52	2.10
Ascorbate, TMPD, cyt. c; low	72	75	81	1.0	1.12
Ascorbate, TMPD; high	78	38	143	1.12	1.80

* RCR (val) = TN (+val)/TN (con)
** RCR (con) = TN (val+nig)/TN (con)

valinomycin was pulsed using small aliquots of reduced horse heart cytochrome *c*. Figure 4.7 shows a typical proton pulse obtained. Added cytochrome *c* is immediately oxidized by the COV and this was accompanied by the ejection of protons with a stoichiometry of approximately 0.5 H^+/cytochrome *c* $^{2+}$ oxidized. The slow subsequent alkalinization is due to the scalar OH^- ions formed by reduction of O_2 (1.0 OH^- /cytochrome *c* $^{2+}$ oxidized) within the COV which slowly diffuse into the bulk phase. Previous attempts of proton pumping of *caa*$_3$ in *Thermus thermophilus* vesicles showed a H^+/e^- stoichiometry of 0.8 (Hon-ami and Oshima, 1984), when using reduced *T. thermophilus* cytochrome c_{552}.

4.2.3 Steady State Reduction of Cytochromes in Bacillus subtilis caa3 COV

The presence of a covalently attached cytochrome *c* in the cytochrome *caa*$_3$ oxidase invites speculation concerning the electron transport through the enzyme. In particular, by what route do electrons travel through the enzyme, and how is it linked to charge separation and proton pumping? The Cu_A centre in *Paracoccus* is located in a globular domain of subunit II, which protrudes into the periplasmic space. This is in close proximity to the covalently bound cytochrome *c* and may suggest the beginning route taken by electrons to the binuclear centre. In order to begin in answering such questions steady state reduction of both cytochromes *c* and *a* in *caa*$_3$ COV was examined. The use of ionophores provided for the opportunity to examine reduction states in both the controlled and uncontrolled states.

Steady state reductions of cytochromes *c* and *a* during steady state respiration by COV in the controlled and uncontrolled state are shown in Figure 4.8. Table 4.3 lists the calculated K_d values of ascorbate and the maximum reduction values for cytochrome *c* and *a*. With increasing ascorbate levels, there is a progressive increase n the reduction levels for haems *c* and haem *a* in the visible region. A Soret ban shows

Figure 4.7: Proton pumping activity in *B. subtilis* caa_3 COV. The pH electrode was placed in a sealed 4.4 mL reaction chamber, with a syringe access port. The vessel was thermostatically controlled and magnetically stirred. The reaction mixture contained 64 mM K^+, pH 7.0 , DOPE/DOPC COV with 0.5 μM outwardly facing caa_3, 400 nM valinomycin, and/or not 10 nM FCCP, at 30°C. Proton pulses were initiated by the addition of 30 nmol ferrocytochrome *c*. The pH of the ferrocytochrome *c* was adjusted to pH 7.0 just prior to injection into the vessel. After equilibrium was reached the pH was readjusted to pH 7.0, and further pulses were performed.

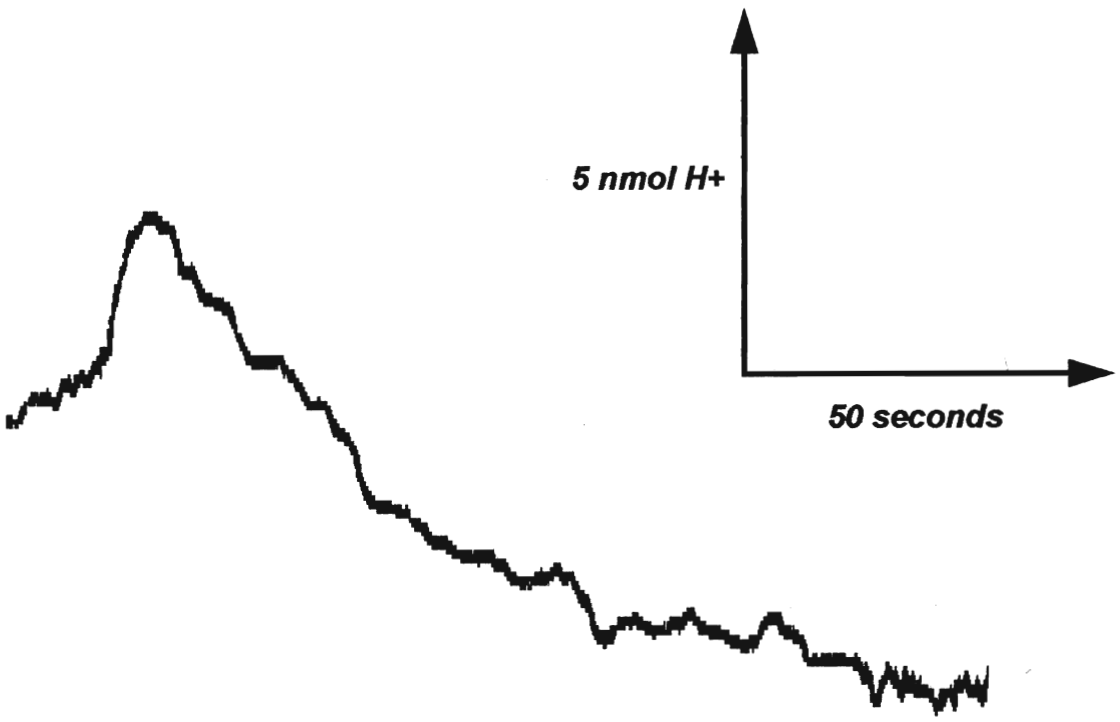
5 nmol H+
50 seconds

~50% reduction of the visible region reduction. Cytochrome a_3 , whose reduced form only contributes in the Soret region, remains oxidized during steady state at high ascorbate concentrations (K_m (O_2)≤1 mM). Unlike the eukaryotic enzyme however, cytochrome *c* and *a* are reduced in parallel. They show near equal redox potentials and a form of the enzyme present during maximal turnover that contains both centres fully reduced. Haem *a* also shows only a modest response to ionophore addition. Euakryotic haem *a* has a redox potential more positive than that of external cytochrome *c* (260 mV) and which becomes more positive on addition of ionophores. Cytochrome caa_3 shows no such redox change. Cytochromes *c* and *a* are near equilibrium with similar E_m values in the controlled state (upper panel), and in uncontrolled COV (lower panel).

Figure 4.8: Steady state reduction of cytochromes *c* and *a* during steady state respiration by *B. subtilis* caa_3 COV. Cytochrome *c* and *a* levels were monitored at varying ascorbate concentrations in the controlled state, partially uncontrolled or the fully uncontrolled states spectrophotometrically with a Beckman DU-7400 diode array spectrometer in 100 mM HEPES, 64 mM K^+, pH 7.0 at 30°C. For partially uncontrolled samples, cuvette mixtures were as above except for the addition of 10 nM valinomycin ($\Delta\Psi$ eliminated), or both valinomycin and nigericin (1.4 mM) in the uncontrolled state. A. Controlled state; B. in the presence of valinomycin; C. Uncontrolled state. ■, cytochrome *c* reduction (550-540 nm absorbence); ▲, cytochrome *a* reduction (604-630 nm absorbence); ◆, cytochrome aa_3 reduction (444-470 nm absorbence).

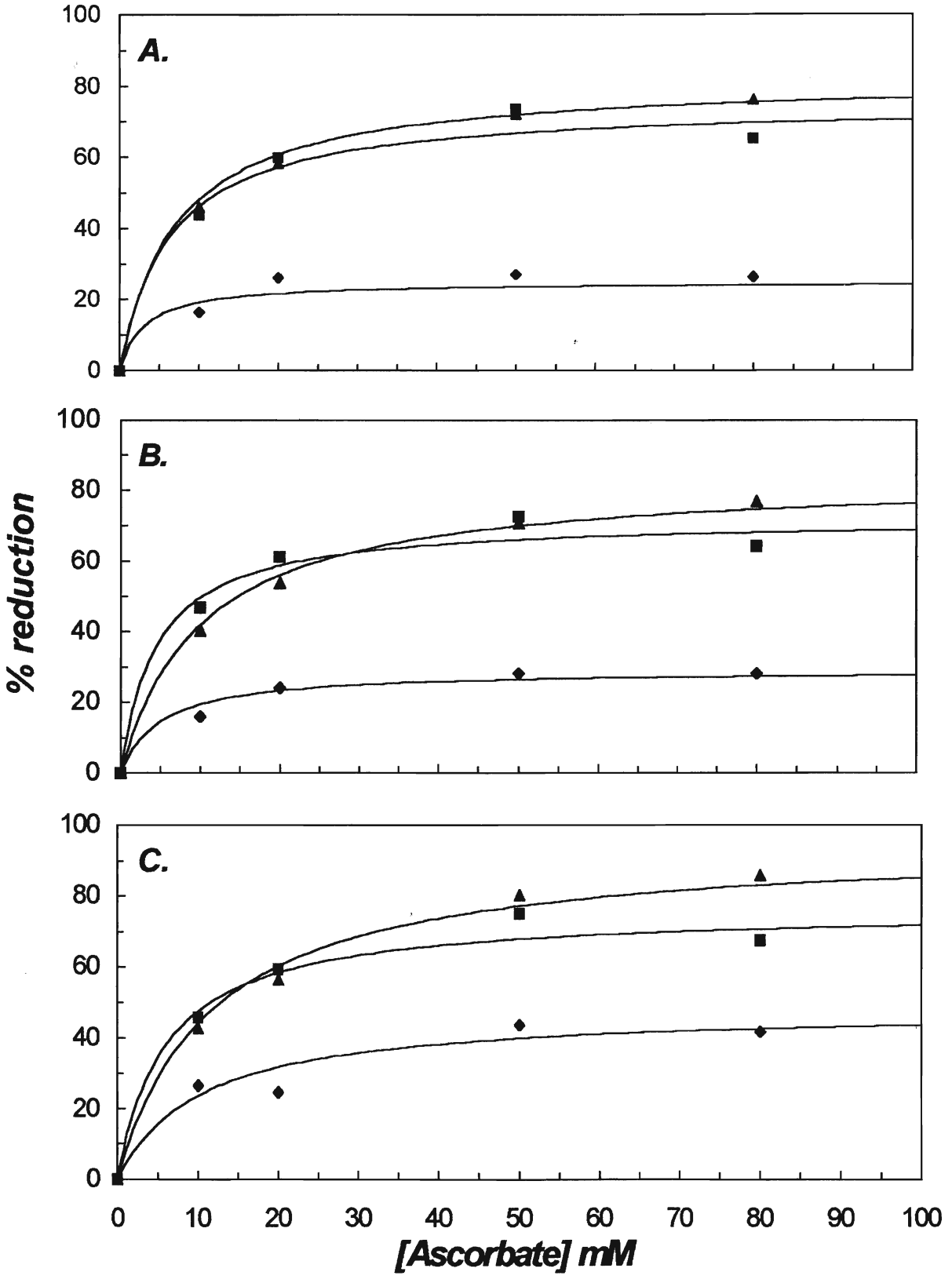
A.
B.
C.
% reduction
[Ascorbate] mM
0
20
40
60
80
100
0
10
20
30
40
50
60
70
80
90
100

Table 4.4: Calculated K_d values for ascorbate, and the maximum % reduction under various energized states.

Wavelengthh pair	K_d (app)			% reduction (max)		
	control	+val	val+nig	control	+val	val+nig
550-540 nm Cyt. *c*	5.60	4.14	5.40	71	69	72
604-630 nm Cyt. *a*	6.19	8.07	9.31	77	76	85
444-470 nm Cyt. aa_3	2.77	4.57	8.65	24	28	44

Chapter 5

Discussion

5.1 Proton Pumping Activity of Bovine Heart COV

Proton pumping activity of cytochrome *c* oxidase was demonstrated by Wikstrom (1977) in mitochondrial particles. This discovery was revolutionary, and created a tremendous amount of debate amongst researchers in the field. The mechanism of proton translocation and its relationship to charge translocation has been studied extensively. Many models have been proposed to explain this relationship of charge and proton translocation. Much controversy has often revolved around the H^+/e^- stoichiometry in cytochrome *c* oxidase turnover. H^+/e^- stoichiometry has been predicted to be as low as 0.5 and as high as 2. The most accepted and consistant value suggests a H^+/e^- stoichiometry of 1. The question of the proton/charge relation has become more prominent with the recent publications of the 3-dimensional structure of cytochrome *c* oxidase for both mitochondrial and bacterial species. Two posibly different proton translocation schemes have been predicted by the authors for their 3-dimensional structures, involving a single (Tsiukahara *et al.*, 1996) or two (Iwata *et al.*, 1995) proton channels. This study examined the action of bovine serum albumin and a possible role for free fatty acids in proton pumping activity of bovine heart cytochrome *c* oxidase in proteoliposomes.

Proton pumping activity in the present bovine heart COV was examined and revealed a H^+/e^- stoichiometry of between 0.8 and 1. This is consistant with the commonly accepted H^+/e^- stoichiometry. Continued proton pulsing of the sample gave a decrease in the H^+/e^- stoichiometry both in the case of ferrocytochrome *c* induced pulses, and for the oxygen induced pulses. However, oxygen induced pulses also showed an initially lower H^+/e^- stoichiometry.Nicholls and Shaughnessy (1985) showed that an autoxidation of ferrocytochrome *c* can occur in vesicles at low ionic strength. This can result in a mimicking of proton re-equilibration across the membrane. This may result in an over estimation of H^+/e^- stoichiometry. A decrease in the H^+/e^- stoichiometry at low ionic strength can be attributed to vesicle heterogeneity or the

retention of alkalinity inside the vesicles between pulses (Nicholls and Shaughnessy, 1985). This can be overcome by the addition of low levels of FCCP or high levels of valinomycin. In this study, low levels of FCCP (10 nM) was added to the mixture. The significant decrease in H^+/e^- stoichiometry for the ferrocytochrome *c* pulses may be due to ferrocytochrome *c* interaction with COV membrane.

Bovine serum albumin is a protein with six high affinity fatty acid binding sites. Spectroscopic studies of BSA action on cytochrome *c* oxidase indicates a red shift in the soret band (Sharpe *et al.*, 1996). This may indicate that the resting enzyme contains intrinsic bound fatty acids. BSA preincubation was also shown to increase the steady state reduction of cytochrome a. The removal of intrinsic FFA may inhibit electron transfer from cytochrome a to a_3. A role for carboxylate groups as ligands has previously been suggested by Moody *et al.* (1991). The carboxylate group of FFA may therefore be implicated as possible ligands. The data presented here has shown that BSA is capable of inhibiting proton pumping activity in COV. Proton pumping activity decreased significantly upon prior incubation with BSA. BSA treated COV were treated with a mixture of FFA, and proton pumping activity was partially restored. A mechanism by which removal of FFA could stop proton translocation is lacking. DCCD inhibits proton translocation (Prochaska *et al.*, 1981) and reacts with carboxylic residues (Asp 90 of bovine subunit II). Could DCCD be involved in binding to intrinsic FFA to abolish proton translocation? Attempts to restore proton pumping activity of DCCD treated COV with FFA were unsuccessful. Possible mechanisms may involve models of a proton shuttle system by acidic residues (Iwata *et al.*, 1995; Tsukihara *et al.,* 1996). Such a mechanism should be insensitive to BSA action. Where do FFA fit in such a mechanism? A possible model may involve FFA as an intraenzymic proton carrier, capable of moving protons electroneutrally from the inner aqueous phase to the binuclear centre. The three dimensional structure of cytochrome

c oxidase may provide a possible binding and active site location for the involvement of FFA in the enzymes activity.

Knowledge of the 3-dimensional structure of cytochrome oxidase may provide more clues to the relationship between proton translocation and charge separation. Required protons are of two types: pumped protons which are translocated across the membrane, and chemical protons which are consumed upon the reduction of oxygen to water. Both processes involve proton channels, which move of protons past amino acid residues to the binuclear centre.

Iwata *et al.* (1995) have proposed that movement of protons occurs exclusively through two separate channels, one for pumped protons, and a second for chemical protons (Figure 5.1). In their model, protons to be pumped enter a channel at Asp124 through to Glu28 and to His325, which is a ligand to Cu_B. His325 is proposed to occur in two possible conformations, and to cycle through imidozolate, imidizole, and imidozolium states. In its initial form (imidazolate state), His325 forms hydrogen bonds with Cu_B and Thr344. Upon a single electron reduction of the binuclear centre, a proton is taken up, converting His325 to the neutral imidazole form. During a second reduction step, a second proton is taken up and will be bound to His325. This can only occur when His325 rotates to an alternate binding configuration, forming a hydrogen bond with the formyl group of haem a_3 and Phe340. After this, protons are passed onto Leu393 and Asp399.

Tsukihara *et al.* (1996) have proposed several possible proton pathways across the membrane. One of these is a channel involving no contact with or influence from haem groups. A second proton translocation channel spans the distance from Asp407 at the entrance onto Arg38, Asn451, and Tyr443 at the exit. This second channel has branch leading to haem *a*, and suggests that proton translocation is in some way controlled by the redox state of that haem. Both proposed channels are remote from the binuclear centre, but may still be coupled to oxygen reduction in some

Figure 5.1: Proposed proton channel involved in the translocation of protons and reduction of molecular oxygen to water in *Paracoccus denitrificans* cytochrome *c* oxidase. Translocated and chemical protons enter the channel at different residues (from Tsukihara *et al.*, 1996).

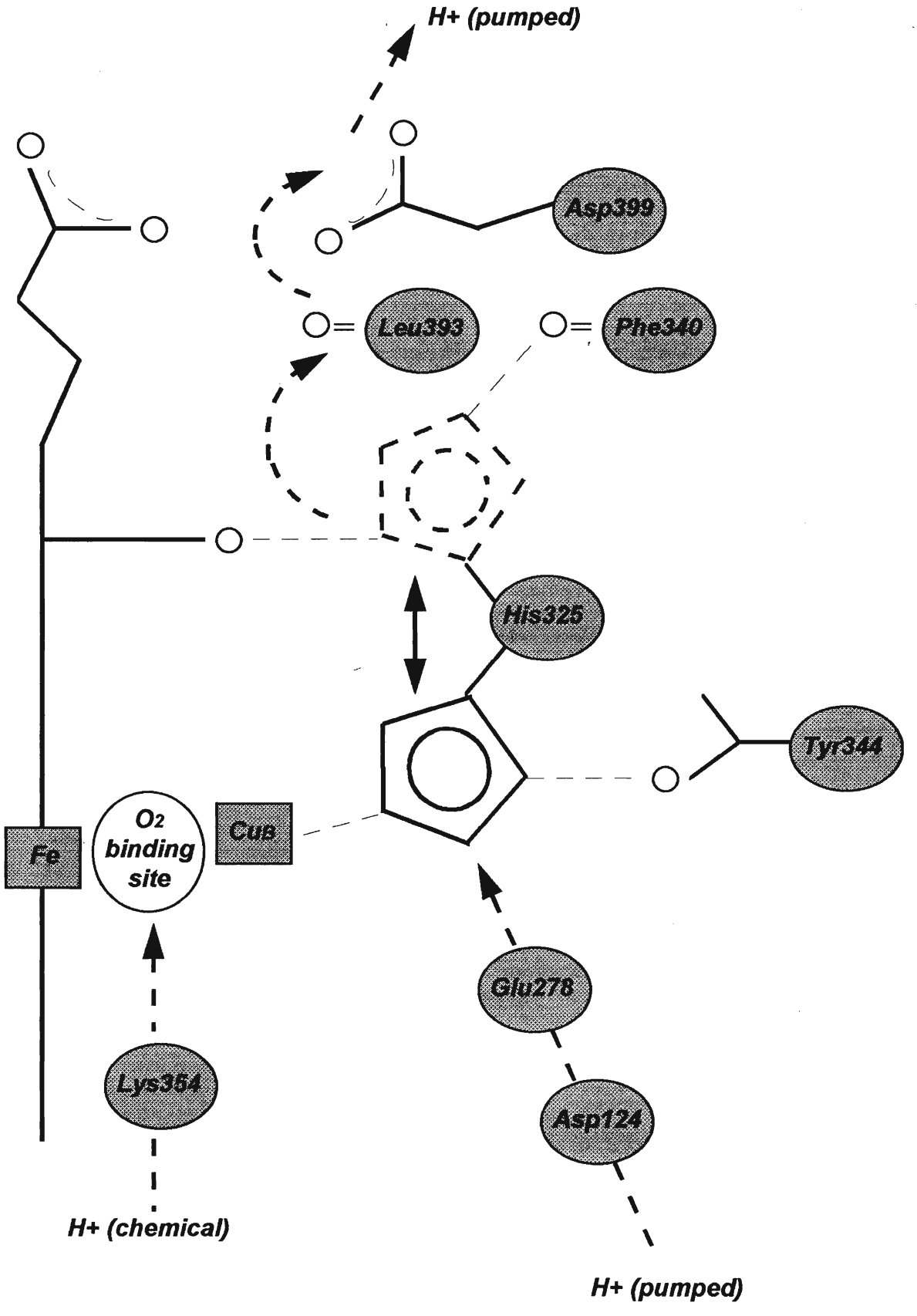
H+ (pumped)
Asp399
Leu393
Phe340
His325
Tyr344
Fe
O2 binding site
CuB
Glu278
Lys354
Asp124
H+ (chemical)
H+ (pumped)

way. A third network, spans the gap from Lys265 to Tyr244 which is connected to His240, a ligand of Cu_B (Figure 5.2). This makes it a likely channel to be involved in the movement of protons for water formation. However, it may also serve as a proton translocation channel through its links to His240, Cu_B and His291. The Cu_B may control the pK values of the two imadazole ligands to produce unidirectional proton transfer, coupled to its redox state.

The action of FFA in proton pumping may involve an association with one or more of the proposed proton channels. The carboxylic group of FFA makes it suitable for the involvement in a proton shuttle system. The question remains on how and where it might be involved in a shuttle system. The relative size of FFA makes it a large molecule to be incorporated deep within the enzyme. The 3-dimensional structure does not indicate the presence of a FFA molecule or possible entrance site for such a molecule. It is the carboxylic group that is required in proton transfer. FFA may wrap themselves to the oxidase in such a way as to expose the polar head group within a prominant position in a channel. The potential position of the head group within the channel is not known, but is most likely in such a place as to accomadate the long carbon tail and polar head group. Possible positions may be close to the entrance or exit of the proton channel. The data presented here has shown that under conditions where proton pumping activity is absent, the addition of FFA results in the restoration of activity. The elimination of proton pumping activity in the presence of BSA is not fully understood. The increase in the reduction of cytochrome *a* in the presence of BSA (Sharpe *et al.*, 1996) may be linked to the decline in proton pumping activity. A proposed proton channel (Tsukihara *et al.*, 1996) suggests a linkage between the redox state of cytochrome *a* and proton transfer. FFA may be involved in electron transfer between cytochrome *a* and the binuclear centre (Sharpe *et al.*, 1996). The removal of FFA may prevent this transfer, increasing the steady-state reduction level of cytochrome *a* and thus stop proton translocation.

Figure 5.2: Proposed proton channel involved in proton translocation from bovine heart cytochrome *c* oxidase. In this channels, protons enter at Lys265 and exit at Tyr244. This channel involves residue His240, which is a ligans to the Cu_B atom (from Tsukihara *et al.*, 1996).

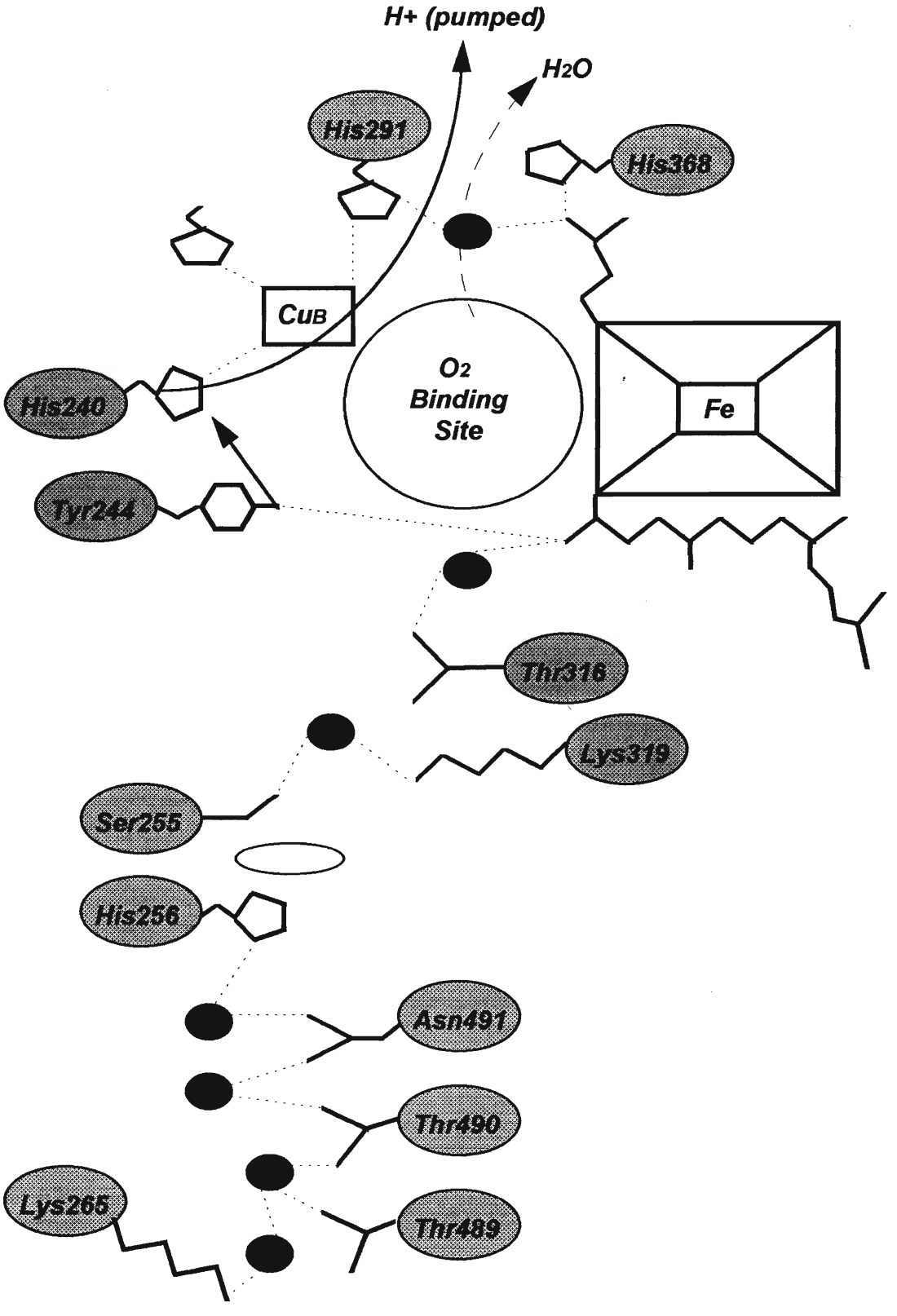
H+ (pumped)
H2O
His291
His368
CuB
O2
Binding
Site
Fe
His240
Tyr244
Thr316
Lys319
Ser255
His256
Asn491
Thr490
Lys265
Thr489

5.2 Influence of Bulk pH on ΔpH Formation in Bovine Heart COV

An influence of ΔpH on cytochrome *c* oxidase activity is well known. The pH gradient provides a greater control over enzyme turnover than does $\Delta\Psi$. A ΔpH of 0.1 unit has been shown to result in a 10% decrease in enzyme activity (Nicholls,1990). However, the effect of ΔpH can be difficult to interpret as results may be due to changes of pH inside the COV instead of ΔpH. This can be probed by observing the effects of bulk pH on enzyme activity. The presented results indicated that the bulk pH has very little influence on ΔpH formation in bovine heart COV. Enzyme turnover on the other hand is highly influenced by bulk pH, where the greatest turnover rates being observed in the acidic region. What is the relationship between enzyme turnover and ΔpH control?

Enzyme turnover results in proton consumption by O_2 reduction and proton translocation, which generate a ΔpH (Figure 5.3A). Prior to turnover and at an acidic external pH, proton equilibration may occur if protons can enter the COV, decreasing the internal pH. A similar equilibration may occur at an alkaline external pH, with protons initially moving out of the COV resulting in an increase of the internal pH (Figure 5.3B). Upon initiation of enzyme turnover, protons are consumed internally and translocated. Lost protons in the proton channels are replaced by the existing internal proton sinks. This allows turnover to continue and produces a ΔpH, alkaline inside. When the initial bulk pH is alkaline, the steady state ΔpH is smaller than at neutral or acid pH. Fewer protons are internally available at alkaline pH values to move into the proton channels to replace protons consumed or translocated. At steady state, the resulting ΔpH formation is therefore decreased. At an acidic pH more protons are available both in the internal sink and the channels, which allows a higher turnover rate and a larger steady state ΔpH to be maintained.

Figure 5.3: Proton equilibration and ΔpH formation at acidic and alkaline bulk pH. A. Proton equilibration at an acidic pH. Protons move into the COV, thus increasing proton availability for turnover and ΔpH formation. B. Proton equilibration at an alkaline pH. Protons move out of the COV, decreasing proton availability for turnover and ΔpH formation.

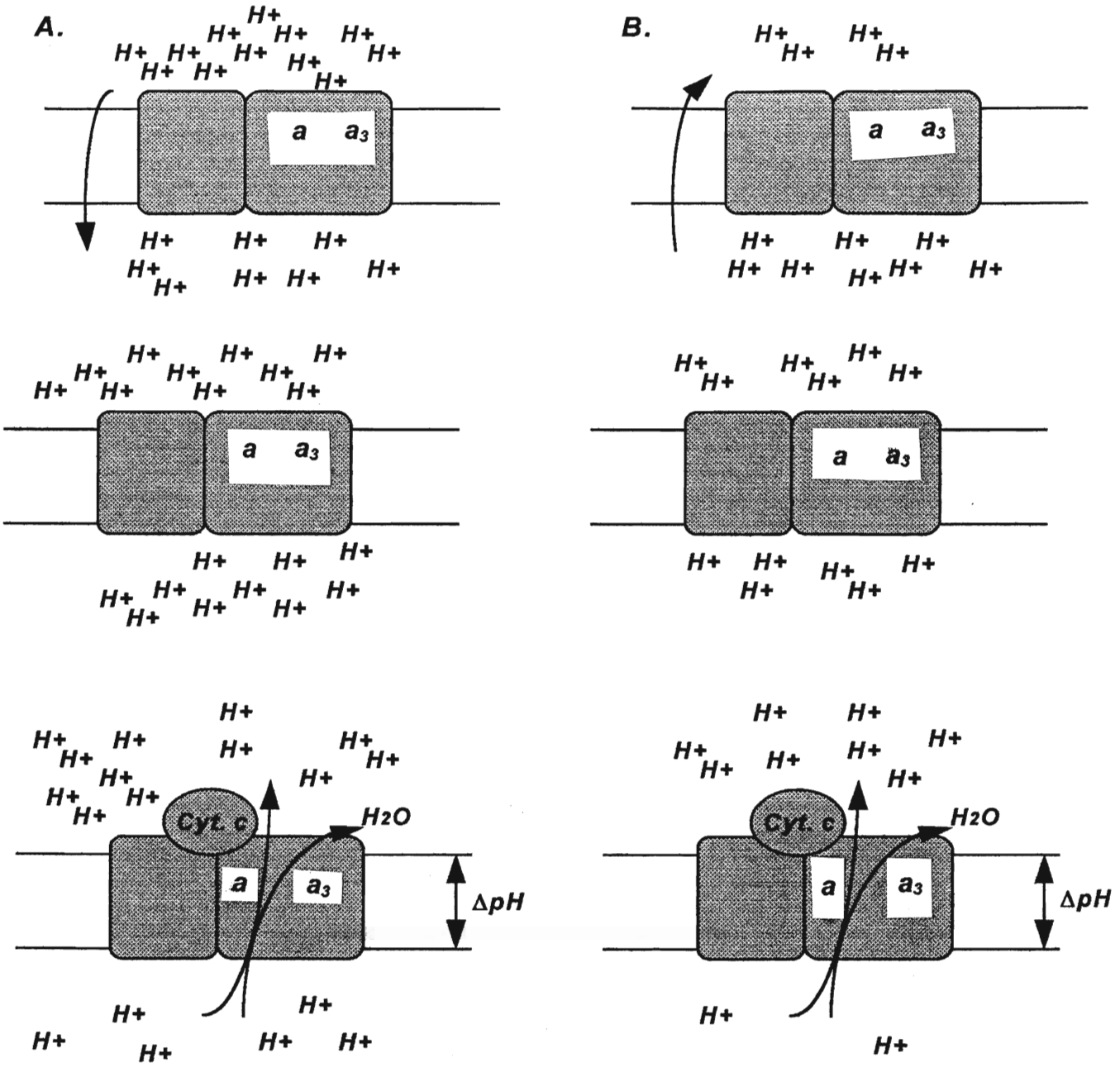
A.
B.
H+
a
a3
Cyt. c
H2O
ΔpH

ΔpH affects electron transfer from cytochrome *a* to the binuclear centre and can decrease enzyme activity 10% for every 0.1 ΔpH unit (Nicholls, 1990). The data presented here indicate that proton pumping and charge separation are not pH ndependent. A decrease in ΔpH at an alkaline pH is advantageous for electrochemical potential formation. A smaller ΔpH will exert less control on enzyme turnover in an environment where proton availability is limited. This feedback system is characteristic of cytochrome *c* oxidase. At low pH values enzyme turnover is high, producing a larger ΔpH, which exerts a greater control on turnover. Conversely at high pH, turnover is low, producing a smaller ΔpH, which exerts less control on turnover. Oxidase induced ΔpH formation exhibited only small trends between external pH values of 6.2 to 7.8. The influence of ΔpH is highly controlled. Large changes in ΔpH would cause an enormous change in enzyme turnover, which may not be advantageous. Small changes in ΔpH allow for a more constant rate of enzyme turnover, and better adaptation to changing environmental conditions.

5.3 pH Effects on the Kinetics of Vesicular Cytochrome c oxidase

Cytochrome *c* oxidase has two cytochrome *c* binding sites. These binding sites are characterized as being either high or low affinity. The influence of bulk pH is most marked at the low affinity binding site. The enzyme turnover is greatly influenced by the gradient across the membrane. Under full or partial control, turnover of COV shows only a small dependence on pH. In the fully uncontrolled state, enzyme turnover drops dramatically at an alkaline pH. The respiratory control ratio of the COV has a maximum at pH 7.0. The K_m values at the low affinity binding site decrease with an increase in pH in both the controlled and uncontrolled states. Bulk pH does influence biphasic kinetics, largely by moderating the enzyme at the low affinity binding site.

The enzyme turnover is greatest in the acidic pH region. Protons are a substrate for cytochrome *c* oxidase. At a lower pH, proton availability is high, and thus the proton channels involved in proton translocation and the formation of water are

maintained in their protonated state. Electron movement to the binuclear centre for oxygen reduction can therefore proceed at a greater rate. The differences in turnover between the controlled or partially controlled states and the uncontrolled state indicate the chemiosmotic control that is being. The V_{max} at the low affinity binding site indicate is the predominant contributor to enzyme turnover. V_{max} at the high affinity binding site represents < 10% of the total turnover of the enzyme. The low affinity K_m decreases with increase in pH. The binding of cytochrome *c* to the enzyme involves electrostatic interaction between amino acid residues. Residues on the enzyme are negatively charged, and attract the positive charges on the cytochrome *c*. However, protons may influence this enzyme-substrate interaction by competing with cytochrome *c* in binding to the negatively charged binding site. At higher proton concentrations, competition for the binding site is greater, and the K_m value will therefore be greater.

At all pH values, the K_m decreases with the loss of chemiosmotic control. The magnitude of this decrease in K_m is pH dependent. Decrease in chemiosmotic control implies an increase in enzyme turnover. The elimination of control affects binding site competition between positively charge ions and cytochrome *c*. When ΔpH is negligible, proton interaction with the enzyme changes in two different areas. Externally, the proton concentration decreases and protons are therefore not available to compete with cytochrome *c* at the negatively charged binding site. This lowers the apparent K_m for cytochrome *c*. Internally, an increase in proton availability allows for protonation of proton channels. The addition of valinomycin eliminates $\Delta\Psi$, and initially results in a decrease in enzyme turnover. The K_m at the low affinity binding site may decreases due to the decrease in positive charges, allowing for increased cytochrome *c* binding. Proton interaction with the cytochrome *c* binding site is greater at an acidic pH. The sudden release of proton equilibrium is therefore more significant at the lower pH. As proton concentration decreases, the sudden release of proton equilibrium is less

significant. In the alkaline pH region, proton concentration is too low to have much initial influence on K_m.

5.4 Steady State Reduction of Cytochromes c and a in Bovine Heart COV

This study has examined the influence of bulk pH on the steady state reduction of cytochromes *c* and *a* in proteoliposomal systems. Using COV Nicholls (1993) have showed specific haem response of cytochrome *c* and cytochrome *a*. Cytochrome *c* reduction was dependent on enzyme flux, while cytochrome *a* reduction was independent of the flux. This was also observed here, in all energetic states. Cytochrome *a* maximal reduction at a given cytochrome *c* reduction is dependent on the energetic state. Cytochrome *a* reduction is greater in the presence of a ΔpH, and small in the presence of $\Delta\Psi$ alone and in the uncontrolled state. The K_{eq} increased with pH and is independent of the energetic state. This suggests that the reduction of cytochrome *a* is associated with the uptake of a proton.

If cytochrome *a* reduction involves the uptake of a proton, where does this proton come from? Protons can come from either the external medium or the interior of the COV. Figure 5.4 presents two possible models that may account for the uptake of a proton associated with cytochrome *a* reduction. In the first model (Model A), a proton is taken up from the external medium. At first glance this model is favourable due to the close proximity of cytochrome *a* to the external surface, and due to the fact that this proton movement is subject only to 1/3 of $\Delta\Psi$ control. Cytochrome *c* oxidase turnover produces a ΔpH through the consumption of protons in the formation of water and proton translocation. Two protons from the interior of the COV are therefore required to produce a ΔpH. One of these protons is consumed, while the other is translocated. The oxidation of cytochrome *a* upon giving up its electron to the binuclear centre also

Figure 5.4: Proposed models for the association of proton uptake and the reduction of cytochrome *a*. A. This model predicts the uptake of a proton to occur from the external medium. Upon oxidation of cytochrome *a* the proton is released back into the external medium. Proton translocation and oxygen reduction obtain their respective protons from the COV interior via other proton channels. B. In this model, cytochrome *a* is protonated by protons from the interior of the COV. This may involve a predicted proton pumping channel and may suggest the involvement of cytochrome *a* in proton translocation.

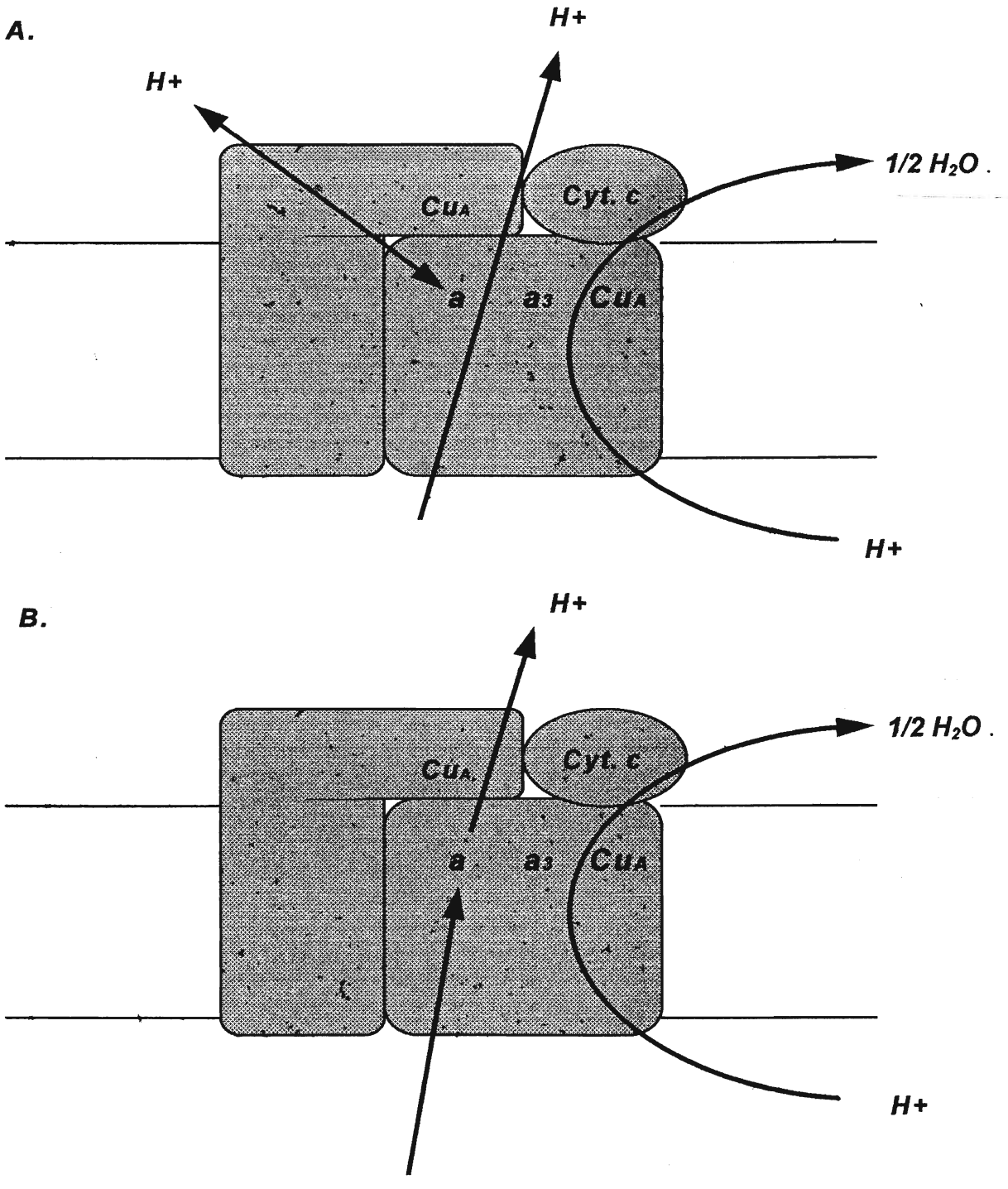
A.
H+
H+
1/2 H2O .
CuA
Cyt. c
a
a3
CuA
H+
B.
H+
1/2 H2O .
CuA
Cyt. c
a
a3
CuA
H+

results in the loss of its proton. This proton is presumably transferred back to the external medium. The movement of the proton into the COV would suggest a reverse proton pump, which is not likely. $\Delta\Psi$ control is minimal in this model. The elimination of $\Delta\Psi$ control would not have a great influence on this model system. The second model (Model B) presents the uptake of a proton from the interior of the COV to be associated with the reduction of cytochrome *a*. A proton channel involving cytochrome *a* has been suggested from the 3-dimensional structure of cytochrome *c* oxidase (Tsiukahara, *et al.*, 1996). The oxidation of cytochrome *a* upon giving up its electron releases its proton. This may suggest that cytochrome *a* is involved in proton translocation. A second proton from the interior is taken up to the binuclear centre and is involved in water formation. In this second model, proton uptake is under 2/3 $\Delta\Psi$ control. The elimination of $\Delta\Psi$ in this model system would greatly influence cytochrome *a* reduction. The data presented here suggests a $\Delta\Psi$ sensitivity to cytochrome *a* reduction.

Model B implicates the protonation of cytochrome *a* through a proton channel. The actual protonated species linked to the haem iron in cytochrome *a* is not yet identified. Inspection of the 3-dimensional structure of cytochrome *c* oxidase reveals no amino side side chains with the appropriate properties. The farnasyl side chain of haem *a* is located nearer the interior side of the enzyme. This side chain does not contain any known protonatable groups is most likely not involved in proton uptake. Propionate residues of the haem ring are located nearer the external surface and are not easily accessible by interior protons. They are however, a more likely candidate to be involved in proton uptake. Studies presented here have indicated a possible involvement of free fatty acids in the proton pumping mechanism of cytochrome *c* oxidase. The carboxylic group of free fatty acids may provide an ideal protonatable group. They may incorporate themselves in close proximity to cytochrome *a*; the reduction of the latter may be linked to proton uptake by the free fatty acids. It however remains unclear where proton uptake occurs with the reduction of cytochrome *a*.

5.5 Structure of Bacillus subtilis caa_3

The cytochrome caa_3 oxidase is unique among the family of bacterial oxidases because of a covalently bound cytochrome *c* attached to subunit II of the enzyme. This type of oxidase has been found in a variety of prokaryotic species, including *Bacillus subtilis, Bacillus stearothermophilus, Thermus thermophilus,* and *Paracoccus denitrifcans.* The caa_3 oxidase is typically associated with other cytochrome oxidases as part of a branched respiratory chain. The existence of multiple oxidases raises the question of the functional role of these secondary oxidases. The vast and harsh environmental conditions under which prokaryotes can be found may be implicated in the evolution of a branched respiratory system. I have attempted to examine the structure of *B. subtilis* caa_3 oxidase as it relates to its role.

The results indicated a possible cytochrome *c* to cytochrome *a* ratio of greater than 1 for *B. subtilis* caa_3. Three different models can be constructed to account for such a ratio (Figure 5.5). Model A requires a second covalently bound cytochrome *c* on the enzyme. However, the genes sequence for the caa_3 protein have been sequenced for both the *B. subtilis* and *B. stearothermophilus* (Saraste *et al.,* 1991; Kusano *et al.*, 1996). The analysis indicated a single cytochrome *c* coding region adjacent to the coding region for subunit II. Approximately 100 amino acids form the cytochrome *c* domain, and contains the consensus haem *c* attachment site, CXXCH. This similar coding region in *T. thermophilus* also codes for cytochrome *c* (Buse *et al.,* 1989). No other cytochrome *c* coding sequence has been identified within the caa_3 genes. This therefore indicates that a second covalently bound cytochrome *c* molecule is not present.

A second model (Model B), postulates a loosely associated cytochrome *c*, isolated along with the caa_3 enzyme. There are available at present only four complete primary structures of Gram-positive bacterial cytochrome *c*: *B. subtilis* cytochrome c_{550},

Figure 5.5: Representative models of observed cytochrome *c* to cytochrome *a* ratios in *Bacillus subtilis* cytochrome *caa3* oxidase. Measurements were obtained by comparing the 550-540 nm vs 604-630 nm of reduced minus oxidized spectra. A. This model suggests two covalently attached cytochrome *c* molecules to subunit II of the enzyme per one cytochrome *a*. B. In this model, exogenous cytochrome *c* is present along with the *caa3* enzyme. C. Two different populations of the *caa3* enzyme are predicted by this model. One population contains the fully functional native enzyme, while a second population contains an active cytochrome *c* portion, but an inactive *aa3* portion of the enzyme.

A.

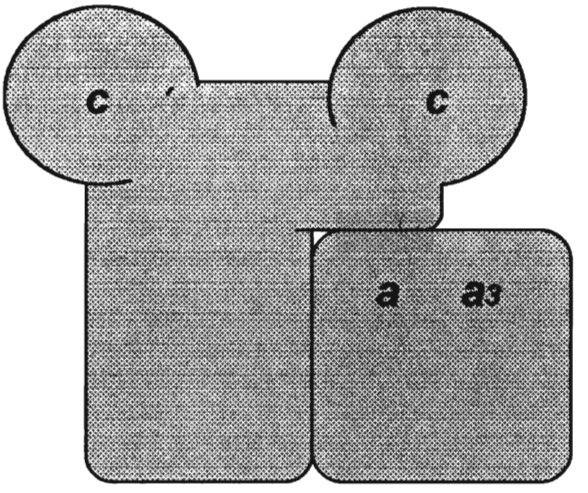

B.

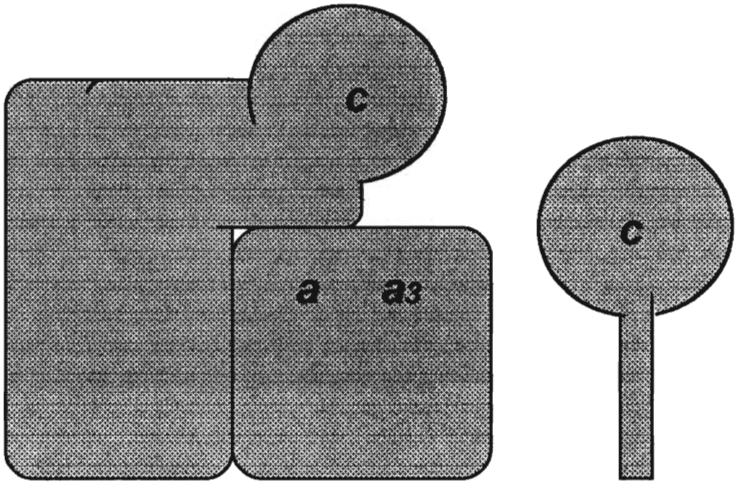

C.

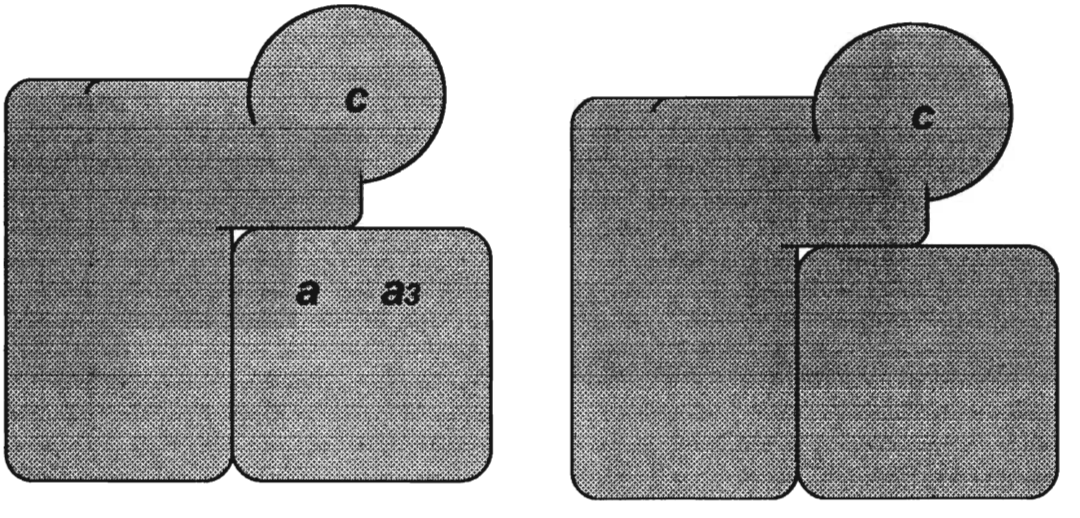

Bacillus PS3 cytochrome c_{551}, and the haem *c* containing subunits II of cytochrome *caa3* oxidase from *B. subtilis* and *Bacillus* PS3 respectively. In the Gram-negative *P. denitrificans*, cytochrome c_{552} is associated with the plasma membrane. In *B. subtilis* four different types of cytochrome *c* have been identified with molecular weights of 16, 22, 29, and 52 kDa (von Wachenfedlt and Hederstedt, 1990) All the *B. subtilis* species of cytochrome *c* are found in the plasma membrane and can be released only by detergent (von Wachenfedlt and Hederstedt, 1990). Cytochrome c_{550} is the smallest of these membrane anchored *c* type cytochromes, with an estimated mass between 13 and 16 kDa, and a two domain structure. A membrane anchored N-terminal domain is composed of 25 to 30 amino acids in an alpha-helical conformation. The haem domain is located on the outer surface of the plasma membrane, and shows similar 3-dimensional structure to that of the eukaryotic cytochromes *c*. *B. subtilis* cytochrome c_{550} is similar to *Pseudomonas aeruginosa* cytochrome c_{551} (von Wachenfedlt and Hederstedt, 1990). De Vriij *et al.* (1987) also described a cytochrome c_{554} of a *B. subtilis* strain W23 with a molecular weight of approximately 30 kDa. The remaining two cytochrome *c* species have yet to be characterized. The cytochrome *c* portion of subunit II shows sequence similarity to the mitochondrial cytochrome *c* group (37% amino acid homology). EPR-spectra of the isolated *caa3* enzyme contain a g = 3.46 signal assignable to the cytochrome *c* domain. This is similar to the EPR spectrum of *B. subtilis* cytochrome c_{550}, indicating structural similarities between the two proteins (Lauraeus *et al.*, 1991). A number of different cytochrome *c* species are therefore possible natural contaminants in the isolated caa_3 enzyme. To examine the possibility of a loosely associated cytochrome *c* molecule with the caa_3 enzyme the SDS-PAGE protein and haem stain analyses were performed. The results showed that no such cytochrome *c* of any kind is associated with the isolated enzyme.

The third model (Model C) postulates two populations of caa_3 enzyme. One population consists of the native fully functional enzyme, while a second population contains an active cytochrome *c*, but inactive cytochromes *a* and a_3. This results in an excess of haem *c* to one haem *a*. Such selectivity could be a result of the sensitivity of the caa_3 enzyme to environmental conditions. Baines and co-workers (1984) examined cytochrome caa_3 oxidase from the thermophilic bacterium PS3. Spectral analysis indicated a disappearance of the haem *aa3* signal in the visible region (605 nm) upon storage of the enzyme at $4^{o}C$ for 30 days. In the Soret region, a broad band at 430 nm appeared. Enzyme stored at $77^{o}K$ for 30 days showed smaller changes in the spectra, but the apparent haem *c* to haem *a* ratio for this enzyme was still greater than 1. The observations of Baines (1984) and those made here might indicate that loss of both haems *a* and *a3* may occur following prolonged storage of the enzyme.

None of the three models presented may prove necessary. Apparent haem *c* to haem *a* ratios of greater than one may be due to the use of erroneous extinction coefficients. Cytochrome *c* extinction coefficients often differ among species (Hon-ami and Oshida, 1984). Cytochrome *a* extinction coefficients may also show differences. Re-analysis of the haem *c* to haem *a* ratios using three extinction coefficients shows substantial change in ratios (Table 5.1). The haem *c* to haem aa_3 ratios of the reduced minus oxidized spectra of caa_3 were calculated using the extinction coefficients indicated by the authors, classical bovine heart values, and those of Henning *et al.* (1995). Fee *et al.* (1980) calculated the haem *c* to haem aa_3 ratio for caa_3 in *T. thermophilus* HB8 to be 0.88 using single wavelength extinction coefficients. A comparison of haem *c* to haem aa_3 ratios using different single wavelength extinction coefficients indicates very similar values. Sone and coworkers (Sone and Yanagita, 1982; Kusano *et al.*, 1996) calculated the haem *c* to haem aa_3 ratios of *Bacillus* PS3 and *B. stearothermophilus* using difference spectra extinction coefficients. The values

obtained were greater than 1 in for both species. The haem *c* to haem aa_3 ratios increased when classical bovine heart extinction coefficients were used. When using the extinction values from Henning *et al.* (1995), the haem *c* to haem aa_3 ratio decreased to a value very near 1. In this work, the haem *c* to haem aa_3 ratio of *Bacillus subtilis* caa_3 was calculated using classical bovine heart extinction values. When recalculated with the values of Henning *et al.* (1995), the haem *c* to haem aa_3 ratio decreased significantly from 2.17 to 1.47. Using the classical extinction values to calculate the haem *c* to haem aa_3 ratio for *B. subtilis* caa_3 in Henning *et al.* (1995) resulted in a 40% increase in the ratio. In all cases, the use of classical bovine heart extinction CO-efficient values resulted in the largest haem *c* to haem aa_3 ratio. Haem *c* to haem aa_3 ratios of very near 1 were obtained in all but the work presented here when extinction values from Henning *et al.* (1995) were used. The haem *c* to haem aa_3 ratio is still greater than 1, indicating possible loss of haem *a* and haem a_3 activity.

Cytochrome *c* extinction coefficients vary greatly among species and may have a profound effect on haem *c* to haem *a* ratio. The cytochrome *a* extinction coefficients (605-630 nm) for the classical bovine heart enzyme and that used by Henning *et al.* (1995) for caa_3 are similar. The difference in the observed ratios is due to the cytochrome *c* extinction co-efficient.

The varying range in cytochrome *c* to cytochrome *a* ratios in *caa3* enzymes observed here and elsewhere may be due to simple enzyme degradation and extinction coefficient determination. The presence of two different enzyme populations due to enzyme degradation produces an underestimation of cytochrome *a* concentration in the enzyme sample. Baines (1984) showed how storage of the caa_3 enzyme resulted in a decrease in the 605 nm peak of the enzyme. Data presented here also shows a decrease in the 604 nm peak along with prolonged extension of the visible region peak over a large nm range. Again this shows a possible degradation of the enzyme. The extinction coefficients used in calculating cytochrome *c* and *a* content vary in values.

Table 5.1: Comparison of cytochrome *c* to *aa3* ratios of various cytochrome *caa3* oxidases. Reduced minus oxidized spectra were obtained from the indicated authors. The extinction coefficients used were from: (a) the indicated authors, (b) classical beef and horse heart values (see text), and (c) Henning *et al.*, (1995).

Spectra Reference (Reduced-oxidized)	#	*ε haem c 550 -540 nm* $mM^{-1}\ cm^{-1}$	*ε haem c 550 nm* $mM^{-1}\ cm^{-1}$	*ε haem aa3 605-630 nm* $mM^{-1}\ cm^{-1}$	*ε haem aa3 605nm* $mM^{-1}\ cm^{-1}$	*[cyt.c] μM*	*[cyt.aa3] μM*	*c:aa3 Ratio*
Fee et al. (1980) T. thermophilus HB8	a	-	22.7	-	23.4	0.38	0.42	0.88
	b	(21.1)	20	(27)	24	0.42	0.41	1.03
	c	(30)	25.7	(26)	23.9	0.33	0.41	0.80
Sone and Yanagita (1982) Bacillus PS3	a	21.2	(21.2)	23.2	(21.0)	2.48	1.96	1.26
	b	21.1	(20)	27	(24)	2.49	1.69	1.48
	c	30	(25.7)	26	(23.9)	1.75	1.75	1.00
Kusano et al. (1996) B. stearothermophilus	a	21.2	(21.2)	23.2	(21.0)	1.08	0.79	1.38
	b	21.1	(20)	27	(24)	1.09	0.68	1.61
	c	30	(25.7)	26	(23.9)	0.77	0.70	1.09
Henning et al. (1995) B. subtilis	a	30	(25.7)	26	(23.9)	0.005	0.005	1.00
	b	21.1	-	27	-	0.007	0.005	1.44
This work (1996) B. subtilis	a	21.1	(20)	27	(24)	1.69	0.78	2.17
	c	30	-	26	-	1.19	0.80	1.47

a, extinction coefficients used by the indicated authors.
b, extinction coefficients from classical beef and horse heart values (see text).
c, extinction coefficients from Henning et al. (1995).

Precise extinction coefficient determination for each sample of enzyme is required in order to determine accurate cytochrome *c* to cytochrome *a* ratios in the *caa3* enzyme.

5.6 Bioenergetics of Bacillus subtilis caa$_3$

The branched respiratory chain in prokaryotes provides an organism with a second terminal electron acceptor, which may be used in times of nutritional stress or to maintain cellular activity under dormant conditions. The function of these secondary oxidases in relation to the major oxidase species is not fully understood. In *B. subtilis*, this secondary terminal electron acceptor is the cytochrome *c* oxidase *caa3*. Further questions arise with *caa3* due to the presence of a covalently bound cytochrome *c* moiety to the enzyme. What is the mechanism of electron transfer through the enzyme? How is it linked to charge separation and proton pumping? Both cytochromes *c* and *a* may be implicated. Answers may provide an insight into the functional role of the *caa$_3$* enzyme as a secondary oxidase. We have attempted to begin to answer such questions by examining the bioenergetic characteristics of the *caa3* enzyme. The respiratory control ratios, the proton pumping, and the steady state reductions were all examined of cytochrome *c* and *a* during steady state respiration in *caa3* COV are discussed.

In reconstituted systems a proportion of the enzyme population will be oriented inside-out. Two different populations of enzyme may also be present in terms of their functionality. One of these is the native active enzyme (A), while the second may contain an active cytochrome *c* portion, but an inactive cytochrome *a* and *a$_3$* (I). These two populations are also subject to different orientations, either right-side-out(R) or inside-out (I). There are therefore four possible populations of enzyme within the COV: AR, AI, IR, and II (Figure 5.6). Both AR and IR vesicles show cytochrome *c* reduction, but only the AR vesicles will show enzyme activity and proton pumping. In the presence of TMPD, which is capable of moving across the membrane, the AI

Figure 5.6: Representative populations of enzyme in *B. subtilis* caa_3 COV. Four different populations of COV are possible: active right-side-out (AR), active inside-out (AI), inactive right-side-out (IR), inactive inside-out (II). The relative proportions of these populations may determine the activity shown by the COV.

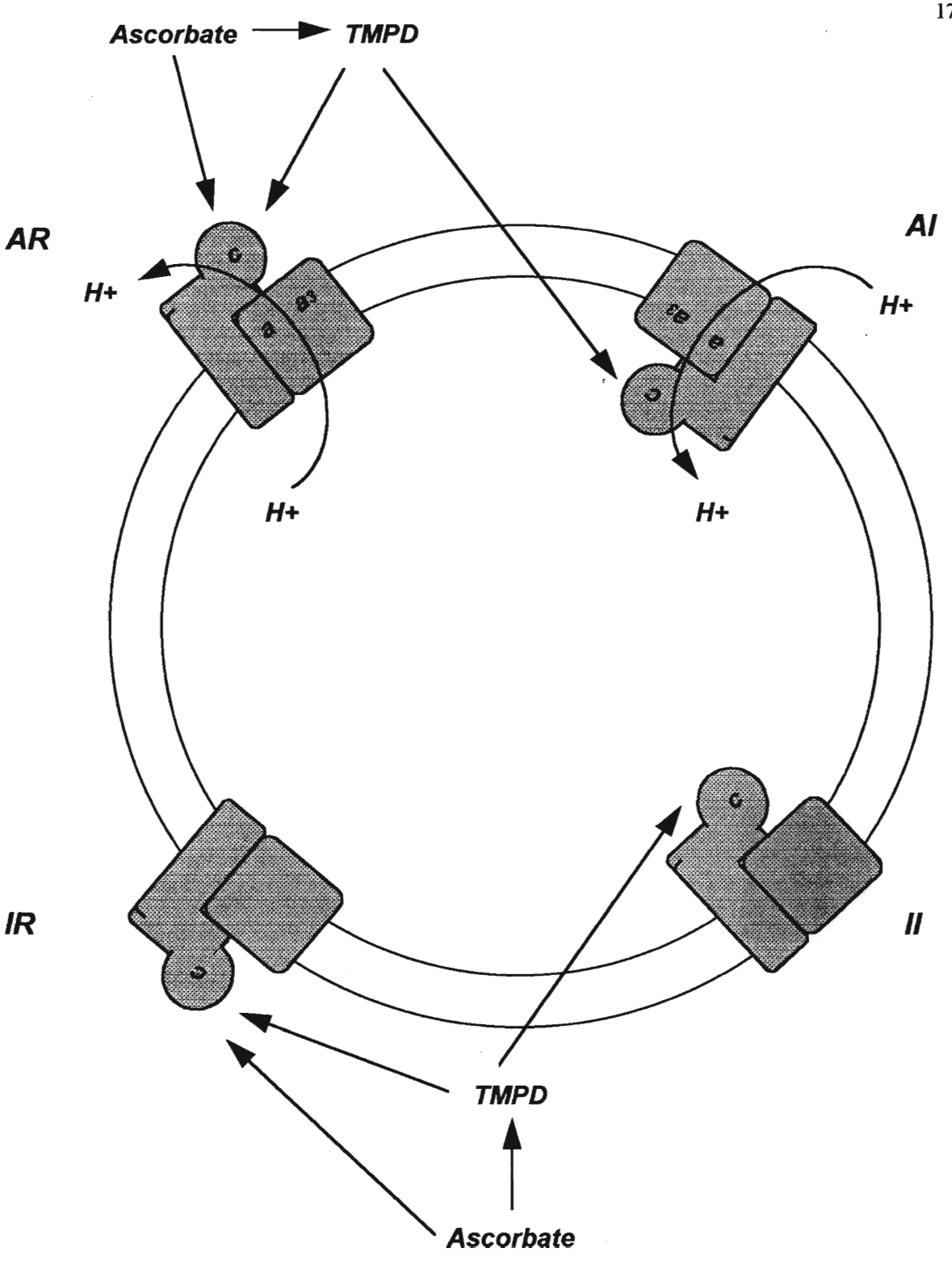
Ascorbate
TMPD
AR
AI
H+
H+
H+
H+
IR
II
TMPD
Ascorbate

vesicles may be able to show cytochrome *c* reduction and proton pumping activity. The extent of inactivation of cytochrome *a* and a_3 may vary from partially to complete.

The respiratory control ratio (RCR) is a measure of the kinetic control of enzyme turnover in the coupled state (when both $\Delta\Psi$ and ΔpH are present) of the COV. The respiratory control ratios observed for the caa_3 COV ranged between 1.1 and 2.2 depending on the respiratory medium used. Under low ionic strengthconditions with ascorbate alone, the respiratory control ratio was maximal. Ascorbate reduces bound externally facing cytochrome *c* at low ionic strength. At a higher ionic strength, enzyme turnover is increased but, TMPD is needed as a redox mediator. In the presence of TMPD, a slightly lower respiratory control ratio was found. TMPD is membrane permeable and may therefore be able to move into the COV and possibly donate its electrons to inward facing caa_3. The turnover of the inward facing caa_3 will pump protons into the internal space of the COV. This will decrease the ΔpH control of enzyme turnover. This is reflected in the lower RCR values, as is seen here.

When exogenous horse heart cytochrome *c* was added in the low ionic strength medium, the respiration rate was substantially higher, but the COV no longer responded to ionophores (RCR = 1.1). As in the case of TMPD at higher ionic strength, reduction of inward facing caa_3 may have occurred. This would normally require the movement of cytochrome *c* across the membrane. However, the presence of cytochrome *c* may also influence membrane permeability to protons. Rapid return of protons into the COV will eliminates pH control.

The caa_3 COV showed proton pumping activity to a level at least 50% that of bovine heart enzyme. Proton pumping activity of caa_3 from various species of prokaryotes has been measured in proteoliposomes by several workers. Using reconstituted vesicles of *T. thermophilus* caa_3, Hon-nami and Oshima(1984) found a H^+/e^- ratio of 0.83. Proton pumping has also been shown for *Bacillus* PS3 (Sone and

Yanagita, 1982; Sone and Hinkle, 1982). Sone and Yanagita (1984) claimed that H^+/e^- ratios in PS3 *caa3* can be as high as 1.4 . Only the ARS enzyme will show proton pumping activity. This population of enzyme will vary in its extent of inactive cytochrome *a* and a_3 . Some of the 'inactive' ARS population may in fact be capable of partial reduction of O_2 to water, thus consuming protons, but be unable to pump protons. Such 'slip' and may account for measured H^+/e^- ratios of 0.50. Subsequent alkalinization of the medium, which occurs as protons move back across the membrane is due to the net consumption of protons in the reduction of oxygen.

In eukaryotic COV, cytochrome *c* and *a* reductions are independent. Cytochrome *c* reduction is linearly related to the flux through the system, and cytochrome *a* reduction is rather independent of flux. Although cytochrome *a* is normally the immediate electron donor to the binuclear centre, its redox state does not change under conditions of increasing flux through the enzyme and remains partially reduced during steady state. This suggests the possibility of a second electron transfer pathway to the binuclear centre, most likely involving Cu_A (Nicholls, 1993). The model proposed by Nicholls (1993) contains a three electron movement from cytochrome *a* (originally received from Cu_A) to the binuclear centre, and a further one electron movement from Cu_A directly to cytochrome a_3. Rereduction of the binuclear centre occurs when oxygen is added to the fully reduced enzyme. This further reduction, required to produce an oxygen-reactive species, may be associated with the direct electron transfer from Cu_A in the steady state where flux increases without any corresponding change in the cytochrome *a* redox state.

The steady state reductions of cytochrome *c* and *a* in caa_3 COV were examined in the controlled, partially uncontrolled and fully uncontrolled state. Increasing levels of ascorbate induced progressively higher rate of reduction in both haems. Cytochrome *c* and *a* were reduced in parallel, with nearly equal redox potentials, giving a form of the

enzyme with both centres fully reduced at maximal turnover. Unlike the eukaryotic system, neither cytochrome *c* nor cytochrome *a* reductions are proportional to flux.

Multiple oxidases have evolved in prokaryotic organisms. The caa_3 enzyme of *B. subtilis* is probably a secondary oxidase and its functional role is still uncertain. Steady state reduction studies of caa_3 COV may provide some clues to a possible functional role for this enzyme. Steady state kinetic studies of *T. thermophilus caa3* have previously been carried out (Yoshida and Fee, 1984) using TMPD, horse heart, and *Candida crusei* cytochromes *c* and cytochrome c_{552} isolated from the periplasmic space of *T. thermophilus.* All mediated a caa_3 catalyzed oxidation of ascorbate with the largest TN of [a] 130 electrons per second per aa_3 . The oxidation of mediators such as TMPD and of cytochromes *c* were independent and additive, suggesting two substrate binding sites on the enzyme (Yoshida and Fee, 1984). It was presumed that TMPD transferred electrons to the cytochrome *c* portion of caa_3, while the cytochromes *c* transferred electrons directly to the aa_3 portion of the enzyme (Yoshida and Fee, 1984). EPR data (Fee *et al.,* 1986) suggested that the binuclear centre may act as a two electron acceptor and not by the sequential one electron transfers observed in the bovine enzyme. The high reduction levels of cytochrome *c* and *a* indicate a rate limiting step between cytochrome *a* and the binuclear centre at maximal turnover rate. Ascorbate is not the natural reducing agent for the caa_3 enzyme; electron transfer *in vivo* occurs via a membrane bound cytochrome *c* molecule. The presence of two different caa_3 populations, one of which contains an active cytochrome *c* portion, but an inactive aa_3 portion of the enzyme, may in part explain the parallel reduction of cytochrome *c* with cytochrome *a*, independent of flux. Electron movement from cytochrome *c* to cytochrome *a* is one possible route involved in enzyme turnover. Electron transfer may also occur simultaneously from the cytochrome *c* portion of free caa_3 species with inactive cytochrome *a* and cytochrome a_3 which has come in contact

with an active caa_3 species. This electron transfer may occur directly to the binuclear centre. Electrons from the active caa_3 cytochrome *c* portion are transferred to Cu_A, where they are subsequently transferred to cytochrome *a*.

In bovine enzyme the four redox centres all have oxidoreduction potentials between 250 and 400 mV. Cytochromes *a* and a_3, and Cu_A at pH 7.0 have standard oxidoreduction potentials of 340, 290, and 240 mV respectively (Blair *et al.*, 1986; Wang *et al.*, 1986). The reduction potential of Cu_B has been estimated at 340 mV. Redox potentials of caa_3 from *T. thermus* (Yoshida and Fee, 1985) indicated that the cytochrome *c* is a separate electron donor with E_m = 200 mV. Cytochromes *a* and a_3 in caa_3 have redox potentials of 270 mV and 360 mV respectively. Cytochrome *a* redox potential is modulated by both reduction of the binuclear centre and by membrane energization (Nicholls 1993). These processes decrease the cytochrome *a* redox potential to values which are 60 to 100 mV more negative. A redox potential that is initially more positive than that of external cytochrome *c* (260 mV) becomes more positive upon the addition of ionophores. Nicholls (1993) showed that valinomycin increased cytochrome *a* redox potential from 275 mV to 282 mV. Nigericin increased the redox potential to 328 mV. Thus, the de-energization of a membrane increases the redox potential of cytochrome *a*.

Cytochrome caa_3 shows no redox changes upon the addition of ionophores. The similarity in redox states of cytochrome *c* and *a* indicates that control of turnover is not determined by electron transfer between these two centres. $\Delta\Psi$ has been implicated in controlling the movement of electrons from cytochrome *c* to cytochrome *a*. In cytochrome *caa3* the control of enzyme turnover is governed elsewhere and does not lie between cytochrome *c* and cytochrome *a*. Upon the addition of valinomycin by itself, no significant change in the respiration rate was observed. The reduction levels of both cytochromes *c* and *a* did not change in the presence of valinomycin. In the uncontrolled state, the rate of respiration only increased slightly over the controlled

state. The reduction levels of cytochromes *c* and *a* in the *caa3* enzyme increased only with the removal of a pH gradient. This suggests that enzyme turnover is possibly governed between cytochrome *a* and the binuclear centre.

The incorporation of mitochondrial oxidase into proteoliposomes does not pose the problems associated with the prokaryotic species. The mitochondrial enzyme is composed of 13 subunits, many of which are involved in structural stability and membrane incorporation. The prokaryotic oxidases are composed of between 2 and 4 subunits, which are representative of the core enzymatically functional enzyme (subunits I-III). The binding subunits found in the mitochondrial species are not present within the prokaryotic oxidases. In the prokaryotes, stability of the oxidase with the membrane may be governed by other factors, such as the membrane itself. The lipid composition of bacteria varies between species and within species, depending on their environment. The pure lipid system for caa_3 COV may not be entirely suitable to this enzyme. Pure lipid systems eliminate charges on the membrane surface which may influence cytochrome *c* binding to the enzyme, but the use of asolectin or soybean lipid mixtures may be preferred, as they contain a variety of lipids which may be useful in stabilizing the caa_3 enzyme within the membrane. Such a system may prove useful for further steady state studies to examine the apparent parallel reduction of cytochromes *c* and *a*.

References

References

Alexandre, A., Reynafarje, B., and Lehninger, A. 1978. Stoichiometry of vectorial proton movements coupled to electron transport and to ATP synthesis in mitochondria. Proc. Natl. Acad. Sci. USA. ***75:*** 5296-5300.

Anraku, Y., and Gennis, R.B. 1988. Trends in Biochem Sci. The aerobic respiratory chain of *Escherichia coli*. ***12:*** 262-266.

Azzone, G., Pozzan, T., and Di Virgilio. 1979. H^+/site, charge/site, ATP/site ratios at coupling site III in mitochondrial electron transport. J. Biol. Chem. ***254:*** 10206-10212.

Baines, B., Hubbard, J., and Poole, R. 1984. Purification and partial characterization of two cytochrome oxidases (*caa*$_3$ and *o*) from the thermophilic bacterium PS3. Biochem. Biophys. Acta. ***766:*** 438-445.

Beavis, A.D. 1987. Upper and lower limits of charge translocation stoichiometry of cytochrome *c* oxidase. Upper and lower limits of charge translocation stoichiometry of cytochrome *c* oxidase. J. Biol. Chem. ***262:*** 6174-6181.

Bisson, R., and Montecucco, J. 1986. Different polypeptides of bovine heart cytochrome *c* oxidase are in contact with cytochrome *c*. FEBS Lett. ***150:*** 49-53.

Blair, D., Ellis, W., Wang, H., Gray, H., and Chang, S. 1986. Spectroelectrochemical study of cytochrome *c* oxidase: pH and temperature dependencies of the cytochrome potentials. J. Biol. Chem. ***261:*** 11524-11527.

Brown, S., and Brand, M. 1986. Changes in permeability to protons and other cations at high proton motive force in rat liver mitochondria. Biochem. J. ***234:*** 75-81.

Brown, G., Moody, A.J., Mitchell, R., and Rich, P.R. 1993. Binuclear centre structure of terminal protonmotive oxidases. FEBS Letts. ***316:*** 216-223.

Buse, G., Hensel, S., and Fee, J. 1989. Evidence for cytochrome oxidase subunit I and a cytochrome *c* subunit II fused protein in the cytochrome *c*$_1$*aa*$_3$ of *Thermus thermophilus*. Eur. J. Biochem. ***181:*** 261-268.

Calhoun, M.W., Oden, K.L., Gennis, R.B., Joost Teixeira de Matlos, M., and Neijssel, O.M. 1993. Energetic efficiency of *Escherichia coli*: Effects of mutations in components of the aerobic respiratory chain. J. Bact. ***175:*** 3020-3025.

Calhoun, M.W., Thomas, J.W., and Gennis, R.B. 1994. The cytochrome oxidase superfamily of redox driven proton pumps. Trends in Biochem Sci. ***19:*** 325-330.

Capaldi, R.A. 1990. Structure and assembly of cytochrome *c* oxidase. Arch. Bioch. Biophys. ***280:*** 252-262.

Capitanio, N., De Nitto, E., Villani, G., Capitanio, G., and Papa, S. 1990. Proton motive activity of cytochrome oxidase: Control of the oxidoreduction of the heme centres by the proton motive force in the reconstituted beef heart enzyme. Biochemistry. ***29:*** 2939-2945.

Capitanio, N., Capitanio, G., De Nitto, E., Villani, G., and Papa, S. 1991. H^+/e^- stoichiometry of mitochondrial cytochrome complexes reconstituted in liposomes. FEBS. Lett. ***288:*** 179-182.

Casey, R., Thelen, M., and Azzi, A. 1979. Dicyclohexylcarbodiimide inhibits proton translocation by cytochrome oxidase. Bioch. Biophys. Res. Commun. ***87:***1044-1051.

Castresana, J., Lubben, M., Saraste, M., and Higgins, D.G. 1994. Evolution of cytochrome oxidase, an enzyme older than atmosheric oxygen. EMBO J. ***13:*** 2516-2525.

Chepuri, V., Lemieux, L., Au, D.T., and Gennis, R.B. 1990. The sequence the of *cyo* operon indicates substantial structural similarities between the cytochrome *o* ubiquinol oxidase of *Escherichia coli* and the aa_3-type family of cytochrome *c* oxidase. J. Biol. Chem. ***265:*** 11185-11192.

Cooper, C. 1990. The steady state kinetics of cytochrome *c* oxidation by cytochrome *c* oxidase. Bioch. Biophys. Acta. ***1017:*** 187-203.

Dermantia, M., Turk, T., and Hollocher, T. 1991. Nitric oxide reductase: Purification from *Paracoccus denitrificans* with the use of a single column and some characteristics. J. Biol. Chem. ***266:*** 10899-10905.

De Vriij, W., Azzi, A., and Konings, W.N. 1983. Kinetic characterization of cytochrome *c* oxidase from *Bacillus subtilis*. Eur. J. Biochem. ***131:*** 97-103.

De Vriij, W., Heyne, R., and Konings, W.N. 1989. Characterization and application of a thermostable primary transport system: Cytochrome *c* oxidase from *Bacillus stearothermophilus*. Eur. J. Biochem. ***178:*** 763-770.

Di Spirito, D. 1990. Soluble cytochromes *c* from *Methylomonas* A4. Methds. Enzym. ***188:*** 289-301.

Einarsdottir, O., and Caughey, W. 1984. Zinc is a constituent of bovine heart cytochrome *c* oxidase preparations. Biochem. Biophys. Res. Commun. ***124:*** 836-842.

Einarsdottir, O., and Caughey, W. 1985. Bovine heart cytochrome *c* oxidase preparations contain high affinity binding sites for magnesium, as well as for zinc, copper, and heme iron. Biochem. Biophys. Res. Commun. ***129:*** 840-847.

Fee, J., Choc, M., Findling, K., Lorence, R., and Yoshida, T. 1980. Properties of a copper containing cytochrome c_1aa_3 complex: a terminal oxidase of the extreme thermophile *Thermus thermophilus* HB8. Proc. Natl. Acad. Sci. USA. ***77:*** 147-151.

Fee, J., Kuila, D., Mathers, M., and Yoshida, T. 1986. Respiration proteins from extremely thermphilic, aerobic bacteria. Biochem. Biophys. Acta. ***853:***153

Ferguson-Miller, S., Brautigan, D., and Margoliash, E. 1976. Correlation of the kinetics of electron transfer activity of various eukaryotic cytochromes *c* with binding to mitochondrial cytochrome *c* oxidase. J. Biol. Chem. ***251:*** 1104-1115.

Gai, W., Sun, S., Sone, N., and Chan, S. 1990. Cytochrome oxidase from a thermophilic bacterium PS3 contains a fourth protein subunit. Biochem. Biophys. Res. Commun. ***169:*** 414-421.

Garcia-Horsman, J.A., Barquera, B., and Escamilla, J.E. 1991. Two different aa_3-type cytochromes can be purified from the bacterium *Bacillus cereus*. Eur. J. Biochem. ***199:*** 761-768.

Garcia-Horsman, J.A., Berry, E., Shapleigh, J., Alben, J., and Gennis, R. 1994. A novel cytochrome *c* oxidase from *Rhodobacter sphaeroides* that lacks Cu_A. Biochemistry. ***33:*** 3113-3119.

Garcia-Horsman, J.A., Puustinen, A., Gennis, R., and Wikstrom, M. 1995. Proton transfer in cytochrome bo_3 ubiquinol oxidase of *Escherichia coli*: Second site mutation in subunit I that restores proton pumping in mutant Asp 135 - Asn. Biochemistry. ***34:*** 4428-4433.

Gregory, L., and Ferguson-Miller, S. 1988. Effect of subunit III removal on control of cytochrome *c* oxidase activity by pH. Biochemistry. ***27:*** 6307-6314.

Gornal, A., Bardawill, C., and David, M. 1949. Determination of serum proteins by the buret method. J. Biol. Chem. ***177:*** 751.

Gutknecht, J. 1988. Proton conductance caused by long chain fatty acids in phospholipid bilayer membrane. J. Memb. Biol. ***106:*** 83-93.

Haltia, T., Finel, M., Harms, N., Nakari, T., Raitio, M., Wikstrom, M., and Saraste, M. 1989. Deletion of the gene for subunit III leads to deffective assembly of bacterial cytochrome oxidase. EMBO J. ***8:*** 3571-3578.

Hendler, R.W., Pardhasaradhi, K., Reynafarje, B., and Ludwig, B. 1991. Comparison of the energy transducing capabilities of the two and three subunit cytochrome aa_3 from *Paracoccus denitrificans* and the 13 subunit beef heart enzyme. Biophys. J. ***60:*** 415-423.

Henning, W., Vo, L., Albanese, J., and Hill, B.C. 1995. High yield purification of cytochrome aa_3 and cytochrome caa_3 oxidases from *Bacillus subtilis* plasma membrane. Biochem. J. ***309:*** 279-283.

Hill, B.C., and Greenwood, C. 1984. The reaction of fully reduced cytochrome oxidase with O_2 studied by low flash spectrometry at room temperature. Biochem. J. ***218:*** 913-921.

Hill, J.J., Alben, J.O., and Gennis, R.B. 1993. Spectroscopic evidence for a haem-haem binuclear centre in the cytochrome *bd* ubiquinol oxidase from *Escherichia coli.* Proc. Natl. Acad. Sci. USA. ***90:*** 5863-5867.

Hill, S., Viollet, S., Smith, A., and Anthony, C. 1990. Roles for enteric *d*-type cytochrome oxidase in N_2 fixation and microaerobiosis. J. Bact. ***172:*** 2071-2078.

Hinkle, P.E., Kim, J.J., and Racker, E. 1972. Ion transport and respiratory control in vesicles formed from cytochrome oxidase and phospholipids. J. Biol. Chem. ***247:*** 1338-1345.

Holm, L., Saraste, M., and Wikstrom, M. 1987. Structural models of the redox centres in cytochrome oxidase. EMBO J. ***6:*** 2819-2823.

Hon-nami, K., and Oshima, T. 1984. Purification and characterization of cytochrome *c* oxidase from *Thermus thermophilus* HB8. Biochemistry. ***23:*** 454-460.

Hosler, J., Ferguson-Miller, S., Calhoun, M., Thomas, J., Hill, J., Lemieux, L., Ma, J., Georgiou, C., Fetter, J., Shapleigh, J., Tecklenburg, M., Babcock, G., Gennis, R. 1993. Insight into the active-site structure and function of cytochrome oxidase by analysis of site directed mutants of bacterial cytochrome aa_3 and cytochrome *bo*. J. Bioenerg. Biomemb. ***25:*** 121-136.

Iwata, S., Ostermeier, C., Ludwig, B., and Michel, H. 1995. Structure at 2.8 A resolution of cytochrome *c* oxidase from *Paracoccus denitrificans*. Nature. ***376:*** 660-669.

Kadenbach, B., Jarausch, J., Hartman, R., and Merle, P. 1982. Separation of mammalian cytochrome *c* oxidase into 13 polypeptides by sodium dodecl sulphate gel electrophoresis procedure. Analyt. Biochem. ***129:*** 517-521.

Kasting, J.F. 1993. Earths early atmosphere. Science. ***259:*** 920-926.

Keilin, D. 1925. On cytochromes, a respiratory pigment, common to animals, yeast, and higher plants. Proc. Roy. Soc. B. ***98:*** 312-339.

Keilin, D., and Hartree, E. 1939. Cytochrome and cytochrome oxidase. Proc. Roy. Soc. B. ***127:*** 167-191.

Krishnamoorthy, V., and Hinkle, P. 1984. Non-ohmic proton conductance of mitochondria and liposomes. Biochemistry. ***23:*** 1640-1645.

Kuboyama, M., Yong, F.C., and King, T.E. 1972. Studies on cytochrome oxidase. VIII. Preparation and some properties of cardiac cytochrome oxidase. J. Biol. Chem. ***247:*** 6375-6383.

Kusano, T, Kuge, S., Sakamoto, J., Noguchi, S., and Sone, N. (1996) Nucleotide and amino acid sequence for cytochrome caa_3 type oxidase of *Bacillus stearothermophilus* K104 and non-Michaelis-type kinetics with cytochrome *c*. Biochim. Biophys. Acta. ***1273:*** 129-138.

Lauraeus, M., Halatia, T., Saraste, M., and Wikstrom, M. 1991. *Bacillus subtilis* expresses two kinds of haem-A containing terminal oxidases. Eur. J. Biochem. ***197:*** 699-705.

Lubben, M., Kolmerer, B., and Saraste, M. 1992. An archaebacteria terminal oxidase combines core structure of two mitochondrial respiratory oxidase complexes. EMBO J. ***11:*** 805-812.

Maison-Peteri, B., and Malmstrom, B.G. 1989. Intrinsic uncoupling in proton pumping cytochrome *c* oxidase: pH dependencies of cytochrome oxidase oxidation in coupled and uncoupled phospholipid vesicles. Biochem. ***28:*** 3156-3160.

Meinhandt, S.W., Gennis, R.B., and Osnishi, T. 1989. EPR studies of the cytochrome *d* complex of *Escherichia coli*. Biochim. Biophys. Acta. ***975:*** 175-184.

Miller, M.J., Hermodson, M., and Gennis, R.B. 1988. The active form of the cytochrome *d* terminal oxidase complex of *Escherichia coli* determined by site directed mutagenesis. J. Biol Chem. ***264:*** 8026-8032.

Mitchell, P. 1961. Coupling of phosphorylation to electron and proton transfer by a chemiosmotic type mechanism. Nature. ***191:*** 144-148.

Mitchell, P. 1966. Chemiosmotic coupling in oxidative and photosynthetic phosphorylation. Glynn Research Ltd., Bodmin, UK.

Mitchell, P. 1968. Chemiosmotic coupling and energy transduction. Glynn Research Ltd., Bodmin, UK.

Mitchell, P., and Hinkle, P. 1970. Effect of membrane potential on membrane poise between cytochrome *a* and cytochrome *c* in rat liver mitochondria. J. Bioenerg. ***1:*** 45-60.

Moody, J., Cooper, C.E., and Rich, P. 1991. Characterization of fast and slow forms of bovine heart cytochrome *c* oxidase. Biochim. Biophys. Acta. ***1059:*** 189-207.

Morgan, J., Verkhovsky, M., and Wikstrom, M. 1994. The histidine cycle: A new model for proton translocation in respiratory heme-copper oxidases. J. Bioenerg. Biomemb. ***26:*** 599-608.

Moyle, J., and Mitchell, P. 1978. Cytochrome *c* oxidase is not a proton pump. FEBS Lett. ***88:*** 268-272.

Murphy, M., and Brand, M. 1988a. Membrane potential dependent changes in the stoichiometry of charge translocation by the mitochondrial respiratory chain. Eur. J. Biochem. ***173:*** 637-644.

Murphy, M., and Brand, M. 1988b. The stoichiometry of charge translocation by cytochrome oxidase and cytochrome bc_1 complex of mitochondria at high membrane potential. Eur. J. Biochem. ***173:*** 645-651.

Nicholls, P., Hildebrandt, V., and Wriglesworth, J.M. 1980. Orientation and reactivity of cytochrome aa_3 haem groups in proteoliposomes. Arch. Bioch. Biophys. ***204:*** 533-543.

Nicholls, P., Shaughnessy, S., and Singh, A.P. 1987. Control of cytochrome oxidase: flux and stoichiometry. *In* Cytochrome systems. Ed. S. Papa, B. Chance, and L. Ernster. Plennum Publishing Co., New York. pp. 391-398.

Nicholls, P., Cooper, C., and Wrigglesworth, J. 1990. Control of proteoliposomal cytochrome *c* oxidase: the overall reaction. Biochem. Cell Biol. ***68:*** 1128-1134.

Nicholls, P. 1990. Control of proteoliposomal cytochrome *c* oxidase: the partial reactions. Biochem. Cell Biol. ***68:*** 1135-1141.

Nicholls, P. 1993. The steady state behaviour of cytochrome *c* oxidase in proteoliposomes. FEBS. Lett. ***327:*** 194-198.

Ostermeier, C., Iwata, S., Ludwig, B., and Michel, H. 1995. F_v fragment-mediated crystallization of the membrane protein bacterial cytochrome *c* oxidase. Nature Struc. Biol. ***2:*** 842-846.

Papa, S., Capitanio, N., and De Nitto, E. 1987. Characteristics of the redox-linked proton ejection in beef-heart cytochrome *c* oxidase reconstituted in liposomes. Eur. J. Biochem. ***164:*** 507-516.

Papa, S., Guerrieri, F., Lorusso, M., Izzo, G., Boffoli, D., Capuano, F., Capitanio, N., and Altamura, N. 1980. The H+/e- stoichiometry of respiration linked H+ translocation in the cytochrome system of mitochondria. Biochem. J. ***192:*** 203-218.

Papa, S., Capitanio, N., Capitanio, G., De Nitto, E., and Minuto, M. 1991. The cytochrome chain of mitochondria exhibits variable H+/e- stoichiometry. FEBS Lett. ***288:*** 183-186.

Poole, R. 1988. Bacterial cytochrome oxidase. *In* Bacterial energy transduction. Ed. C. Anthony. Academic Press, London. pp.231-291.

Preisig, O., Anthamatten, D., and Hennecke, H. 1993. Genes for a microaerobically induced oxidase complex in *Bradyryzobium japonicum* are essential for a nitrogen fixing endosymbiosis. Proc. Natl. Acad. Sci. USA. ***90:*** 3309-3313.

Prochaska, L., Bisson, R., Capaldi, R., Steffens, G., and Buse, G. 1981. Inhibition of cytochrome *c* oxidase function by dicyclohexylcarbodimide. Biochim. Biophys. Acta. ***637:*** 360-373.

Puustinen, A., Finel, M., Haltia, T., Gennis, R.B., and Wikstrom, M. 1991. Properties of two terminal oxidases of *Escherichia coli*. Biochem. ***30:*** 3936-3942.

Racker, E. 1972. Reconstitution of cytochrome oxidase vesicles and conferral of sensitivity to energy transfer inhibitors. J. Memb. Biol. ***10:*** 221-235.

Rice, C., and Hempfling, W. 1978. Oxygen limited continuous culture and respiratory energy conservation in *Escherichia coli*. J. Bact. ***134:*** 115-124.

Rich, P.R., West, I.C., and Mitchell, P. 1988. The location of Cu_A in the mammalian cytochrome oxidase. FEBS Lett. ***233:*** 25-30.

Santana, M., Kunst, F., Francoise, H., Rapoport, G., Danchin, A., and Glasser, P. 1992. Molecular cloning, sequencing, and physiological characterization of the *qox* operon from *Bacillus subtilis* encoding the aa_3-600 quinol oxidase. J. Biol. Chem. ***267:*** 10225-10231.

Saraste, M., Metso, T., Nakari, T., Jalli, T., Lauraeus, M., and van der Oost, J. 1991. The *Bacillus subtilis* cytochrome *c* oxidase: Variations on a conserved protein theme. Eur. J. Biochem. ***195:*** 517-525.

Saraste, M., and Castresana, J. 1994. Cytochrome oxidase evolved by tinkering with denitrification enzymes. FEBS Letters. ***341:*** 1-4.

Shaughnessy, S., and Nicholls, P. 1985. Control of respiration in sonicated cytochrome oxidase proteoliposomes by gated and ungated ionophores. Biochim. Biophys. Res. Comm. ***128:*** 1025-1030.

Sharpe, M., Cooper, C.E., and Wrigglesworth, J. 1991. Transport of K+ and other cations across phospholipid membranes by non-esterified fatty acids. J. Memb. Biol. ***141:*** 21-28.

Sharpe, M., Cooper, C., and Wrigglesworth, J. 1994. Transport of K^+ and other cations across phospholipid membranes by non-esterified fatty acids. J. Memb. Biol. ***141:*** 21-28.

Sharpe, M., Wrigglesworth, J., Loewen, J., and Nicholls, P. 1995. Small pH gradients inhibit cytochrome *c* oxidase: implications for H+ entry to the binuclear centre. Biochem. Biophys. Res. Commun. ***216:*** 931-938.

Sharpe, M., Perin, I., and Nicholls, P. 1996. Action of bovine serum albumin on cytochrome *c* oxidase activity and proton pumping: a role for free fatty acids in enzyme function? FEBS Lett. ***391:*** 134-138.

Sone, N., and Hinkle, P. 1982. Proton transport by cytochrome *c* oxidase from the thermophilic bacterium PS3 reconstituted in liposomes. J. Biol. Chem. ***257:*** 12600-12604.

Sone, N., and Yanagita, Y. 1982. A cytochrome aa_3 terminal oxidase of a thermophilic bacteria: purification, properties and proton pumping. Biochim. Biophys. Acta. ***682:*** 216.

Sone, N., and Yanagita, Y. 1984. High vectorial proton stoichiometry by cytochrome *c* oxidase from the thermophilic bacterium PS3 reconstituted in liposomes. J. Biol. Chem. ***259:*** 1405-1408.

Steverding, D., Kadenbach, B., Capitanio, N., and Papa, S. 1990. Effect of chemical modification of Lys amino groups on redox and protonmotive activity of bovine heart cytochrome *c* oxidase rconstituted in phospholipid membranes. Biochem. ***29:*** 2945-2950.

Taha, T., and Ferguson-Miller, S. 1992. Interaction of cytochrome *c* with cytochrome *c* oxidase studied by monoclonal antibodies and a protein modifying reagent. Biochemistry. ***31:*** 9090-9097.

Thomas, J., Puunstinen, A., Alben, J., Gennis, R., and Wikstrom, M. 1993. Substitution of Asparagine for Aspartate 135 In subunit I of the *bo* ubiquinol oxidase of *Escherichia coli* eliminated proton pumping activity. Biochemistry. ***32:*** 10923-10928.

Tsukihara, T., Aoyama, H., Yamashita, E., Tomizaki, T., Yamaguchi, H., Shinzawa-Itoh, K., Nakashima, R., Yaono, R., and Yoshikawa, S. 1995. Structures of metal sites of oxidized bovine heart cytochrome *c* oxidase at 2.8 A. Science. ***269:*** 1069-1074.

Tsukihara, T., Aoyama, H., Yamashita, E., Tomizaki, T., Yamaguchi, H., Shinzawa-Itoh, K., Nakashima, R., Yaono, R., and Yoshikawa, S. 1996. The whole structure of the 13 subunit oxidized cytochrome *c* oxidase at 2.8 A. Science. ***272:*** 1136-1144.

von Wachenfeldt, C., and Hederstedt, L. (1992). Molecular biology of *Bacillus subtilis* cytochromes. FEMS Microbiology Letters. ***100:*** 91-100.

Wang, H., Blair, D., Ellis, W., Gray, H., and Chan, S. 1986. Temperature dependence of the reduction potential of Cu_A in carbon monoxide inhibited enzyme. Biochemistry. ***25:*** 167-171.

Wikstrom, M. 1977. Proton pump coupled to cytochrome *c* oxidase in mitochondria. Nature. ***266:*** 271-273.

Wikstrom, M., and Krab, K. 1979. Proton pumping cytochrome *c* oxidase. Biochim. Biophys. Acta. ***549:*** 177-222.

Woese, C.R. 1987. Bacterial evolution. Microb. Rev. ***51:*** 221-271.

Wrigglesworth, J.M. 1985. Quantization of membrane potential generation by cytochrome *c* oxidase in small vesicles. J. Inorg. Bioch. ***23:*** 311-316.

Wrigglesworth, J., Wooster, M., Elsden, J. and Danneel, H. 1987. Dynamics of proteoliposome formation. Biochem. J. ***246:*** 737-744.

Wrigglesworth, J., Elsden, J., Chapman, A., Vanader Water, N., and Grahn, M. 1988. Activation by reduction of resting form of cytochrome *c* oxidse: tests of different models and evidence for the involvement of Cu_B. Biochim. Biophys. Acta. ***936:*** 452-464.

Wrigglesworth, J., Cooper, C., Sharpe, M., and Nicholls, P. 1990. The proteoliposomal steady state: Effect of size, capacitance and membrane permeability on cytochrome oxidase-induced ion gradients. Biochem. J. ***270:*** 109-118.

Yonetani, T. 1961. Studies on cytochrome oxidase III: Improved preparation and some properties. J. Biol. Chem. ***236:*** 1680-1688.

Yoshida, T., and Fee, J.A. 1984. Studies on cytochrome *c* oxidase activity of the cytochrome c_1aa_3 from *Thermus thermophilus*. J. Biol. Chem. ***259:*** 1031-1036.

Yoshida, T., and Fee, J.A. 1985. Protentiometric study of cytochrome c_1aa_3 from *Thermus thermophilus*. J. Inorg. Bioch. ***23:*** 279-288.

Yoshikawa, S., Terra, T., Takahashi, Y., Tsukihara, T., and Caughey, W.S. 1988. Crystalline cytochrome *c* oxidase of bovine heart mitochondrial membrane: Composition and x-ray diffraction. Proc. Natl. Acad. Sci. USA. ***85:*** 1354- 1358.